CENTRAL RESEARCH LIBRARY
DOCUMENT COLLECTION

OAK RIDGE NATIONAL LABORATORY
operated by
UNION CARBIDE CORPORATION • NUCLEAR DIVISION
for the
U.S. ATOMIC ENERGY COMMISSION

LOCKHEED MARTIN ENERGY RESEARCH LIBRARIES
3 4456 0514517 0

ORNL-TM-3446

cy. 2

PREIRRADIATION DATA FOR ORNL SERIES II AND B & W OXIDE FUEL TESTS IN EBR-II

A. R. Olsen

OAK RIDGE NATIONAL LABORATORY
CENTRAL RESEARCH LIBRARY
DOCUMENT COLLECTION
LIBRARY LOAN COPY
DO NOT TRANSFER TO ANOTHER PERSON
If you wish someone else to see this document, send in name with document and the library will arrange a loan.

NOTICE This document contains information of a preliminary nature and was prepared primarily for internal use at the Oak Ridge National Laboratory. It is subject to revision or correction and therefore does not represent a final report.

This report was prepared as an account of work sponsored by the United States Government. Neither the United States nor the United States Atomic Energy Commission, nor any of their employees, nor any of their contractors, subcontractors, or their employees, makes any warranty, express or implied, or assumes any legal liability or responsibility for the accuracy, completeness or usefulness of any information, apparatus, product or process disclosed, or represents that its use would not infringe privately owned rights.

ORNL-TM-3446

Contract No. W-7405-eng-26

METALS AND CERAMICS DIVISION

PREIRRADIATION DATA FOR ORNL SERIES II AND B & W OXIDE FUEL TESTS IN EBR-II

A. R. Olsen

Babcock & Wilcox Company

C. J. Baroch
A. H. Bremser
R. V. Carlson
L. J. Ferrell
E. N. Harbinson
J. M. Kerr

Oak Ridge National Laboratory

R. A. Bradley
W. H. Bridges
F. J. Homan
W. J. Leonard
W. H. Pechin
R. B. Pratt
M. K. Preston
C. F. Sanders
J. D. Sease
A. F. Zulliger

NOVEMBER 1971

OAK RIDGE NATIONAL LABORATORY
Oak Ridge, Tennessee 37830
operated by
UNION CARBIDE CORPORATION
for the
U.S. ATOMIC ENERGY COMMISSION

LOCKHEED MARTIN ENERGY RESEARCH LIBRARIES

3 4456 0514517 0

CONTENTS

Page

Abstract 1

Introduction 1

Experiment Description and Requirements 2

Purposes and Objectives of the Experiments 2

Desired Irradiation Conditions 3

Desired Out-of-Reactor Services 7

Identification of Fuel Elements and Subassembly Loading Description 8

Fuel Pin Descriptions 9

Thermal Performance of Fuel Pins 14

Thermal Performance of Subassembly 22

Fuel Pin Stress and Strain Analysis 25

Fuel-Cladding Mechanical Interaction 26

Thermal Gradient and Internal Gas Pressure 28

Cladding Damage Effects 29

Revised Stress-Strain Analysis 31

Effect of Increased Diameter of Pins on Coolant Flow and Subassembly Thermal Analysis 32

Effect of Increased Pin Diameters on Subassembly Dimensions . 36

Safety Analysis 37

Operation at 110% of Normal Heat Rate 37

Abnormal Operations 38

Power Excursions 38

Loss-of-Coolant Flow Operation 42

Cladding Failure 44

Gas Blanketing 44

Solid Debris Flow Blockage 47

Reactor Environment Contamination 48

Sodium Removal from Failed Pin 50

Subassembly Criticality Analysis 50

Criteria for Reinsertion of Pins 50

Quality Assurance Descriptions and As-Built Information 51
Fabrication and Inspection of ORNL Pins 52
Fabrication and Quality Assurance Procedures 52
Fuel Pin Assembly 53
As-Fabricated Data 57
Quality Assurance Certifications 57
Fabrication and Testing of B&W Unencapsulated Fuel Pins . . . 73
Description of Fuel Pin 73
Fuel Material 77
Tubing for Cladding 80
End Fittings 81
Reflector, Spring, and Plenum Tube 82
Fiberfrax Pad 82
Fuel Pin Assembly and Quality Control 83
Quality Assurance Certifications 85
Acknowledgments 87
References 88
Appendix A
Sample Calculations 93
Heat Generation in Fuel 93
Calculations of Flow Rate and Flow Area 96
Gas Pressure 102
Stress and Strain Analysis 108
Preliminary Stress-Strain Analysis 110
Effects of Fast Flux on Cladding Volume Changes 112
Appendix B
ORNL Quality Assurance Specifications and Procedures 155
Weld Repairs 159
Bottom End Plug to Clad Tube Weld W-1 159
Top End Plug to Clad Tube W-3 159
Top End Cap Top End Plug Weld W-5 159

PREIRRADIATION DATA FOR ORNL SERIES II AND B & W OXIDE FUEL TESTS IN EBR-II

ABSTRACT

This data package was prepared to satisfy the requirements for approval of irradiations in the EBR-II. The subassembly includes $(U,Pu)O_2$ fuel pins fabricated by Babcock & Wilcox and Oak Ridge National Laboratory. The objectives of the tests, a performance and safety analysis for the subassembly, and the as-fabricated fuel pin descriptions together with the appropriate fabrication procedures and Quality Assurance documentation are presented. The analysis predicts safe operation of these experimental pins to burnup levels of 100,000 MWd/metric ton of U + Pu at a nominal peak linear heat rate of 14 kW/ft with cladding temperatures in the temperature range 550 to 650°C.

INTRODUCTION

This data package was prepared in accordance with the requirements for approval of experimental irradiations in the Experimental Breeder Reactor (EBR-II). The experiment described here includes $(U,Pu)O_2$ fuel elements fabricated by both the Babcock & Wilcox Company (B & W) and Oak Ridge National Laboratory (ORNL) for irradiation in a shared experimental subassembly.

Each site has previously proposed similar experimental irradiations to be conducted with encapsulated fuel pins.[1,2] Approval was granted to ORNL (ref. 3) for five encapsulated fuel pins to be irradiated as lead experiments for revised test programs[3,4] with unencapsulated experimental pins using a 37-pin shared subassembly. The experimental programs of the two sites have been coordinated to provide complementary performance data on $(U,Pu)O_2$ fuel. The request for Approval-in-Principle[5] of the combined experimental test programs was approved.[6]

Each organization has individual responsibility for the design, fabrication, inspection, and shipment of its own test pins. However, this data package is a common submission of the fabrication information

and safety analysis required for irradiation of the shared subassembly. This report has been organized in accordance with the directions in the Guide[7] to assure recognition of each of the EBR-II project requirements.

EXPERIMENT DESCRIPTION AND REQUIREMENTS

Purposes and Objectives of the Experiments

Both B & W and ORNL have programs for the development and evaluation of oxide fuels for liquid-metal fast breeder reactor (LMFBR) application.[8,9] The program at each site includes specific objectives for the test pins it has included in this shared subassembly. However, the coordination of the programs is such that the objectives of all the tests can be reduced to the following:

1. to obtain data on the operational characteristics of vibratorily compacted $(U,Pu)O_2$ particulate fuel required to qualify it for LMFBR use. The particulates include spheres produced by the sol-gel process and angular particles produced by crushing pellets made from a coprecipitated powder.
2. to compare the performance characteristics and limitations in a fast flux environment of $(U,Pu)O_2$ fuels prepared by different processes, including pellets prepared from coprecipitated $(U,Pu)O_2$ and pellets from $(U,Pu)O_2$ sol-gel-derived powders, and
3. to obtain data on the as-fabricated fuel characteristics required for oxide fuels to provide the performance required for advanced LMFBR applications.

To meet these objectives these tests are designed to place particular emphasis on the effects of fuel form and void distribution on fission-gas release and fuel-cladding mechanical interaction at extended burnup levels (greater than 50,000 MWd/metric ton of heavy metal), with cladding temperatures in the range 550 to 650°C.

The distribution of fuel pins for the first 37-pin subassembly loading is summarized in Table 1 by fabrication form and fuel production process. This subassembly is designed for irradiation to a peak burnup level of 50,000 MWd/metric ton of actinide before interior examination and pin replacement.

Table 1. Number of Test Pins of Various Fuel Forms in Test Subassembly

Fabrication Form	Fuel Production Process	Oxygen-to-Metal Ratio	Number of Test Pins at Each Design Smear Density (% of theoretical)				Total Pins of Each Fuel Form
			80	83	85	90	
Sphere-Pac	Sol-gel	1.98	4	4	6		14
Sphere-Pac	Sol-gel	1.94	2	1	1		4
Pellet	Sol-gel	1.98			2	2	4
Pellet	Coprecipitation	1.98		5			5
Pellet	Sol-gel	1.94	2		1		3
Vi-Pac	Coprecipitation	1.98	6	1			7
TOTALS			14	11	10	2	37

The postirradiation examination will permit a detailed comparison of fuel form, density, and voidage deployment effects on fission-gas release, fuel swelling, in-reactor restructuring, and fuel-component and fission-product redistribution as a function of fuel burnup.

Desired Irradiation Conditions

These tests involve two requirements (high cladding temperatures and extended burnup) which required assistance from the EBR-II Project to obtain subassembly designs which would assure achievement of the objectives. Since we are interested in peak cladding temperatures in the range 550 to 650°C, we contacted the EBR-II Project for a revised J-37 subassembly design to accommodate pins with a 0.250-in. cladding diameter.[10] The J-37-A subassembly design is the result of this request. This design was also used in establishing the flow requirements for the subassembly and selecting the reactor location for irradiation. Subsequently, we requested[11] an alternate design for the subassembly which would not involve a bypass flow and a high risk subassembly design modification, both of which would accept the same test pins as those

designed for irradiation in the J-37-A. The N-37 subassembly is a less expensive subassembly alternate for the J-37-A. The E-37-B is the high risk subassembly design which may be used in the latter stages of the irradiation program if the risks associated with the highest burnup levels are adjudged to require such protection.

Since the element and coolant flow cross-sectional area relationships are identical for all three subassembly designs, a single thermal analysis for the pins will fit all three subassembly designs.[12] However, the total subassembly heat generation, the total sodium coolant flow, and the mean coolant outlet temperature will vary with each design.

The desired irradiation conditions for these test pins were initially analyzed using a J-37-A subassembly design which will provide the required test temperatures and meet the subassembly exit coolant temperature as required by Appendix C, p. 66 of the Guide.[13,14] At the request of the EBR-II Project,[15] we also evaluated the use of the less expensive N-37 subassembly. This analysis indicated we would exceed the permissible subassembly mean coolant outlet temperature under the flow conditions existing at the start of life and at the end of life by only a very small amount. The EBR-II experiment manager felt[16] the calculated results were sufficiently uncertain and the over temperature predicted sufficiently small to justify the use of an N-37 subassembly. We have included the flow requirements and thermal analysis for a J-37-A subassembly as well as an N-37 subassembly in this data package to prevent delays should the interim examination data indicate the need to use the J-37-A subassembly for the second or third subassembly loading.

The desired irradiation conditions are summarized in Table 2. Since the replacement pins to be introduced in each subassembly reloading are currently scheduled to be duplicates of the pins removed, no change in the desired irradiation conditions is anticipated throughout this experimental program. A total of 58 pins are to be irradiated.

Table 3 presents the combined B & W and ORNL program for the subassembly together with the proposed pin removal and replacement schedule. No additional interim examinations are proposed.

Table 2. Irradiation Conditions

	Desired	Alternate
Reactor location	6-N3	6-N4
Subassembly type	N-37	J-37-A
Subassembly flows, gpm at 800°F		
Pin area	45	45
Bypass	Negligible	17
	45	62
Acceptable linear heat rates, kW/ft		
Maximum pin	14 ± 0.5	14 ± 0.5
Minimum pin	10 ± 2.0	8 ± 2.0
Lead pin peak burnup after exposure in:		
Initial subassembly, % FIMA	6.1 ± 0.3	6.1 ± 0.3
First reconstituted subassembly, % FIMA	8.7 ± 0.2	8.7 ± 0.2
Second reconstituted subassembly, % FIMA	12.8 ± 0.2	12.8 ± 0.2
Maximum pin average, MWd/metric ton U + Pu	103,000 ± 2,000	103,000 ± 2,000
Estimated reactor residence time		
Initial subassembly (reactor MWd)[a]	16,000	16,000
First reconstituted subassembly (reactor MWd)[a]	8,000	8,000
Second reconstituted subassembly (reactor MWd)[a]	13,000	13,000
	37,000	37,000

[a]Based on a reactor power level of 62.5 MW.

Table 3. Test Pin Distribution and Replacement Schedule

Subassembly Location	Sponsor	Fabrication[a] Form	Smear Density (% of theoretical)	Pin Identification		
				First Subassembly	Second	Third
1	B & W	SP	80	D-2	D-2	D-39
2	ORNL	PELL	80	OP-7	OP-7	OP-7
3	ORNL	SPL	80	OS-4	OS-16	OS-16
4	ORNL	SP	85	OS-9	OS-9	OS-9
5	B & W	SP	80	D-30	D-30	D-30
6	ORNL	SP	80	OS-8	OS-8	OS-8
7	ORNL	SPL	83	OS-12	OS-12	OS-12
8	B & W	PEL	83	D-9	D-9	D-42
9	ORNL	PEL	85	OP-5	OP-5	OP-5
10	ORNL	PELL	80	OP-3	OP-10	OP-10
11	B & W	VP	83	D-20	D-20	D-20
12	B & W	SP	83	D-10	D-35	D-35
13	ORNL	SP	85	OS-2	OS-14	OS-14
14	ORNL	SP	85	OS-6	OS-6	OS-18
15	B & W	VP	83	D-22	D-22	D-38
16	ORNL	SPL	80	OS-11	OS-11	OS-11
17	B & W	VP	83	D-21	D-21	D-37
18	B & W	VP	85	D-31	D-31	D-31
19	ORNL	SP	85	OS-7	OS-7	OS-19
20	B & W	PEL	83	D-17	D-17	D-43
21	ORNL	SP	80	OS-1	OP-4	OP-4
22	ORNL	SP	80	OS-13	OP-11	OP-11
23	ORNL	SP	85	OS-10	OS-10	OS-10
24	B & W	PEL	83	D-12	D-12	D-12
25	B & W	SP	83	D-19	D-19	D-40
26	B & W	VP	83	D-18	D-34	D-34
27	ORNL	SP	85	OS-3	OS-15	OS-15
28	B & W	PEL	83	D-14	D-14	D-14
29	B & W	SP	83	D-27	D-27	D-41
30	B & W	PEL	83	D-4	D-36	D-36
31	ORNL	SPL	85	OS-5	OS-17	OS-17
32	B & W	VP	83	D-25	D-25	D-25
33	ORNL	PEL	90	OP-2	OP-9	OP-9
34	ORNL	PEL	85	OP-1	OP-8	OP-8
35	B & W	SP	83	D-29	D-29	D-29
36	ORNL	PEL	90	OP-6	OP-6	OP-6
37	B & W	VP	83	D-5	D-5	D-5
	Desired maximum pin peak burnup, % FIMA			6.1 ± 0.3	8.7 ± 0.2	12.8 ± 0.2
	Estimated incremental exposure period:					
	Reactor MWd			16,000	8,000	13,000
	Approximate EBR-II cycles			10	5	7–8
	Number of pins removed at end of exposure period			12	9	37

[a]Fabrication forms: VP = Vi-Pac; SP = Sphere-Pac; PEL = pellets, all with oxygen-to-metal ratio of 1.98. SPL = Sphere-Pac; PELL = pellets, both with oxygen-to-metal ratio of 1.94.

Desired Out-of-Reactor Services

1. Neutron radiographs of each pin are to be obtained before they are initially introduced into the subassembly and each time the subassembly is dismantled for replacement of test pins.

2. As indicated in our request for Approval-in-Principle and in a previous communication,[11] we would like to have the 0.040-in.-diam spiral wrap stainless steel wire installed by the EBR-II Project on each pin to be irradiated in this program.

3. Each fuel pin is to be weighed to the nearest 0.1 g after the wire wrap has been installed and to the nearest 0.1 g (currently listed EBR-II capability) each time the subassembly is dismantled.

4. Following wire wrapping, it is desirable to obtain a balance point measurement on a limited number of pins to survey any fuel relocation during operation. These pins are to be:

Pin Identifications

OS-2	OP-2 OP-3	D-2
OS-8	OP-5	D-20
OS-12	OP-7	D-30

The balance point on these pins is to be measured each time they are removed from a subassembly whether or not they are to continue their irradiation. Please note Item 6 on pin handling which may affect balance point measurements.

5. Each fuel pin scheduled for reinsertion into a new subassembly is to be subjected to dimensional inspection for compliance with the "reinsertion criteria" defined in the safety analysis section of this data package. The dimensioning shall be done in conformance with the procedures and precisions defined in Appendix F, paragraph 1-C of the Guide as revised on Feb. 27, 1970, with the exception that any local abnormal configuration observed in visual examination is to be dimensioned at smaller axial increments and at rotational increments of 0, 30, 60, 90, 120, and 150°.

6. It is desirable to have the pins handled in a vertical orientation as much as possible during all preirradiation, interim examination,

and postirradiation activities. When the pins are handled in a non-vertical orientation, they should be provided with a support such as a Vee-trough to prevent incidental mechanical bending or damages.

7. No special procedures are required during normal subassembly handling, cooling, sodium removal with washing,[17,18] or dismantling.

In the event the subassembly is suspected of containing a failed fuel pin, the sodium removal procedure will have to be resolved with the EBR-II at the time on the basis of the data leading to the suspicion. The presence of plutonium in the EBR-II coolant sodium, for example, makes water washing of a suspect subassembly undesirable, while the presence of only xenon tag in the EBR-II cover gas might justify water washing to prevent caustic attack of the good pins during interim examination. Because of these variables and the unknown capabilities of the EBR-II Fuels Examination Facility in the future, we would prefer not to set specific sodium removal procedures for suspect subassembly handling at this time.

8. Shipping procedures for completed experiments: currently, it is planned to ship all pins that have completed their irradiation to ORNL for examination. The procedures to be used will be the same as those used for ORNL Series I experimental capsules.[19,20]

Identification of Fuel Elements and Subassembly Loading Description

The identification of each test pin is listed in Table 3, together with its assigned location in the subassembly. These subassembly positions are shown graphically in Fig. 1, which also defines the subassembly orientation for the preferred 6-N3 or alternate 6-N4 reactor grid locations.

Details of the method of marking each pin are included in the sections describing the fabrication, inspection, and quality assurance procedures used by each sponsor.

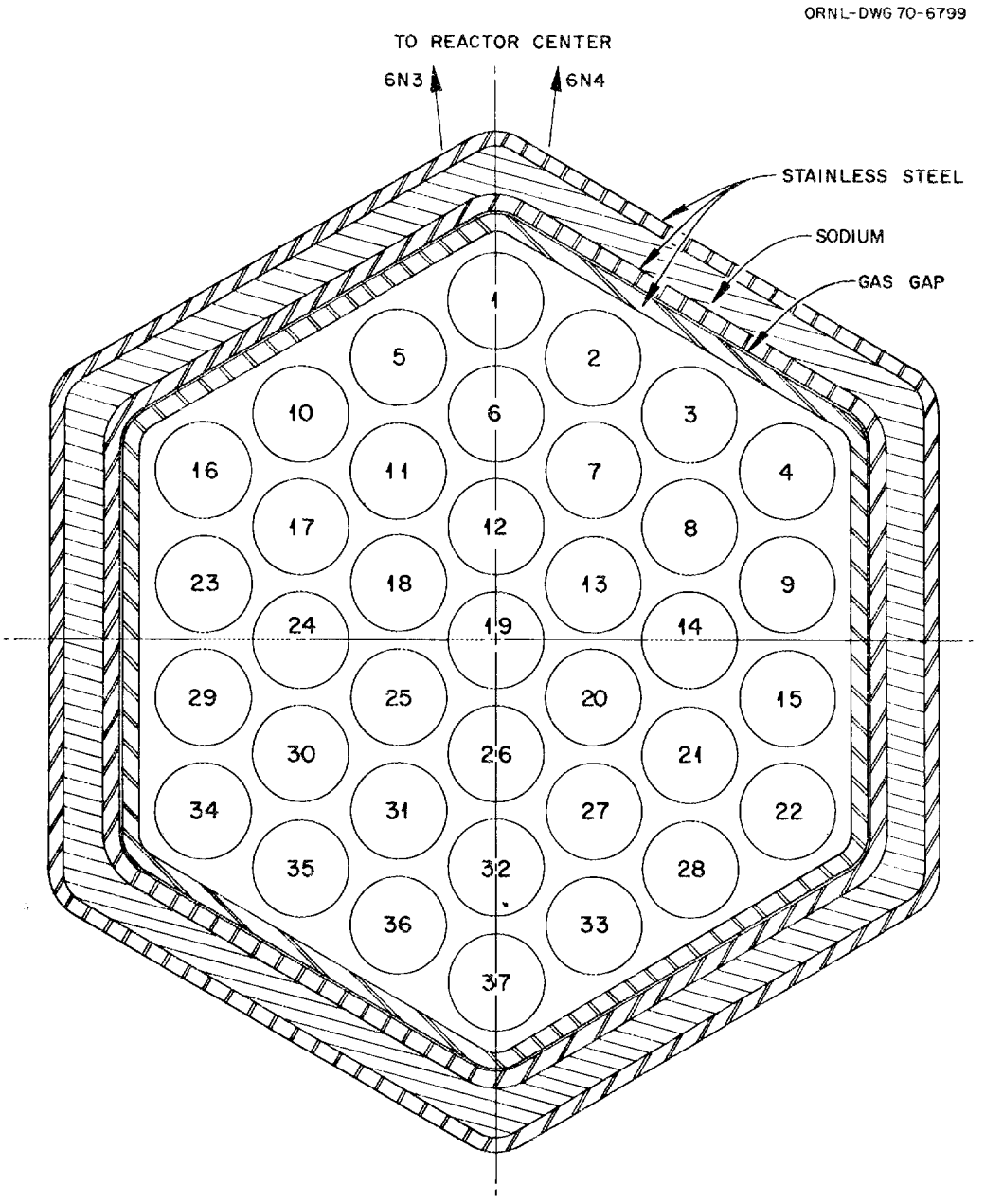

Fig. 1. Cross Section of J-37-A Subassembly with Location Identifying Numbers for ORNL Series II and B & W Pin Placement.

Fuel Pin Descriptions

The detailed designs of the fuel pins provided by each sponsor are shown in Figs. 2 and 3.

The principal difference between the two pin designs is the top end plug configuration which is associated with the xenon tagging procedure

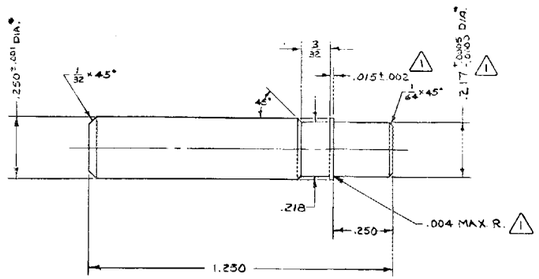

* DIAS. TO BE CONCENTRIC WITHIN .002 T.I.R.

(1) TOP END CAP

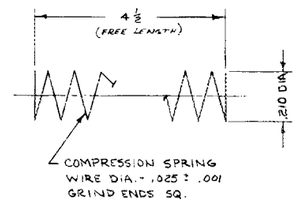

(5) SPRING
302 S.ST

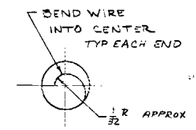

DATE	REV NO	REVISION DESCRIPTION
4-8-70	1	GENERAL REVISION

BILL OF MATERIAL

ITEM	DWG. NO.	DESCRIPTION	QUAN	MAT'L
1	NDC 1730D	TOP END CAP	1	316 SST.
2	NDC 1730D	TUBE .250 ± .001 OD × .218 ± .001 I.D. × 57 3/8 LONG	1	316 SST.
3	NDC 1730D	TUBE .187 ± .002 OD × .014 ± .001 WALL 10.430 LONG	1	316 SST.
4	NDC 1730D	PLUG	1	316 SST.
5	NDC 1730D	SPRING	1	AS NOTED
6	NDC 1730D	ROD .212 ± .001 DIA. × 2 7/32 LG	1	NICKEL
7	NDC 1730D	PAD 7/32 DIA. × 1/16 THICK	2	FIBERFRAX
8	NDC 1730D	INSULATOR PELLET 'X' DIA × 1/4 LG.	4	DEPLETED UO_2
9	NDC 1730D	SPHERE-PAC, VIPAC OR PELLET FUEL	AS REQ'D	$(U_{.35}-20\%PU)O_2$
10	NDC 1730D	BLANKET PELLETS 'X' DIA × 1/4 LG.	AS REQ'D	DEPLETED UO_2
11	NDC 1730D	WIRE .040 DIA. (TO BE INSTALLED BY ANL)	AS REQ'D	316 SST.
12	NDC 1730D	BOTTOM END CAP	1	316 SST.

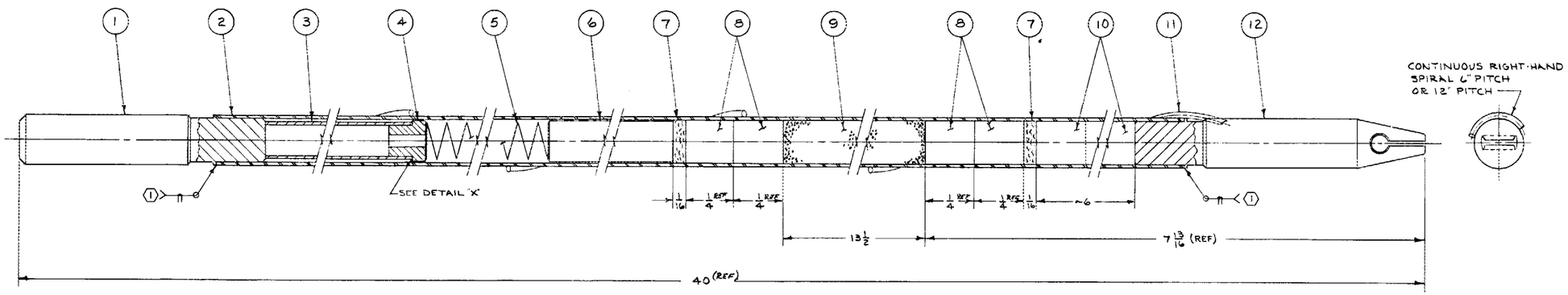

WELDING NOTE

(1) FULL PENETRATION FUSSION WELD REQUIRED (1-T WITH 1 1/4 T LAND)

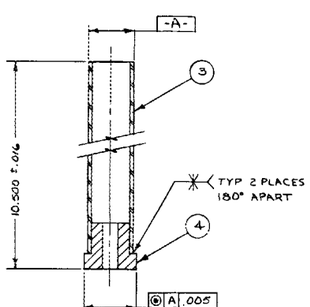

('X') PLENUM SLEEVE ASSEMBLY

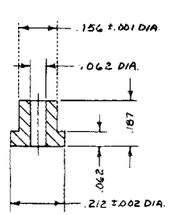

(4) PLUG

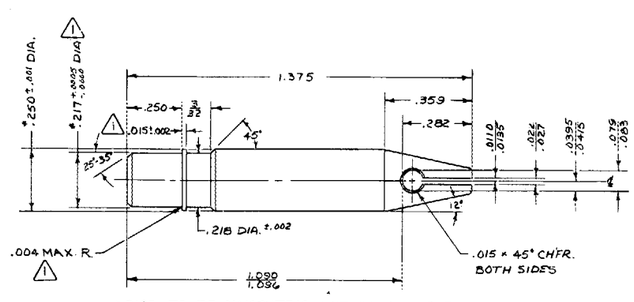

* DIAS. TO BE CONCENTRIC WITHIN .002 T.I.R.

(11) BOTTOM END CAP

Fig. 2. Babcock & Wilcox Pin Design.

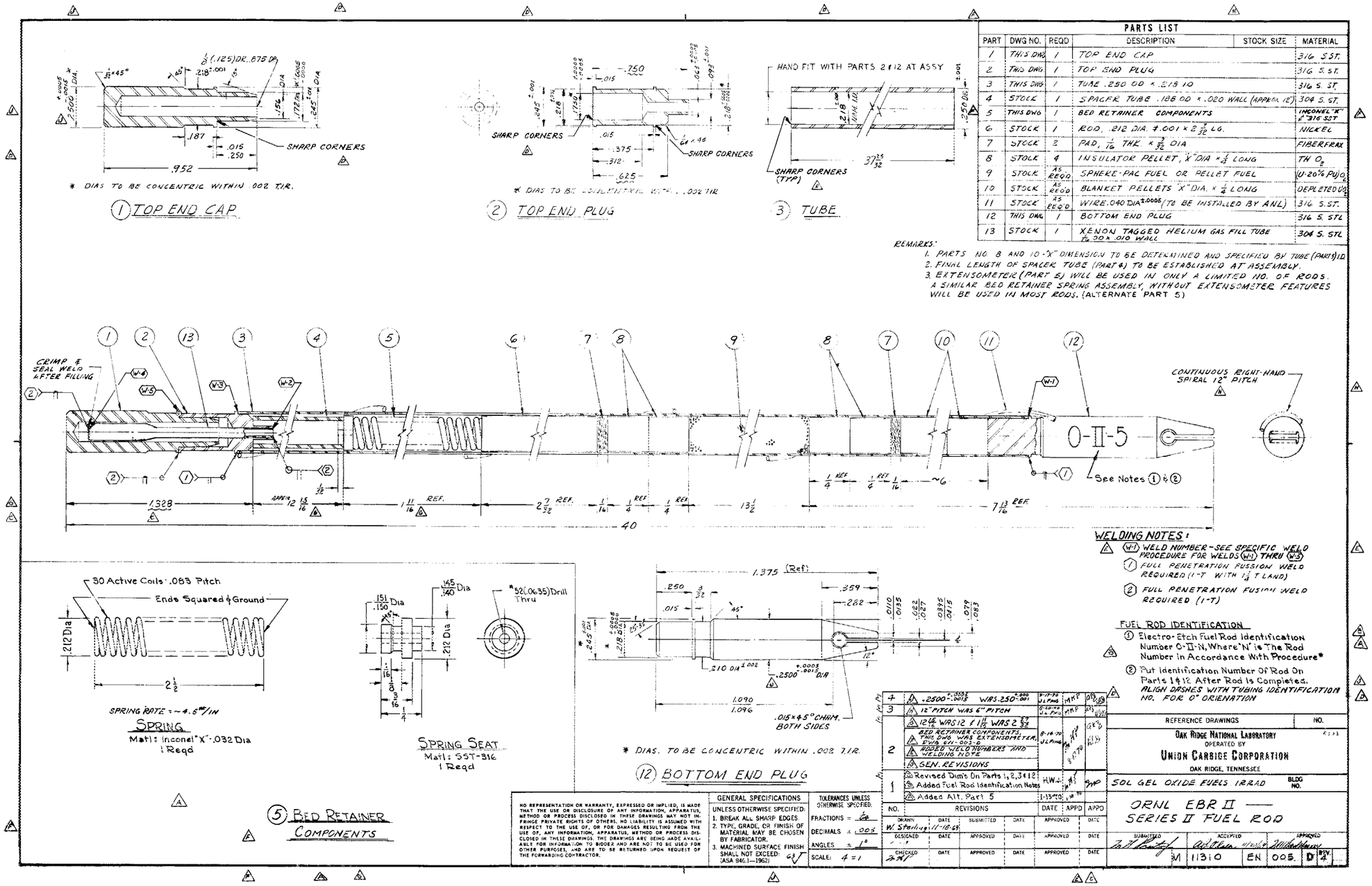

Fig. 3. ORNL Pin Design.

used at each site. However, these detailed design differences do not change the principal pin features so that a common performance analysis can be used.

A general pin description is presented in Table 4. The as-fabricated information on each pin is detailed in the appropriate sponsor fabrication sections.

The only material in these pins which is unusual is the Fiberfrax pads located at each end of a fuel bed. Fiberfrax is a glass wool-like material made of alumina-silica fibers and manufactured by the Carborundum Company. The fibers have a mean diameter of 2.5 μm and range in length from very short up to a maximum of 1.5 in. The analysis of this material is given in Table 4. This material has been used in a variety of irradiation tests at ORNL as porous restraining pads for Sphere-Pac beds. It was used in the ORNL Series I tests[20] and has also been used as a low density filler for the gas plenum in a number of thermal flux reactor tests.[21,22] Although we have not run specific sodium compatibility tests on this material, similar material has been tested by others. A data search by the Liquid Metal Engineering Center[23] revealed two investigations of interest. The Mine Safety Appliance Company immersed samples of Fiberfrax in 500°F sodium under an inert atmosphere for 10-min and 1-hr periods.[24] "There was no apparent reaction with the sodium other than a slight charring at the outer surface of the insulation." The Chemical Engineering Division at Argonne National Laboratory reported[25] on experimentation with a fume trap which consisted of a crucible of molded Fiberfrax. The fume traps worked on the principle of absorption and chemical reaction with the trap surface, and the effectiveness of the trap was apparently unaffected by operation, with sodium on the trap, at furnace temperatures up to 1400°C.

We have had three cases of in-reactor cladding failures when NaK-44 was subsequently in contact with the Fiberfrax material under irradiation. In the high-temperature regions involving molten $(U,Pu)O_2$ fuel and sodium, the material lost its fibrous nature, forming small blackened beads. This reaction is expected since the material will bead up when exposed for extended periods to temperatures above 2300°F (1250°C) and

Table 4. Nominal Test Pin Description

Fuel:		
Material	$(U,Pu)O_2$	
$Pu/(U + Pu)$	0.20 ± 0.01	
$^{235}U/U$	0.93	
$(^{239}Pu + {}^{241}Pu)/Pu$	0.90	
Fuel bed length	13.5 in.	
Theoretical density	10.90 g/cm^3 at 1.98 oxygen-to-metal ratio	
Bed smear density	Variable (80 to 90% of theoretical)	
Cladding:		
Material	Type 316 stainless steel (solution treated)	
Outer diameter	0.250 ± 0.001 in.	
Inner diameter	0.218 ± 0.001 in.	
Wall thickness	$0.015 {}^{+0.0015}_{-0.0010}$ in.	
Insulator Pellets:	ORNL	B & W
Material	ThO_2	$^{238}UO_2$
Length	1 in.	1 in.
Blanket Pellets:		
Material	$^{238}UO_2$	
Length (of stack)	~ 6 in.	
Shield Rod:		
Material	Nickel	
Length	2 7/32 in.	
Diameter	0.212 in.	
Bed Retainers:	ORNL	B & W
Material		
Plug	Type 316 stainless steel	None
Spring	Inconel X	Type 302 stainless steel

Table 4. continued

	ORNL	B & W
Plenum Liner:		
Material	Type 304 stainless steel	Type 316 stainless steel
Outer diameter	0.188 in.	0.187 in.
Wall thickness	0.020 in.	0.014 in.
Pads:		
Material	"Fiberfrax" Al_2O_3-SiO_2	
	Al_2O_3 50 ± 5% SiO_2 50 ± 5% Other oxides < 3%	

below the melting point of approximately 3200°F (1760°C). However, the fibrous mat was only darkened in color approximately 1/16 in. away from the fuel-Fiberfrax interface.

These experimental observations clearly indicate that in the unlikely event of a fuel pin failure the Fiberfrax material will remain in the cladding. The observations of the Argonne National Laboratory group further indicate that there would be no significant contamination of the reactor coolant sodium even though there was direct exposure.

Thermal Performance of Fuel Pins

In order to proceed with the design of the test subassembly and safety analysis of these test pins prior to the availability of final as-fabricated data, we used a single fuel composition and nominal smear densities for individual pins to do the performance analysis. This approach was approved by the EBR-II Project Experiment Manager.[26]

Peak fission heat generation rates were calculated for each of the four assumed fuel densities using the fission rates listed for grid positions 6-N3 and 6-N4 in Table C-1 of the Guide. The listed fission rates were multiplied by 1.25 to account for the change in EBR-II operating power from 50 MW to 62.5 MW. A value of 192 MeV/fission was used; so no gamma heating in the fuel was considered. The axial distribution of fission heat generation was in accordance with Fig. C1 of the Guide.

The curves given in Fig. C-3 were extrapolated to give an estimate of the fission rates for the $^{238}UO_2$ in the lower end of the pins.

The gamma heat generation in nonfuel components was derived from Fig. C-4 of the Guide with an axial distribution in accordance with Fig. C-5 of the Guide.

Peak axial fission heat generation rates for fuels of different smear densities as a function of test pin location in the subassembly are shown in Fig. 4. The gamma heating in the nonfuel components for the various pin locations was held constant at the value for the center line of the subassembly derived from Fig. C-4 of the Guide (2.4 W/g for iron and 6.5 W/g for uranium).

The coolant flow distribution in the experimental subassembly used was the same as the distribution for an H-37 subassembly[27] published in Table D-II of the Guide. No mixing between channels was assumed in making the temperature analysis for each pin.

We used the same computer codes used previously for the ORNL Series I test analysis[20] to do the heat transfer and temperature distribution analysis. The computer program[28] "MAMU" was used to calculate the coolant temperatures and the temperature distribution from the coolant to the fuel surface. The fuel temperatures were calculated with PRØFIL.[29] Iterative calculations were performed to establish the desired coolant flow (45 gpm of 800°F sodium).

The following thermal conductivity values were used in the computer programs. Types 304 and 316 stainless steel:

$$k = 8.49 + 4.3 \times 10^{-3} t \text{ Btu hr}^{-1} \text{ ft}^{-1} \text{ °F}^{-1} .$$

Sodium:

$$k = 51.3 - 0.0135t \text{ Btu hr}^{-1} \text{ ft}^{-1} \text{ °F}^{-1} .$$

Fuel: Determined from empirical formula included in the PRØFIL code and originally proposed by General Electric.[30] Our experience with thermal flux irradiation tests has shown that this formulation provides a reasonable fit with experimental integral conductivities. All fuel center temperatures are quoted for restructured fuel.

ORNL-DWG 70-13098

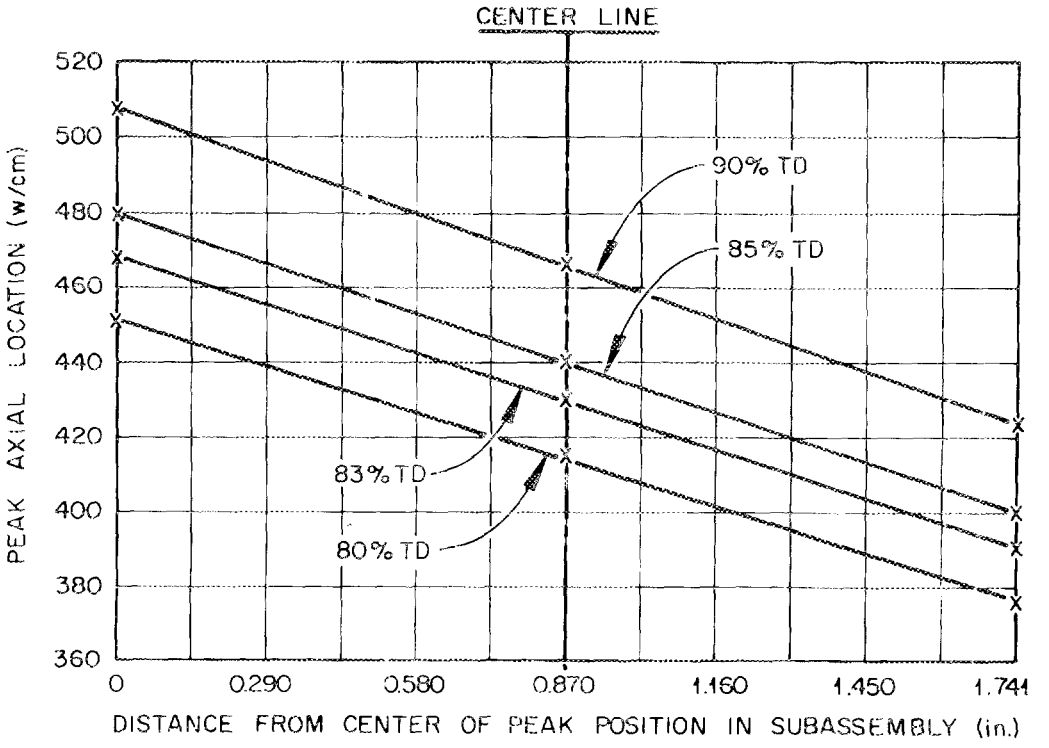

SUBASSEMBLY POSITION												
1	5	6	4	12	9	19	15	26	22	32	33	37
–	2	3	7	8	13	14	20	21	27	28	36	–
–	–	10	11	17	18	24	25	30	31	35	–	–
–	–	–	16	–	23	–	29	–	34	–	–	–

Fig. 4. Peak Axial Fission Heat Rate as a Function of Radial Location for EBR-II Subassembly Positions 6-N3 and 6-N4.

Fuel-Cladding Gap: 1800 Btu hr^{-1} ft^{-2} $°F^{-1}$. Although this gap conductivity may be too low for Sphere-Pac fuels, where the effective geometrical gap is less than 0.001 in., we have used it to provide a conservative estimate of the central fuel temperatures.

These calculations resulted in the individual pin thermal performance data given in Table 5. Example calculations are presented in Appendix A. In addition to the peak values, we have examined the axial temperature profiles for selected pins to cover the full range of maximum to minimum heat ratings and the three different coolant flow rates. These analyses are presented graphically in Figs. 5, 6, 7, 8, and 9.

Uncertainty analyses were made for the axial midplane locations on the two highest heat rate pins. Certain of the factors such as the

Table 5. Fuel Pin Thermal Performance Predictions

Subassembly Location	Fuel Smear Density[a] (% of theoretical)	Peak Linear Heat Rate (kW/ft)	Total Heat Generation[b] (kW)	Peak Fuel Center Line Temperature (°C)	Peak Fuel Surface Temperature (°C)	Peak Cladding Inner Surface Temperature (°C)	Peak Cladding Outer Surface Temperature (°C)	Peak Local Coolant Temperature (°F)	(°C)
1	80	13.76	14.45	2210	767	552	518	936	502
2	80	13.58	14.26	2190	767	558	525	951	511
3	80	13.40	14.07	2180	761	556	523	948	509
4	85	14.04	14.73	2300	775	556	521	941	505
5	80	13.58	14.26	2190	767	558	525	951	511
6	80	13.40	14.07	2210	829	643	614	1114	601
7	83	13.70	14.38	2270	839	650	617	1123	606
8	83	13.51	14.18	2250	832	645	614	1117	603
9	85	13.64	14.32	2260	768	559	526	952	511
10	80	13.40	14.07	2180	837	648	616	1121	605
11	83	13.70	14.38	2270	839	650	617	1123	606
12	83	13.51	14.18	2250	832	645	614	1117	603
13	85	13.64	14.32	2290	837	648	616	1121	605
14	85	13.44	14.11	2270	830	644	613	1115	602
15	83	12.92	13.59	2160	748	549	518	939	504
16	83	13.70	14.39	2240	765	551	518	935	502
17	83	13.51	14.18	2250	832	645	614	1117	603
18	85	13.64	14.32	2290	837	648	616	1121	605
19	85	13.62	14.11	2270	830	644	613	1115	602
20	83	12.92	13.58	2190	813	633	603	1099	593
21	83	12.72	13.37	2160	806	629	600	1093	589
22	85	12.82	13.49	2160	740	540	508	920	493
23	85	13.64	14.32	2260	768	559	526	952	511
24	83	13.12	13.79	2210	820	637	607	1106	597
25	83	12.92	13.58	2190	813	633	603	1099	593
26	83	12.72	13.37	2160	806	629	600	1093	589
27	85	12.82	13.48	2190	809	632	602	1096	591
28	83	12.30	12.96	2090	730	541	511	928	498
29	83	12.92	13.59	2160	748	549	518	939	504
30	83	12.72	13.37	2160	806	629	600	1093	589
31	85	12.82	13.48	2190	809	632	602	1096	591
32	83	12.30	12.95	2120	792	621	593	1081	583
33	90	13.12	13.80	2230	753	552	520	943	506
34	85	12.82	13.49	2160	740	540	508	920	493
35	83	12.30	12.96	2090	730	541	511	928	498
36	90	13.12	13.80	2230	753	552	520	943	506
37	83	11.90	12.55	2020	714	528	499	905	485

[a]These are nominal design densities used in all thermal performance analyses.

[b]Including gamma heating in sodium coolant associated with each pin.

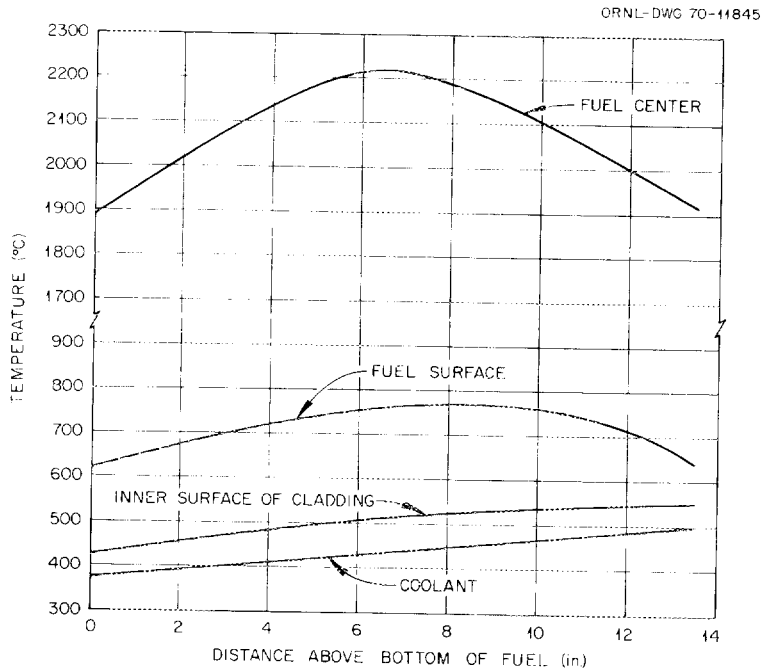

Fig. 5. Partial Temperature Distribution for Pin in Subassembly Position 1.

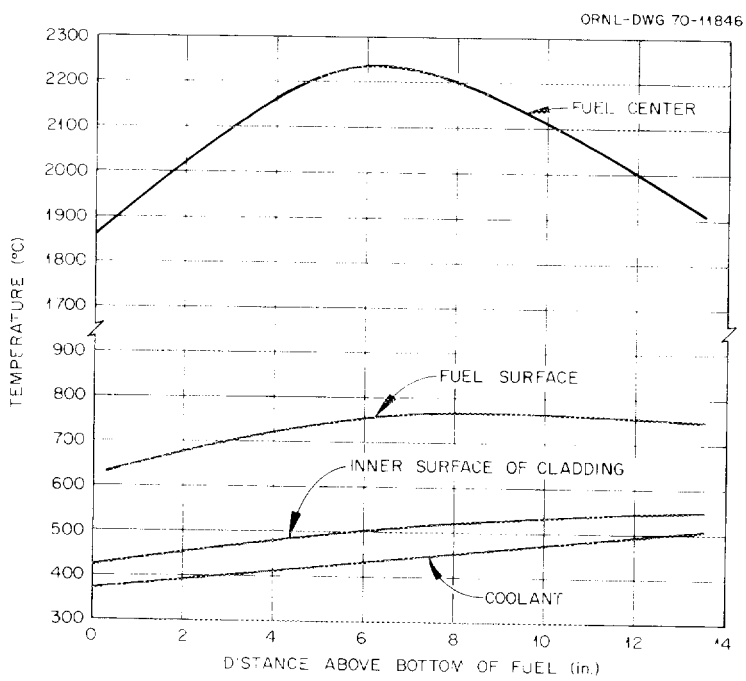

Fig. 6. Partial Temperature Distribution for Pin in Subassembly Position 2.

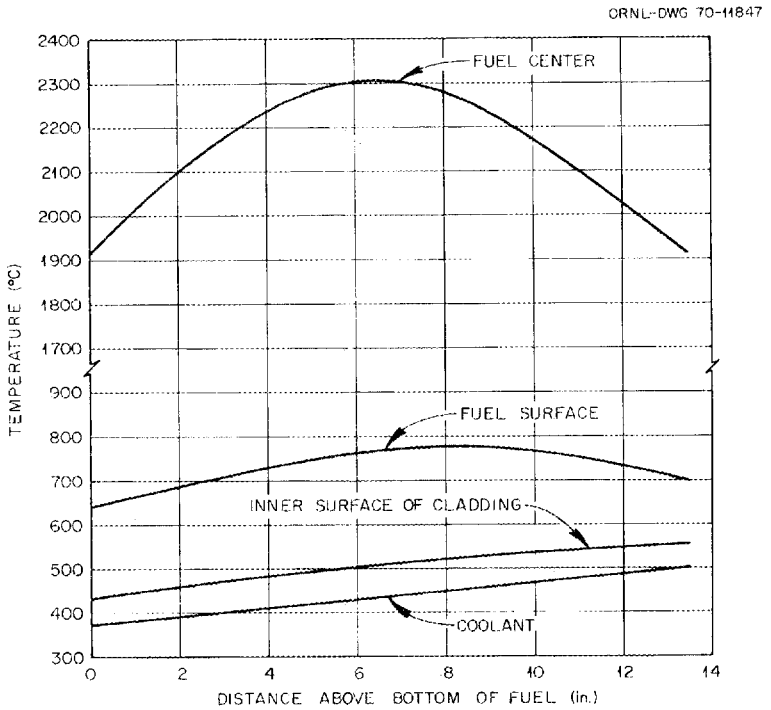

Fig. 7. Partial Temperature Distribution for Pin in Subassembly Position 4.

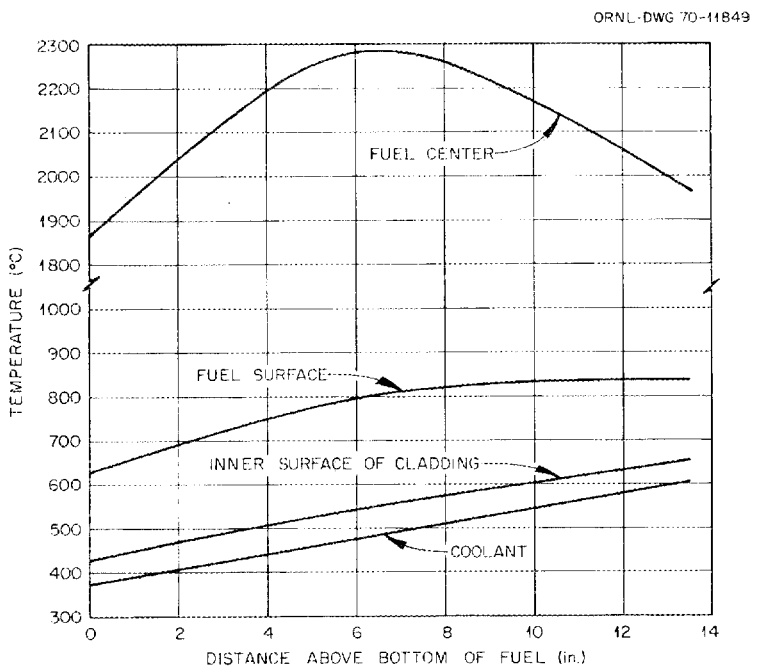

Fig. 8. Partial Temperature Distribution for Pin in Subassembly Position 7.

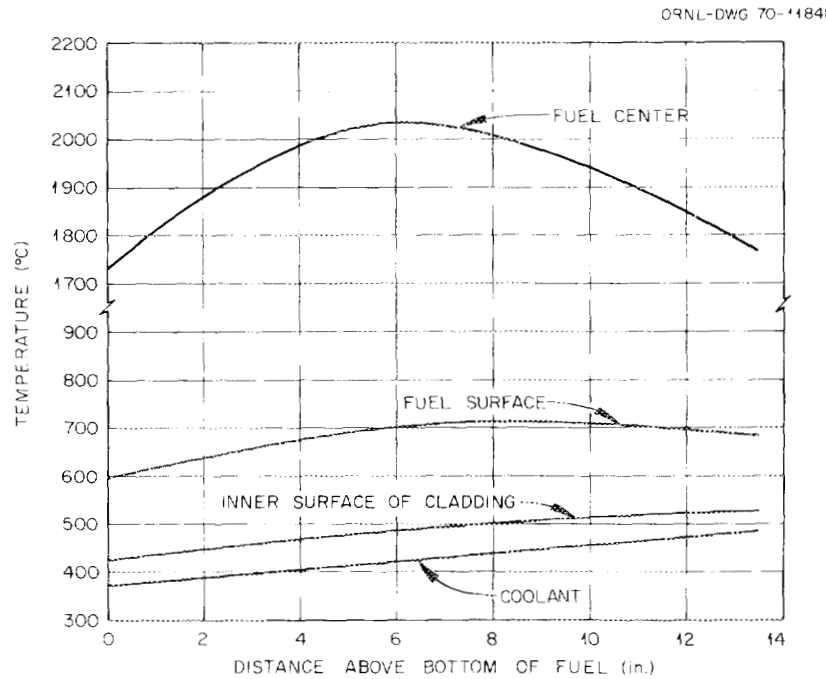

Fig. 9. Partial Temperature Distribution for Pin in Subassembly Position 37.

uncertainty in neutron and gamma flux, the subassembly flow rate, subassembly flow distribution, the power level measurement, and the transient overload are reactor parameters; and therefore, we have no justification for altering these from the information presented[31] in ANL-5719. We performed a statistical analysis of our data on cladding thickness, fuel dimensions, and fuel composition which yielded uncertainty factors of 1.050, 1.003, and 1.008, respectively. We chose the larger and more conservative uncertainty factors from ANL-5719 to cover possible variations in the fabrication of the replacement pins, thus hopefully avoiding the necessity of repeating these calculations. The results are given in Tables 6 and 7. These analyses indicate that all uncertainty factors, including a 10% increase in the fission rate, would yield a 3% maximum increase in cladding inner surface temperature and a maximum fuel center line temperature of 2630°C, which is below the melting point of the $(U,Pu)O_2$ fuel. Since the anticipated fission rate per the note on the bottom of Table C-I of the Guide is probably a −5% instead of the +10% which we used, no more detailed uncertainty analyses were made.

Table 6. Uncertainty Calculations for Axial Midplane of Fuel for Subassembly Position 7[a]

Thermophysical Quantity	$\theta_{coolant}$ = 204.2			θ_{film} = 34.2				θ_{clad} = 80.3				$\theta_{fuel\ clad\ interface}$ = 453.8				θ_{fuel} = 2663.5			
	F	d_1	d_1^2	F	d_2	$\Sigma d_{1\to2}$	$(\Sigma d_{1\to2})^2$	F	d_3	$\Sigma d_{1\to3}$	$(\Sigma d_{1\to3})^2$	F	d_4	$\Sigma d_{1\to4}$	$(\Sigma d_{1\to4})^2$	F	d_5	$\Sigma d_{1\to5}$	$(\Sigma d_{1\to5})^2$
Neutron and gamma flux	1.07	14.29	204.32	1.10	3.42	17.71	313.64	1.10	8.03	25.74	662.55	1.10	45.38	71.12	5058.1	1.10	266.35	337.45	113,886.00
Flow rate through subassembly	1.05	10.21	104.24																
Flow profile within subassembly	1.05	10.21	1104.24																
Manufacturing Deviations from Nominal: Cladding Dimensions								1.05	4.01	4.01	16.12								
Manufacturing Deviations from Nominal: Fuel Dimensions				1.02	0.684	0.684	0.468	1.02	1.61	2.29	5.24	1.02	9.08	11.37	129.18	1.02	53.27	64.64	4,178.33
Manufacturing Deviations from Nominal: Fissile Material Concentration	1.01	2.04	4.17	1.01	0.342	2.38	5.67	1.01	0.80	3.18	10.11	1.01	4.54	7.72	59.57	1.01	26.64	34.36	1,180.27
Thermal Conductivity: Cladding								1.10	8.03	8.03	64.48								
Thermal Conductivity: Fuel-Cladding Interface												1.10	45.38	45.38	2059.34				
Thermal Conductivity: Fuel																1.15	399.53	399.53	159,620.2
Heat transfer coefficient				1.20	6.84	6.84	46.79												
Power level measurement	1.02	4.08	16.68	1.02	0.684	4.764	22.70	1.02	1.61	6.37	40.58	1.02	9.08	15.45	238.58	1.02	53.27	68.72	4,722.44
Transient overload	1.05	10.21	104.24	1.05	1.71	11.92	142.09	1.05	4.01	15.94	253.92	1.05	22.69	38.63	1492.28	1.05	133.18	171.81	29,516.96
$\Sigma(\Sigma d_i)^2$			537.90				531.35				1053.01				9037.01				313,104.22
$[\Sigma(\Sigma d_i)^2]^{1/2}$			23.19				23.05				32.45				95.06				559.56
Without uncertainty	Tc = 904.2°F (484.5°C)			TO = 938.4°F (503.6°C)				T1 = 1018.7°F (548.2°C)				T2 = 1472.5°F (800.3°C)				$T_{\mathcal{L}}$ = 4136.0°F (2280.0°C)			
With uncertainty	Tc = 927.4°F (497.4°C)			TO = 961.5°F (516.4°C)				T1 = 1051.2°F (566.2°C)				T2 = 1567.6°F (853.1°C)				$T_{\mathcal{L}}$ = 4695.6°F (2590.9°C)			

[a] F is uncertainty factor; d_i is the temperature deviation in °F.

Tc is coolant temperature

TO is clad outer surface temperature

T1 is clad inner surface temperature

T2 is fuel outer surface temperature

θ is temperature variation across region at normal condition

$T_{\mathcal{L}}$ is fuel center temperature.

Table 7. Uncertainty Calculations for Axial Midplane of Fuel for Subassembly Position 4[a]

Thermophysical Quantity	$\theta_{coolant}$ = 116			θ_{film} = 44				θ_{clad} = 84.5				$\theta_{fuel\ clad\ interface}$ = 454.9				θ_{fuel} = 2775.1			
	F	d_1	d_1^2	F	d_2	$\Sigma d_{1\to2}$	$(\Sigma d_{1\to2})^2$	F	d_3	$\Sigma d_{1\to3}$	$(\Sigma d_{1\to3})^2$	F	d_4	$\Sigma d_{1\to4}$	$(\Sigma d_{1\to4})^2$	F	d_5	$\Sigma d_{1\to5}$	$(\Sigma d_{1\to5})^2$
Neutron and gamma flux	1.07	8.12	65.93	1.10	4.4	12.52	156.75	1.10	8.45	20.97	439.74	1.10	46.49	67.46	4550.85	1.10	277.5	344.97	119,004.3
Flow rate through subassembly	1.05	5.8	33.64																
Flow profile within subassembly	1.05	5.8	33.64																
Manufacturing Deviations from Nominal: Cladding Dimensions								1.05	4.23	4.23	17.85								
Manufacturing Deviations from Nominal: Fuel Dimensions				1.02	0.88	0.88	0.77	1.02	1.69	2.57	6.60	1.02	9.30	11.87	140.85	1.02	55.50	69.37	4,538.99
Manufacturing Deviations from Nominal: Fissile Material Concentration	1.01	1.16	1.35	1.01	0.44	1.6	2.56	1.01	0.85	2.45	5.98	1.01	4.65	7.60	50.40	1.01	27.75	35.35	1,249.69
Thermal Conductivity: Cladding								1.10	8.45	8.45	71.40								
Thermal Conductivity: Fuel-Cladding Interface												1.10	46.49	46.49	2161.3				
Thermal Conductivity: Fuel																1.15	416.27	416.27	173,276.55
Heat transfer coefficient				1.20	8.8	8.8	77.44												
Power level measurement	1.02	2.32	5.38	1.02	0.88	3.2	10.24	1.02	1.69	4.89	23.91	1.02	9.30	14.19	201.30	1.02	55.50	69.69	4,856.97
Transient overload	1.05	5.8	33.64	1.05	2.2	8.0	64.0	1.05	4.23	12.23	149.45	1.05	23.25	35.48	1258.48	1.05	138.76	174.24	30,357.84
$\Sigma(\Sigma d_i)^2$			173.58				311.76				714.93				8312.78				333,284.34
$[\Sigma(\Sigma d_i)^2]^{1/2}$			13.17				17.66				26.74				91.17				577.31
Without uncertainty	Tc = 816.1°F (435.6°C)			TO = 860.1°F (460.0°C)				T1 = 944.6°F (507.0°C)				T2 = 1409.5°F (765.3°C)				$T_{\mathcal{L}}$ = 4184.6°F (2307.0°C)			
With uncertainty	Tc = 829.3°F (442.9°C)			TO = 877.8°F (469.9°C)				T1 = 971.3°F (521.8°C)				T2 = 1500.7°F (815.9°C)				$T_{\mathcal{L}}$ = 4761.9°F (2627.7°C)			

[a] F is uncertainty factor; d_i is the temperature deviation in °F.

Tc is coolant temperature

TO is clad outer surface temperature

T1 is clad inner surface temperature

T2 is fuel outer surface temperature

θ is temperature variation across region at normal condition.

$T_{\mathcal{L}}$ is fuel center temperature.

Thermal Performance of Subassembly

The thermal analysis of the subassembly was done with the same "MAMU" code[28] as used for the individual pins.

The assumptions on which the analysis was based are:

1. For a J-37-A subassembly a total flow of 62 gpm of 800°F sodium is acceptable and within the orifice adjustment capabilities for such a subassembly in row 6 of the EBR-II.[32]

2. For an N-37 or an E-37-B, the total subassembly flow can be equivalent to that for a J-37-A.

3. We assumed there was no radial heat transfer to or from adjacent subassemblies.[33] Thus, all heat generated within the subassembly must be removed by the sodium passing through the subassembly.

4. As indicated in the section on fuel pin performance, the flow distribution used in the fuel pin area was the distribution for an H-37 subassembly. Since the MAMU code is based on a pure radial heat transfer mechanism, we subdivided the individual flow channels to obtain an equivalent cylindrical flow area. This procedure resulted in three flow areas, depending on the pin locations in the center, along the edge, or at the corner of the inner hexagonal can of the subassembly. The relative coolant flow for each pin in the array was derived from a similar geometric analysis and the relative flow for each of the channels, as described in Appendix D of the Guide. These calculations are summarized in Table 8.

A mean sodium temperature of 800°F (427°C) was used to convert the sodium flow rate to pounds per hour. Iterative calculations were then made to establish the desired flow. The cladding inner surface temperature for the highest heat rate pin in an inner location was limited to 650°C. No interchannel mixing was assumed; so the calculated flow rate may be slightly too high. With the flow rate for this pin established, the flow rate for all the pins was defined by proportioning.

5. The MAMU code was also used to calculate the total gamma heating in the subassembly components. In the case of a J-37-A subassembly, this heat was transferred to the bypass sodium coolant. The subassembly component gamma heating for the N-37 subassembly was transferred to the pin coolant sodium.

Table 8. Flow Distribution Inside Inner Hexagonal Can

Pin Location	Flow Area (in.^{2})	Relative Flow	Number of Pins	Percent of Total Flow	
				Each	Total
Center	0.02249	1.00	19	2.014	38.27
Edge	0.03329	1.66	12	3.343	40.12
Corner	0.02945	1.79	6	3.602	21.61

With these assumptions, we were able to establish the subassembly thermal performance data reported in Table 9 for each of the subassembly types. Details of the subassembly thermal performance by pin locations are included in Table 10.

Table 9. Subassembly Thermal Performance

Characteristics	Subassembly Type	
	N-37	J-37-A
Coolant Flow Rate:		
Inner hex can, lb/hr of 800°F Na	19,083	19,083
Bypass, lb/hr of 800°F Na		6,665
TOTAL, lb/hr of 800°F Na	19,083	25,748
TOTAL, gpm at 800°F	45.02	60.74
Total Heat Generated:		
Pins and sodium, Btu/hr	1,748,400	1,748,400
Subassembly hardware,[a] Btu/hr	64,000	74,300
TOTAL, Btu/hr	1,812,400	1,822,700
Temperature Rise in Coolant:		
Inner hex can, °F	313.4	302.4
Bypass, °F		36.8
Mixed Mean Outlet Temperature:		
°F	1,013.0	934.0
°C	545.0	501.0

[a]Including bypass sodium for J-37-A subassembly.

Table 10. Fuel Pin Thermal Analysis Start of Life

Pin Position	Coolant Flow Rate (lb/hr)	Total Heat Production (Btu/hr)	Maximum Cladding Wall Temperature (°F)	(°C)	Coolant Outlet Temperature (°F)	(°C)
1	687	49,312	1,026	552	936	502
2	638	48,668	1,037	558	951	511
3	638	48,032	1,032	556	948	509
4	687	50,267	1,032	556	941	505
5	638	48,668	1,037	558	951	510
6	384	48,009	1,189	643	1,114	601
7	384	49,069	1,200	649	1,123	606
8	384	48,401	1,193	645	1,117	603
9	638	48,880	1,038	559	952	511
10	638	48,032	1,198	648	948	509
11	384	49,069	1,200	649	1,123	606
12	384	48,401	1,193	645	1,117	603
13	384	48,856	1,198	648	1,121	605
14	384	48,168	1,191	644	1,115	602
15	638	46,368	1,021	549	939	504
16	687	49,100	1,024	551	935	502
17	384	48,401	1,193	645	1,117	603
18	384	48,856	1,198	648	1,121	605
19	384	48,168	1,191	644	1,115	602
20	384	46,344	1,172	633	1,099	593
21	384	45,644	1,165	629	1,093	589
22	687	46,037	1,004	540	920	493
23	638	48,880	1,038	559	952	511
24	384	47,065	1,179	637	1,106	597
25	384	46,344	1,172	633	1,099	593
26	384	45,644	1,165	629	1,093	589
27	384	46,005	1,169	632	1,096	591
28	638	44,226	1,006	541	928	498
29	638	46,368	1,021	549	939	504
30	384	45,644	1,165	629	1,093	589
31	384	46,005	1,169	632	1,096	591
32	384	44,202	1,150	621	1,081	583
33	638	47,089	1,026	552	943	506
34	687	46,037	1,004	540	920	493
35	638	44,226	1,006	541	928	498
36	638	47,089	1,026	552	943	506
37	687	42,825	983	528	905	485
TOTAL	19,083	1,748,399				

Fuel Pin Stress and Strain Analysis

The fuel pin cladding stress is the net result of a variety of conditions. A stress component can result from mechanical interaction between the fuel and the cladding, initially as a result of differential thermal expansion and at high enough burnup levels as a result of fuel swelling. The principal sources of stress during most of the fuel pin life are the net result of the radial temperature gradient in the cladding and the internal pressure from sorbed gases, moisture, fill gas, and fission-product gases. Finally, a stress component may result from radial differences in cladding volume changes because of fast neutron damage in the temperature gradients across the cladding. In evaluating the performance of these pins we made two analyses.

The preliminary analysis was a simplified analysis in which we assumed the as-fabricated fuel porosity plus cladding volume changes during irradiation would provide space to accommodate all fuel swelling; so no fuel-cladding mechanical interaction would occur after the initial startup. In this analysis we also assumed a constant fission rate during the life of the experiment which results in an overestimation of the fission-gas production. Further, our observations to date on Sphere-Pac fuel irradiation tests have indicated negligible fuel-cladding chemical interaction at temperatures up to 590°C and burnup levels up to 5% FIMA.[21,22] Therefore, we made no allowance for fuel-cladding chemical interaction. The results of this analysis, which were used in the subsequent subassembly thermal performance analysis, are given in Appendix A.

A revised analysis was made at the request of the EBR-II Project following the review of our preliminary data package. This revised analysis includes the amount of fuel-cladding chemical interactions specified in Revision 4 of the Guide, fuel swelling to affect fuel-cladding mechanical interaction, and flux enhanced creep of the stainless steel cladding. This revised analysis is discussed in the subsequent sections.

Fuel-Cladding Mechanical Interaction

The stress which might derive from mechanical interaction between the fuel and the cladding has been examined in two ways:

1. The FMØDEL code[34] was used to examine the start-of-life interaction as a result of differential thermal expansion. To make this analysis we chose the pin in position 7 of the array. This is a Sphere-Pac pin; the fuel-to-cladding gap is zero, which is the worst condition for this analysis. Since the initial startup rate of the reactor is unknown, we chose to bring the pin to a full operating power peak of 14 kW/ft in four steps of 25% each, holding the power at each level for 24 hr before stepping to the next level. In addition, we assumed restructuring to occur as a function of temperature to 98% of theoretical for fuel above 1800°C, to 92% of theoretical for fuel between 1450 and 1800°C with no change in density for fuel at temperatures below 1450°C. Further restructuring as a function of time at temperature was allowed in accordance with the "hot-pressing" densification rates built into the code.

The maximum density allowed by this process is 98% of theoretical; this was further restricted so that fuel between 1450 and 1850°C could not have less than 6% porosity, or fuel at temperatures less than 1450°C could not have less than 10% porosity.

The cladding mechanical property data used in these calculations are from a recent compilation.[35] Table 11 summarizes those properties pertinent to this evaluation. The thermal and flux enhanced creep formulas used in the FMØDEL code are presented in Appendix A.

The results of these calculations are shown graphically in Fig. 10. From these calculations it is apparent that any mechanical interaction stress between the fuel and cladding as a result of differential thermal expansion is gone after approximately 8 days (5 days at the full power level).

2. The effects of fuel swelling on fuel-cladding mechanical interaction were calculated with the FMØDEL code. To define fuel swelling it is necessary to input additional parameters. These parameters are:

(a) Solid fission product swelling, 0.32% $\Delta V/V$ per % FIMA,

Table 11. Cladding Mechanical Property Data[a]

Temperature (°C)	Elastic Modulus (psi)	Shear Modulus (psi)	Temperature (°C)	Coefficient of Thermal Expansion (in./in.-°C)	Temperature (°C)	Yield Stress (psi)
	$\times 10^8$			$\times 10^{-4}$		
24	0.283	0.113×10^8	100	0.1602	427	23,180
149	0.272	0.108×10^8	300	0.1620	482	22,530
260	0.264	0.102×10^8	500	0.1746	538	21,810
371	0.256	0.960×10^7	600	0.1854	593	21,060
482	0.238	0.910×10^7	800	0.1998	649	20,300
593	0.225	0.850×10^7			704	19,000
704	0.210	0.800×10^7				
816	0.186	0.750×10^7				

[a]See Appendix A for creep formula and constants.

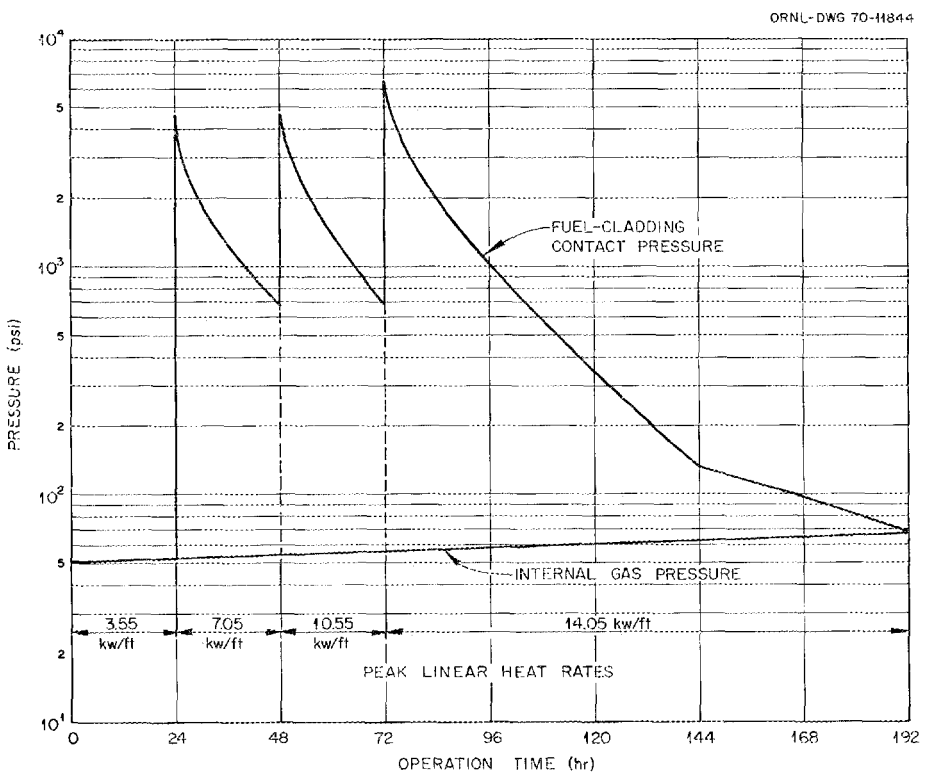

Fig. 10. Start-of-Life Fuel-Cladding Mechanical Interaction.

(b) Fission-gas release rates as a function of temperature in the fuel,

Temperature, °C	Gas Release, %
> 1800	98
< 1800 > 1450	50
< 1450	30

The fuel densification limits used for this analysis were the same as those described under the preceding Item 1. Since the final amount of fuel swelling is included in the total stress-strain analysis presented later, no separate tabulation of the results is presented here.

Thermal Gradient and Internal Gas Pressure

The thermal gradient across the cladding varies with power production and coolant temperatures along the length of each pin. This radial temperature gradient in the cladding is a primary source of stress. From our heat transfer analysis this temperature differential in the peak heat rate locations for the pins is 45 ± 1°C.

A second source of stress is that produced from gas pressure in the pin. This pressure is the result of expansion of the sorbed gases, moisture, helium and xenon tag gas sealed in the pin, plus the gradual accumulation of fission-product gases, and is affected by the burnup rate, the total burnup, plenum volume, and the plenum temperature. To obtain the values of internal gas pressure for each of the pins, we have made the following conservative assumptions:

1. For the revised stress analysis we took into account the effects of fissile element depletion with its effect on decreasing the rate of fission-product gas production.

2. One hundred percent of the fission-product gases are released.

3. We assumed that there was no available volume in the fuel, leaving only the plenum volume to accommodate the gas.

4. For the revised analysis we calculated the initial gas content by adding the amount of sorbed gases, including moisture, to the measured volume of helium and xenon added to each pin. This gas content contribution was assumed to remain constant throughout the test. The plenum volume for each pin was derived from the fabrication data.

Using these assumptions and the gas plenum temperatures calculated by the MAMU code, we have obtained the beginning and end-of-life gas pressures for each of the pins. These are listed in Table 12, together with the gas pressures used in the preliminary analysis.

Sample calculations are presented in Appendix A, together with a table (A-5) showing the change in gas pressure as a function of burnup for the pin with the highest pressure throughout the entire planned irradiation period.

Cladding Damage Effects

The EBR-II Guide, on p. 7 of the Guide, requires the inclusion of a stainless steel sodium corrosion allowance in making stress analysis as well as an allowance for defects, fuel-cladding interaction, and fabrication tolerances. The FMØDEL code will not currently permit such gradual changes in wall thickness. Therefore, we simulated these conditions by reducing the wall thickness of the cladding at the start of irradiation and maintaining all other conditions constant. This approach is recognizably overly conservative. To obtain the reduced wall thickness, we used the following assumptions:

1. based on the recommended corrosion curve (p. 8 of the Guide) at our peak cladding outer surface temperature of 617°C, the corrosion rate is 0.45 mil/year. Thus, for 600 effective full power days of operating the wall reduction is:

$$0.45 \left(\frac{600}{365}\right) = 0.74 \text{ mil} = 0.00074 \text{ in.},$$

2. reduction of 0.001 in. for fabrication tolerance,
3. reduction of 0.001 in. for nondetected flaws, because tubing with defects in excess of a standard notch of 0.001 in. deep by 0.030 in. long was rejected and not used for cladding,
4. fuel-cladding chemical interaction — we used the recommended EBR-II reaction rate formula to obtain a maximum loss of wall thickness by calculating it for the highest inner surface temperature as follows:

$$\begin{aligned} \text{thickness loss in mils/\% FIMA} &= 0.00125\ [T(^\circ C) - 370] \\ &= 0.00125\ (649 - 370) \\ &= 0.349 \text{ mil/\% FIMA}\ . \end{aligned}$$

Table 12. Internal Gas Pressures in Each Pin at Operating Temperatures

Subassembly Location	Peak Linear Heat Rate (kW/ft)	Target Average Burnup (% FIMA)	Gas Plenum Temperature (°C)	Gas Plenum Temperature (°K)	Internal Gas Pressure, psi: Initial, Preliminary	Internal Gas Pressure, psi: Initial, Revised	Internal Gas Pressure, psi: Final, Preliminary	Internal Gas Pressure, psi: Final, Revised
1	13.76	[illegible]	504	777	53	93	950	740
2	13.58	11.3	512	785	54	88	1440	1150
3	13.40	5.3	510	783	54	93	640	600
4	14.04	10.9	505	778	53	84	1480	1130
5	13.58	11.3	512	785	54	94	1440	1040
6	13.40	11.1	603	876	60	75	1590	1200
7	13.70	10.9	607	880	60	104	1630	1300
8	13.51	7.3	604	877	60	60	1050	750
9	13.64	6.3	513	786	54	82	1450	1200
10	13.40	5.3	510	783	54	86	640	580
11	13.70	10.9	607	880	60	99	1630	1120
12	13.51	5.1	604	877	60	105	720	590
13	13.64	5.1	607	880	60	95	730	640
14	13.44	7.1	603	876	60	94	1040	850
15	12.92	7.0	506	779	53	88	890	670
16	13.70	10.9	504	777	53	92	1440	1140
17	13.51	7.3	604	877	60	99	1050	780
18	13.64	10.6	607	880	60	100	1620	1100
19	13.62	7.1	603	876	60	91	1060	860
20	12.92	7.0	595	868	59	60	990	710
21	12.72	4.8	591	864	59	77	670	590
22	12.82	4.8	495	768	53	66	600	500
23	13.64	10.6	513	786	54	85	1450	1100
24	13.12	10.5	598	871	60	60	1540	1040
25	12.92	7.0	595	868	59	104	990	760
26	12.72	4.8	591	864	59	98	670	540
27	12.82	4.8	593	866	59	93	670	590
28	12.30	9.9	499	772	53	60	1280	870
29	12.92	7.0	506	779	53	93	890	680
30	12.72	4.8	591	864	59	60	670	510
31	12.82	4.8	593	866	59	103	670	610
32	12.30	9.9	584	857	59	96	1420	970
33	13.12	4.6	508	781	53	77	620	580
34	12.82	4.7	495	768	53	81	770	570
35	12.30	9.9	499	772	53	92	1280	[illegible]
36	13.12	9.7	508	781	53	73	1380	1080
37	11.90	9.5	487	760	52	86	1220	860

The total loss in wall thickness for the pin in position 7 at an average burnup of 10.9% FIMA then calculates to 3.81 mils or 0.00381 in.

In order to retain the effects of fuel-cladding mechanical interaction during power changes and as fuel swelling occurs, we retained the initial cladding inner radius and reduced the 0.0165 in. average wall thickness to 0.00995 in. by decreasing the cladding outer diameter to 0.2379 in.

Revised Stress-Strain Analysis

The revised stress-strain analysis calculations were made with the FMØDEL code and, therefore, include the effects of fuel-cladding mechanical interaction, flux enhanced creep, and the effects of fast flux exposure on cladding density changes. The code also predicts fission-gas release as a function of fuel temperature and burnup. Since these predictions are generally in agreement with experimental results and less than 100%, we used a version in which the gas pressure in the plenum calculated for 100% release was input for discrete time intervals. The code uses a linear extrapolation of pressure for the time increments between these intervals. Simultaneously, the calculated gas release fractions for various fuel temperatures were retained in the section of the code calculating the fuel swelling.

The actual cyclic conditions used are listed in Table 13. The incremental times were altered from our preliminary calculations to save computer time. Cycles 1 and 6 were extended from instantaneous to 3 hr to more nearly represent the rate of bringing the EBR-II to power. The ends of cycles 4, 8, and 10 roughly approximate the irradiation increments proposed for this test series.

We evaluated three axial increments for the pin in subassembly position 7. The results of these analyses are presented in Table 14.

The results of these calculations are quite comparable with the preliminary analysis reported in Table A-8 in Appendix A. The preliminary analysis indicates a greater overall dimensional change for the peak heat rate and top of the fuel column, while the revised analysis shows a greater predicted dimensional change for the bottom of the pin.

Table 13. FMØDEL Incremental Conditions for Revised Analysis

Cycle	Interval Time (hr)	Reactor Power Level	Pin 7 Plenum Conditions		
			Temperature (°C)	Pressure, psi	
				Initial	Final
1	3	Zero to full	607	15	104
2	2400	Full	607	104	347
3	2400	Full	607	347	570
4	1200	Full	607	570	674
5	480	Zero	371	674	494
6	3	Zero to full	607	494	674
7	2400	Full	607	674	872
8	1200	Full	607	872	965
9	2400	Full	607	965	1140
10	2400	Full	607	1140	1301
11	1200	Full	25	1301	410

These differences are the result of the higher internal gas pressure effect at high cladding temperatures while irradiation creep of the cladding predominates at the cooler temperatures at the bottom of the pin.

Effect of Increased Diameter of Pins on Coolant Flow and Subassembly Thermal Analysis

The actual dimensional profile of each pin as a function of axial location will be a complex interrelation of cladding swelling and plastic deformation. Because of the uncertainties associated with both of these calculations and the varied history of the different pins in the subassembly at the end of life, we chose to make a very conservative assumption for the calculation of end-of-life coolant flow and temperatures. We have assumed a uniform 100% of the maximum calculated diameter change without any corrosion allowance along the full length of each pin. In addition, we have reduced the fission heat rate by only 10% although the reduction in fissile inventory will be in excess of 13%.

Table 14. Pin 7 — Stress-Strain Deformation Analysis with Allowances for Fabrication and Corrosion Effects

Cycle Number	Axial Location	Start of Cycle	End of Cycle		Inner Surface		Outer Surface[b]	End of Life		
		Linear Heat Rate (kW/ft)	Burnup (% FIMA)	Fuel Swelling (% ΔV/V)	Stress[a] (psi)	Radius (cm)	Stress (psi)	Cladding Swelling (% ΔV/V)	Change in Diameter (%)	Plastic Strain[c] (%)
1	Bottom of fuel	11.1	0.0	0.0	29,190[d]	0.2806	48,900[d]			
2		11.1	2.0	0.03	−9,054	0.2806	14,930			
3		10.8	3.9	0.20	−9,789	0.2811	20,564			
4		10.5	4.84	0.33	−11,380	0.2814	21,330			
5		0.0	4.84	0.33	−770	0.2811	10,090			
6		0.0	4.84	0.33	−14,170	0.2814	23,160			
7		10.4	6.69	0.69	−19,700	0.2823	34,140			
8		10.2	7.59	0.94	−15,670	0.2828	24,130			
9		10.1	9.39	1.53	−18,070	0.2839	31,370			
10		9.9	11.14	2.58	−18,050	0.2852	34,120			
11		0.0	11.14	2.58	−12,940	0.2831	24,520	1.38	2.18	0.003
1	Peak heat rate	13.8	0.0	0.0	1,990[d]	0.2791	21,620[d]			
2		13.8	2.37	0.37	−7,220	0.2801	13,330			
3		13.5	4.66	0.83	−1,350	0.2813	11,810			
4		13.2	5.77	1.14	1,960	0.2819	10,930			
5		0.0	5.77	1.14	16,620	0.2809	−3,060			
6		0.0	5.77	1.15	810	0.2814	13,220			
7		13.0	7.99	1.83	4,830	0.2834	14,520			
8		12.7	9.06	2.24	8,810	0.2844	13,150			
9		12.6	11.21	3.47	15,870	0.2865	11,290			
10		12.4	13.30	4.78	20,350	0.2889	10,070			
11		0.0	13.30	4.78	27,900	0.2862	12,000	3.22	3.24	0.0008
1	Top of fuel	10.4	0.0	0.0	72,260[d]	0.2798	81,460[d]			
2		10.4	1.84	0.05	−4,350	0.2805	9,940			
3		10.2	3.60	0.25	2,370	0.2815	7,540			
4		9.9	4.46	0.37	5,920	0.2817	6,530			
5		0.0	4.46	0.37	16,630	0.2798	−4,900			
6		0.0	4.46	0.37	9,480	0.2813	2,360			
7		9.8	6.17	0.68	9,500	0.2827	6,150			
8		9.6	7.00	0.87	9,960	0.2831	7,400			
9		9.5	8.64	1.40	10,900	0.2842	11,620			
10		9.3	10.26	2.22	12,240	0.2855	14,740			
11		0.0	10.26	2.22	23,780	0.2818	4,850	1.49	1.74	0.0018

[a]The stress values are for tangential stress in the increment adjacent to the surface identified. Positive values are tensile, and negative (−) values are compressive. The cladding thickness was divided into five radial increments for this analysis.

[b]At room temperature the outer surface radii were assumed to have been decreased by 0.00655 in. to account for fuel-cladding and Na-cladding interactions plus mechanical flaws. Therefore, the fictitious radii are not included in this table.

[c]The plastic strain is the calculated total creep strain including second-stage thermal creep and a flux-enhanced creep based on the proposal of T. T. Claudson, BNWL-SA-328B.

[d]The start of life stresses are the result of differential thermal expansion in the fuel and cladding. Since the FMØDEL code is written for pellet fuels with radial gaps between the fuel and cladding, the use with Sphere-Pac fuels and no gap will give erratic start of life stresses. A very small amount of primary creep not included in the present code will relieve these stresses.

Calculations of the effect of the diameter change on coolant flow are summarized in Table 15.

Table 15. Comparison of Start-of-Life Coolant Flow Rates with End-of-Life Flow Rates

Pin Location	Start of Life		End of Life		Decrease, %	
	Flow Area per Pin (in.^{2})	Flow Rate per Pin (lb/hr)[a]	Flow Area per Pin (in.^{2})	Flow Rate per Pin (lb/hr)[a]	Area	Flow
Corner	0.0369	687.3	0.0330	595.0	10.5	13.4
Edge	0.0333	638.0	0.0295	544.3	11.4	14.7
Center	0.0225	384.4	0.0186	304.7	17.3	27.0

[a]Based on a mean sodium coolant temperature of 911°F.

Although only certain pins are currently scheduled for irradiation to the maximum burnup level, there is a significant probability that the results of interim examinations may alter the choice of which pins. Therefore, we used the MAMU code to calculate the end-of-life thermal conditions for each location in the subassembly. The results of these calculations are summarized in Table 16.

In Table 17 we have summarized the subassembly conditions for the hypothetical case where all pins are taken to full burnup. In this case the mixed mean outlet coolant temperature for an N-37 subassembly would have reached 1058°F or 11°F above the permissible temperature of 1047°F for a 6-N3 position listed in Table C-VIII, p. C-50 of the Guide. This is a very conservative estimate.

Since these calculations are all based on extremely conservative assumptions, we would propose that no orifice change be made for the second N-37 subassembly loading. Further, we propose to use the results of the interim examination at the time of fabricating the second subassembly together with all available data from other experiments available at that time to evaluate more precisely the end-of-life conditions and define the orificing requirements for the third subassembly. Similar adjustments to a J-37-A internal orificing may be made for the third

Table 16. Fuel Pin Thermal Analysis, End of Life

Pin Location in Subassembly	Fuel Smear Density (% of theoretical)	Coolant Flow Rate (lb/hr)	Total Heat Production (Btu/hr)	Maximum Cladding Inner Surface Temperature (°F)	(°C)	Coolant Outlet Temperature (°F)	(°C)	Extra Thermal Expansion[a] (in. $\times 10^{-3}$)
1	80	595	44,518	1,026	552	946	508	Negative
2	80	544	43,937	1,042	561	966	519	Negative
3	80	544	43,365	1,037	558	962	517	Negative
4	85	595	45,376	1,033	556	951	511	Negative
5	80	544	43,937	1,042	561	966	519	Negative
6	80	305	43,341	1,237	669	1,171	633	0.1
7	83	305	44,295	1,249	676	1,189	638	0.1
8	83	305	43,694	1,241	672	1,175	635	0.1
9	85	544	44,128	1,043	562	967	519	Negative
10	80	544	43,365	1,037	558	962	517	Negative
11	83	305	44,295	1,249	676	1,181	638	0.1
12	83	305	43,694	1,241	672	1,175	635	0.1
13	85	305	44,104	1,246	674	1,179	637	0.1
14	85	305	43,485	1,238	670	1,173	634	0.1
15	83	544	41,867	1,026	552	953	512	Negative
16	83	595	44,327	1,025	552	945	507	Negative
17	83	305	43,694	1,241	672	1,175	635	0.1
18	85	305	44,104	1,246	674	1,179	637	0.1
19	85	305	43,485	1,238	670	1,173	634	0.1
20	83	305	41,844	1,218	659	1,155	624	0.1
21	83	305	41,214	1,210	654	1,148	620	0.1
22	85	595	41,570	1,005	540	930	499	Negative
23	85	544	44,128	1,043	562	967	519	Negative
24	83	305	42,492	1,226	663	1,162	628	0.1
25	83	305	41,844	1,218	650	1,155	624	0.1
26	83	305	41,214	1,210	654	1,148	620	0.1
27	85	305	41,538	1,214	657	1,151	622	0.1
28	83	544	39,939	1,011	544	941	505	Negative
29	83	544	41,867	1,026	552	953	512	Negative
30	83	305	51,214	1,210	654	1,148	620	0.1
31	85	305	41,538	1,214	657	1,151	622	0.1
32	83	305	39,916	1,194	646	1,134	612	0.1
33	90	544	42,516	1,031	555	957	514	Negative
34	85	595	41,570	1,005	541	930	499	Negative
35	83	544	39,939	1,011	544	941	505	Negative
36	90	544	42,516	1,031	555	957	514	Negative
37	83	595	38,679	984	529	914	490	Negative
TOTAL		15,434	1,662,279					

[a]The extra thermal expansion denotes the increase in cladding diameter due to the change in temperature from beginning-of-life to end-of-life conditions.

Table 17. Subassembly Thermal Performance, End of Life

Characteristics	Subassembly Type	
	N-37	J-37-A
Coolant Flow Rate:		
Inner hex can, lb/hr of 800°F Na	15,891	15,891
Bypass, lb/hr of 800°F Na		7,665
TOTAL, lb/hr of 800°F Na	15,891	23,556
TOTAL, gpm at 800°F	36.4	54.5
Total Heat Generated:		
Pins and sodium, Btu/hr	1,662,300	1,662,300
Subassembly hardware,[a] Btu/hr	64,000	74,300
TOTAL, Btu/hr	1,726,300	1,736,600
Temperature Rise:		
Inner hex can, °F	358	345
Bypass, °F		32
Mixed Mean Outlet Temperature:		
°F	1,058	943
°C	570	506

[a]Including bypass sodium for J-37-A subassembly.

subassembly to level test conditions, even though the worst case is well within the EBR-II coolant outlet temperature limitations.

Effect of Increased Pin Diameters on Subassembly Dimensions

The effects of increasing pin diameters on the subassembly dimensions must be considered in two ways: (1) mechanical interaction during irradiation, and (2) changes in subassembly hardware at each interim examination.

During irradiation of any subassembly the increased diameter of each of the pins will result in a gross dimensional change in the pin bundle periphery dimensions which vary as a function of axial location. Since these dimensional changes are predominantly the result of cladding and wire wrap density changes as a function of fluence and the subassembly

hardware is subjected to the same fluence at each of the axial locations, the change in relative dimensions across flats for the pin bundle and the subassembly inner can will be essentially zero. In fact, because of the temperature of the inner can (generally close to 500°C), the initial as-fabricated clearance between the inner can and the pin bundle may increase slightly.

However, it may be necessary to alter the dimensions of the inner can for the second and third subassemblies to provide assembly clearance for the irradiated pins. On the basis of our dimensional analysis, the inner hex-can distance across flats will have to be increased by 0.020 in. to 1.866 in. nominal for the second subassembly. This will reduce the effects of pin swelling on coolant flow described in the previous section. It is possible that a further increase in the inner hex can flat-to-flat dimension by 0.010 in. may be required for the third subassembly; but this is unlikely and can only be determined when the results of the interim examination of the first subassembly are available.

SAFETY ANALYSIS

Operation at 110% of Normal Heat Rate

An increase of 10% in the steady-state heat rate of all the pins in this subassembly will have a negligible effect on fuel restructuring with the maximum fuel center temperature increasing from 2300 to 2420°C. No axial fuel movement is expected, and the effect of the increased peak cladding temperatures (1140 to 1190°F) on sodium cladding reactions is likewise negligible.

The effect on fuel-cladding reactions is more nebulous. One of the secondary objectives of this test series is to obtain more information on fuel-cladding interactions at cladding temperatures above 600°C. There have been tests in which reactions up to 0.005 in. at 750°C have been reported.[36] These reactions were with fuel having a reported initial oxygen-to-metal ratio of 2.00, and lowering the ratio should lower the fuel-cladding reaction rate. The reaction rate with our hypostoichiometric fuel is uncertain. In view of these uncertainties

and the fact that we have used a conservative approach in making our stress-strain analysis, we feel the possibility of a 10% overpower operation will not jeopardize the integrity of these pins because of fuel-cladding interaction.

The very remote possibility of a 10% greater burnup for the maximum burnup pins will increase the swelling of the fuel and vary the swelling of the cladding. The higher fuel temperatures would increase the plasticity of the fuel and increase the actual fission-gas release. This would improve the utilization of available porosity to reduce the rate of fuel swelling. Even without the increase in volume provided by the stainless steel void swelling effect on the cladding dimensions, which will be less according to the current formulations as the cladding temperatures go farther above the 550°C peak swelling temperature, there should still be adequate void volume to accommodate the fuel swelling without serious mechanical interaction with the cladding.

The effect of changes in swelling of the cladding on coolant annuli will be negligible because of similar changes in the fluence-temperature effects on the swelling of the inner hex can.

The mechanical properties of the cladding will experience a range of property changes because of the increased range in temperatures. The higher temperatures are expected to decrease the effects of irradiation on both yield strength and ductility, thus making our assumptions of unirradiated properties more valid.

Abnormal Operations

Power Excursions

Nuclear Excursion in a Core at Zero Power. — Acting on instructions from the EBR-II Experiments Manager,[37] we have not considered Case 1 in Appendix E of the Guide.

Accidental Insertion of a Control Rod in a Core at Normal Power. — Case 2 of Appendix E of the Guide defines the transient. In analyzing this case, we chose to analyze the peak heat rate pin in position 7 of the subassembly. We further assumed that the accident occurred after

172 hr of full power operation so that there would be a gas plenum pressure of 130 psi absolute inside the pin.

The thermal analysis was done by a series of steady-state analyses using the MAMU code. This is conservative since the actual coolant temperatures during the transient will be less than the steady-state temperatures. The resulting maximum temperatures at various times during the transient are listed in Table 18 and shown graphically in Fig. 11.

Table 18. Nuclear Excursion Subassembly Thermal Analysis for Pin in Position 7

Time (sec)	Reactor Power[a] (%)	Maximum Cladding Surface Temperature, °C		Coolant Outlet Temperature	
		Inner	Outer	(°C)	(°F)
0	100	650	616	604	1120
5	101.9	654	621	610	1130
10	104.2	660	627	616	1140
15	107.1	668	635	621	1150
20	110.5	677	743	632	1170
25	115.0	688	654	643	1190
30	119.7	704	666	652	1205
35	125.0	718	679	666	1230
40	130.4	732	693	677	1250
45	136.4	749	710	693	1280

[a]Based on a reactor power level of 62.5 MW as 100%.

The stress analysis for this case was made by using the MAMU temperatures and calculated by the FMØDEL code for three 0.5-in.-long axial locations, the bottom of the fuel column, the peak heat rate section, and the top of the fuel column. The critical values resulting from these calculations are listed in Table 19.

Three failure criteria can be assumed:

1. cladding temperatures reach the melting point,

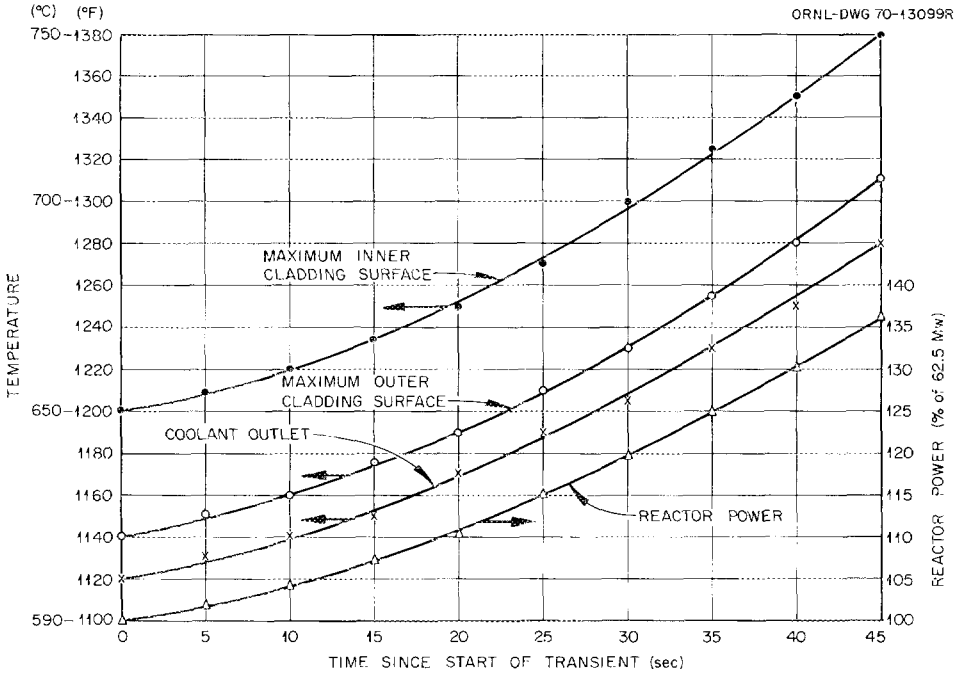

Fig. 11. Partial Thermal Analysis of Power Transient on Pin in Subassembly Position 7.

2. cladding tangential stresses exceed the ultimate strength of the material, or
3. sufficient fuel melting occurs to provide a serious threat to pin integrity. For this case, we believe the unirradiated fuel tests in TREAT[38] justify the assumption that less than 50 vol % melting is below the transient failure threshold.

Based on our analysis and the results given in Tables 18 and 19, none of these failure criteria are met provided the power transient is terminated within 45 sec. The maximum cladding temperature is only 749°C (1380°F), well below the melting point of 1380°C (2520°F). The cladding tangential stresses at the outer surface are high, but the mean wall stress is below the ultimate strength of the material. Finally, the volume of fuel melting is calculated to be 45% of the volume, which is below the failure criterion but would obviously exceed this criterion if the transient was allowed to continue beyond the 45 sec that we have analyzed.

Table 19. Nuclear Excursion Analysis for Three Axial Locations on a Pin in Subassembly Position 7

Time (sec)	Reactor Power[a] (%)	Gas Plenum Pressure (psi)	Bottom of Fuel				Peak Heat Rate Position				Top of Fuel			
			Fuel Center Temperature (°C)	Fuel Melting (vol %)	Cladding Tangential Surface Stress, psi		Fuel Center Temperature (°C)	Fuel Melting (vol %)	Cladding Tangential Surface Stress, psi		Fuel Center Temperature (°C)	Fuel Melting (vol %)	Cladding Tangential Surface Stress, psi	
					Inner	Outer			Inner	Outer			Inner	Outer
0	100	131	1900	0	−15,700	16,000	2170	0	−18,800	18,600	1950	0	−12,600	12,600
5	101.9	132	1940	0	−10,000	21,700	2220	0	−16,000	21,800	1990	0	−11,800	13,900
10	104.2	133	1990	0	−1,300	30,100	2270	0	−11,200	26,900	2040	0	−10,400	15,600
15	107.1	134	2050	0	3,100	34,900	2340	0	−5,800	32,700	2100	0	−7,000	19,100
20	110.5	135	2120	0	6,800	39,100	2420	0	1,300	40,200	2170	0	−1,800	25,200
25	115.0	136	2210	0	7,300	40,800	2530	0	4,000	44,200	2260	0	2,300	28,900
30	119.7	138	2310	0	7,800	42,400	2650	0	4,900	46,700	2360	0	3,100	30,500
35	125.0	140	2420	0	8,000	44,000	2780	0	4,900	48,600	2470	0	4,300	32,500
40	130.4	142	2540	0	8,200	45,600	Molten	14	4,600	50,000	2580	0	4,500	33,600
45	136.4	144	2660	0	8,600	47,400	Molten	45	4,800	51,500	2710	0	4,600	34,400

[a]Based on a reactor power of 62.5 MW as 100%.

Loss-of-Coolant Flow Operation

To investigate the effects of a loss-of-coolant pump power with immediate scram of the reactor, we again made a series of thermal analysis calculations using the MAMU code and assuming steady-state operation at fixed time increments during the event (Figs. E-3 and E-4 of the Guide). We did these calculations for the pin located in subassembly position 7, the peak heat rate pin with the minimum coolant flow. We assumed this occurred during the initial startup of the reactor following introduction of the pin; no fuel restructuring was considered. The latter assumption raises the fuel center temperatures to the maximum. The results of these calculations are summarized in Table 20 and shown graphically in Fig. 12.

Table 20. Loss-of-Coolant Flow Accident Pin in Subassembly[a] Position 7

Time (sec)	Flow (%)	Reactor Power (%)	Maximum Cladding Surface Temperature, °C		Fuel Center Temperature (°C)	Coolant Outlet Temperature	
			Inner	Outer		(°C)	(°F)
0	100	100	650	616	2340	604	1120
1	100	24	438	429	680	427	800
10	47	15	451	446	590	445	833
20	23.5	11	483	202	570	479	895
30	15	8.9	511	508	585	509	948
40	10.5	7.5	537	535	600	537	998
50	7.5	6.6	576	575	630	575	1067
60	5.3	6.0	634	633	685	633	1172
70	4.0	5.4	684	684	730	684	1264
75	3.6	5.0	693	693	735	693	1279
80	3.4	4.9	706	706	750	705	1301
90	3.2	4.5	697	697	730	697	1287
100	3.0	4.2	696	696	730	696	1284

[a]Full flow = 384.35 lb/hr; sodium heat capacity = 0.306 at 750°F; sodium density = 53.3 lb/ft^3 or 0.8538 g/cm^3.

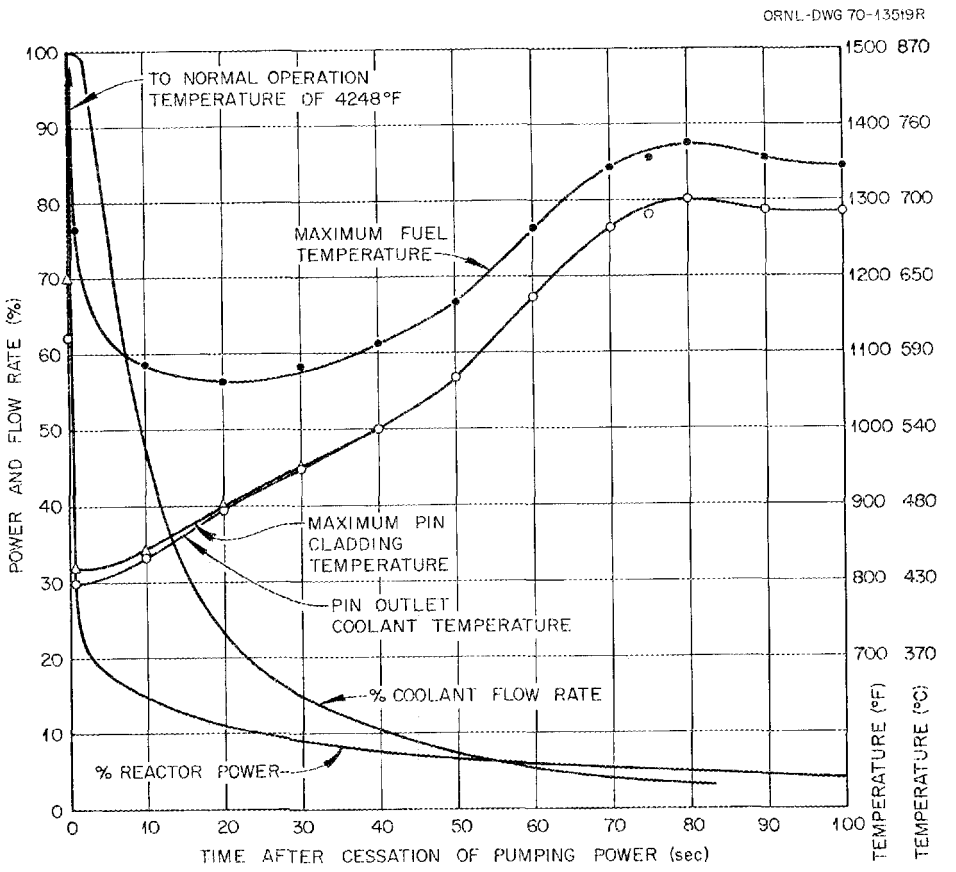

Fig. 12. Partial Thermal Analysis of Loss-of-Coolant Flow on Pin in Subassembly Position 7.

Because of the immediate scram of the reactor, all fuel temperatures are well below the normal operating temperatures, and the thermal gradients in the cladding and fuel rapidly approach near zero values. The only significant temperature differences occur in the cladding temperatures and coolant outlet temperatures. These two temperatures, after an initial drop, will rise above the normal steady-state operating conditions to peaks approximately 80 sec after the loss of pump power. The peak cladding and coolant outlet temperatures will be approximately 1300°F (700°C). Since there is essentially no thermal gradient stress in the cladding at this time and the internal gas pressure will only rise 10% above normal, because of the increased plenum temperature, the effective stress in the cladding will be well below that under normal steady-state operation.

Cladding Failure

Gas Blanketing

The failure of the cladding on one pin in the subassembly will release its gas to the coolant and cause a temporary deterioration of the heat transfer characteristics of the subassembly. The extent of the heat transfer deterioration and the length of time that such a temperature transient will endure depends on the nature and location of the cladding failure together with the burnup level at the time of failure.

We have chosen to analyze two cases of failure similar to those selected by others.[39] We have used the HEATING code[40] to analyze the temperature transients. In making these analyses we have assumed that the failure occurs at the bottom of the fuel pin and at the peak burnup level when the fission-product gas accumulation is maximum. In both cases we have assumed that the gas escapes at a rate defined by the flow area of sodium displaced with the gas bubble moving at a velocity equivalent to the sodium flow before failure. The gas-blanketed flow channels were defined as shown in Fig. 13. In Case A the gas blanket is distributed to all coolant channels surrounding the failed pin, while in Case B the gas blanket is restricted by the wire wrap to one-third of the available channels. Figures 14 and 15 show the maximum calculated fuel and cladding temperatures as a function of time for Cases A and B, respectively. As can be seen in Fig. 14, no fuel melting is anticipated for Case A. The calculated volume percentage of molten fuel for Case B as a function of time is given in Table 21. These values are only approximate since only radial heat flow was assumed in the analysis and the actual molten volume would be significantly less because of tangential heat flow to the two-thirds of the fuel still having full coolant flow in the unblanketed channels.

These calculations were made with the assumption that the gas blanket was a perfect insulator so that no cooling was available to the cladding covered by the gas during the time the gas was escaping. This assumption is undoubtedly too pessimistic but even so in Case A, where the entire pin is blanketed for 1.49 sec, only incipient melting of the cladding at the highest heat rate location of the pin is indicated, and

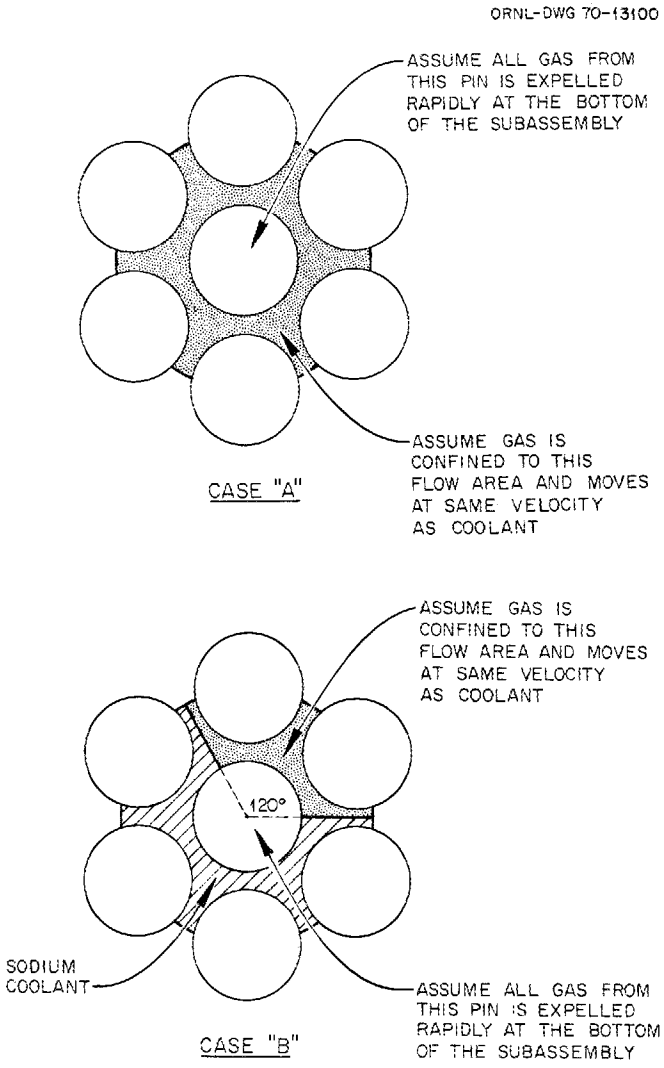

Fig. 13. Flow Model for Calculating Pin Temperatures During Hypothetical Gas Blanketing Incident.

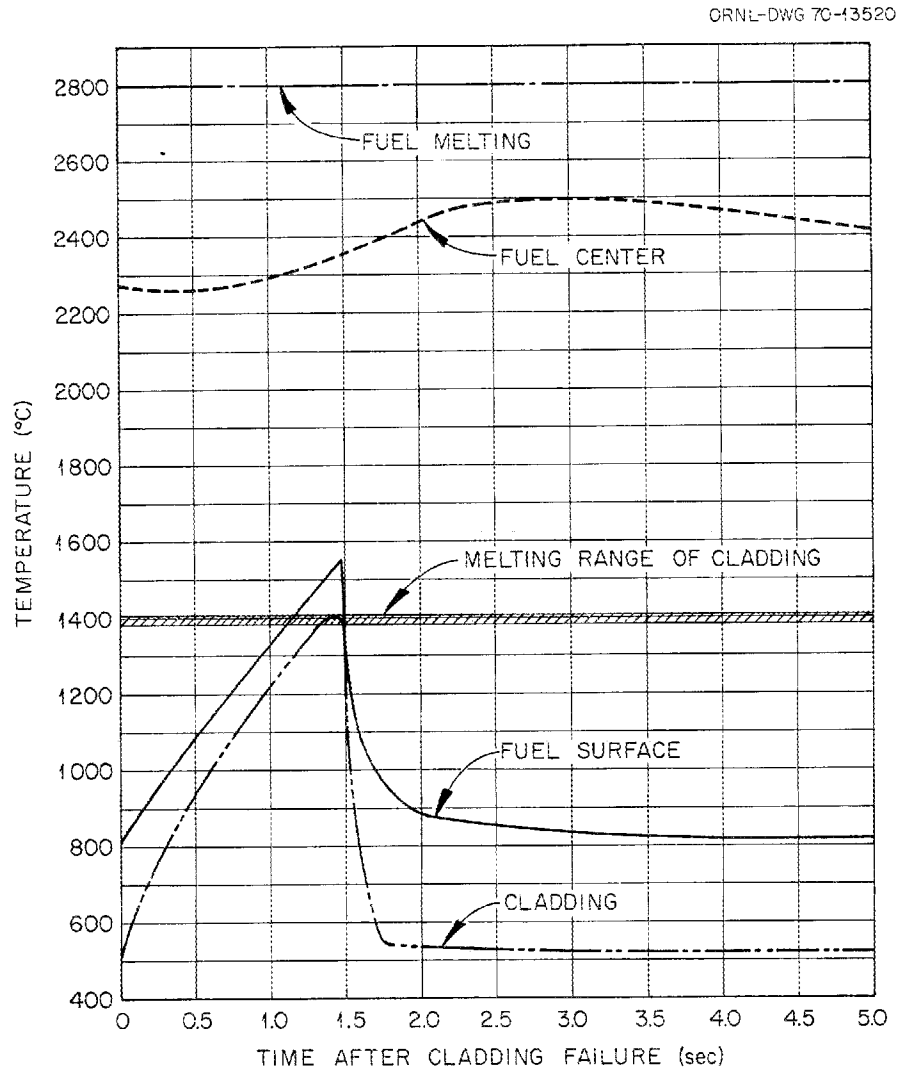

Fig. 14. Maximum Temperatures During Gas Blanketing, Case A.

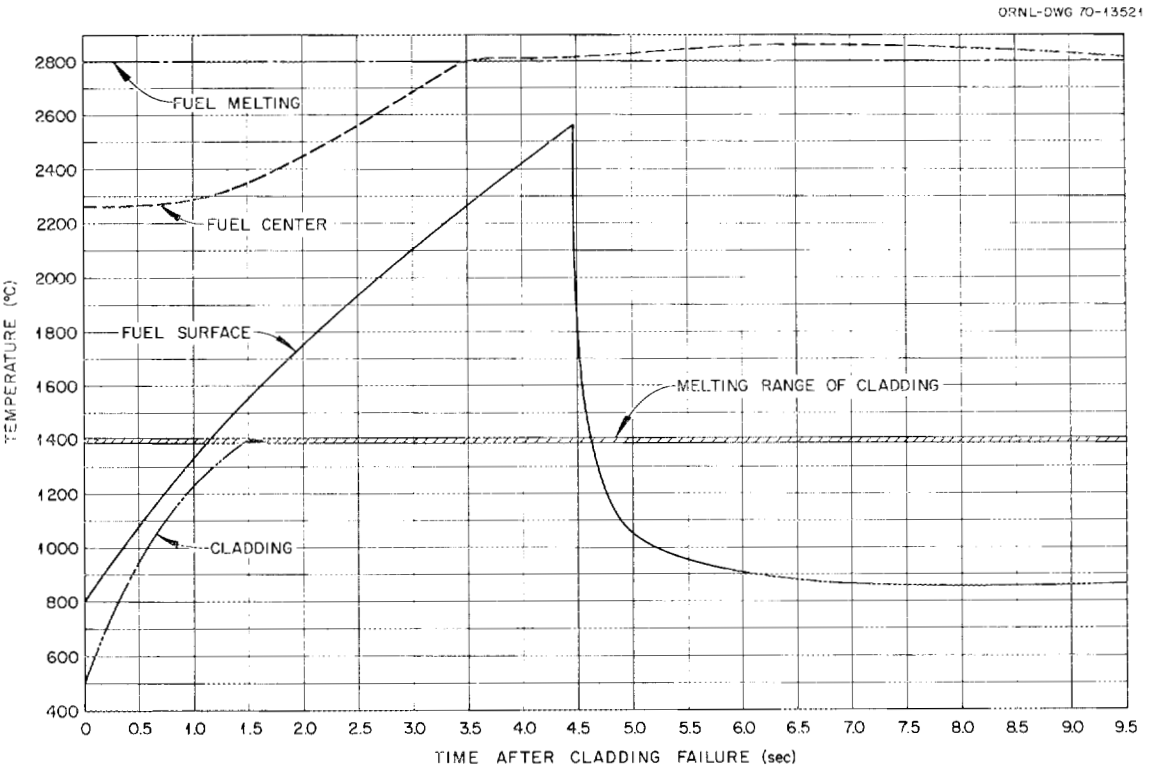

Fig. 15. Maximum Temperature During Gas Blanketing, Case B.

Table 21. Volume of Fuel Molten During Gas Blanketing Thermal Transient, Case B (4.47 sec duration)

Time After Failure (sec)	Maximum Volume of Molten Fuel (%)
0.5	0
1.0	0
1.5	0
2.0	0
2.5	0
3.0	0
3.5	2
4.0	11
4.47	18
4.5	19
5.0	15
6.0	9
7.0	7
8.0	6
9.0	5
10.0	4

the partially cooled adjacent pins should survive the less severe localized temperature transient without failure.

If the gas is trapped in the restricted channel defined in Case B, cladding melting will occur on the failed pin and failure of the adjacent pins is probable. However, since the gas escaping from these pins would also be trapped in the same coolant annuli, additional failures beyond the adjacent pins are highly unlikely.

Solid Debris Flow Blockage

The possible effects on coolant flow blockage by solid or molten material from a failed pin are, to a large extent, dependent on whether or not the material can become lodged in the subassembly and the effective reduction in coolant flow from such blockage.

Brook[41] did an extensive analysis of the effects of flow blockage on PFR fuel subassemblies. The agreement between Brook's analysis and our calculations for the gas release Case A is excellent. Therefore, we feel the use of his analysis is a valid analogy for this subassembly. From Brook's analysis, blockage of a single flow channel would not cause severe damage; but complete blockage of six to eight flow channels would initiate boiling in the stagnant coolant and melting of the pins. The basis of Brook's analysis was that flows of the magnitude of 2 to 4% of full flow would restrict the temperature rise in the coolant for short blockages to the point where sodium boiling would not occur and the cladding temperature at 4% flow would be below the melting point as a result of heat conduction to adjacent channels. We did not attempt to duplicate his analysis for our case since such calculations are extremely sensitive to the assumptions of the length of such blockages, the amount of interchannel mixing, etc. Failure debris is more likely to be swept out of this subassembly with wire wrap spacing than with the grid structure investigated by Brook. Therefore, we feel the probability of failure propagation within the subassembly as a result of debris from a single failure is extremely remote.

Localized bulging of a fuel pin as a result of the initial failure would impair the coolant flow in the adjacent channels, but is very unlikely to lead to a total blockage of even one coolant channel. Thus,

again citing the analysis of Brook, the continuation of as little as 4% of the initial coolant flow will prevent failure propagation.

Reactor Environment Contamination

We examined the effect of cladding failure of one pin on reactor coolant and cover gas contamination with the assumption that the failure occurred in a peak burnup pin with an initial fuel smear density of 85% of theoretical. The fission-product inventory was calculated by the ØRIGEN code.[42] Because of the probable thermal transient and high burnup, the assumption of 100% gas release (krypton and xenon) from this pin to the cover gas volume is probably reasonable. On the other hand, the assumption that all of the fuel and nongaseous fission-product activity is released to the coolant is unreasonable. Nevertheless, using these assumptions, we have plotted both the cover gas and coolant contamination as a function of decay time following the assumed failure in Fig. 16. It is our considered opinion that the extent of fuel washout from any failure will be less than 1%; so the actual coolant contamination will be about 1% of the values given.

The exposure of the fuel to the primary coolant will probably result in some additional fuel swelling from sodium-fuel-fission product interaction. The maximum change in diameter associated with a pin failure in which this reaction may have been a contributing factor is 22%, as reported by General Electric[43] (pin F-2-A). This failed fuel pin was in an encapsulated test in the EBR-II with a reported burnup of 71,000 MWd/metric ton. The cladding was type 347 stainless steel welded and drawn tubing, and the fuel had a reported oxygen-to-metal ratio of 2.03. The initial failure was reportedly associated with the tube weld and extended the full length of the fuel. The extent of reaction with the sodium (approximately 0.020 in.) was approximately four times the reaction depth seen in another failed pin (F-4-D) where the fuel oxygen-to-metal ratio was 2.00. Since all of the fuel in this subassembly has initial oxygen-to-metal ratios less than 2.00, it is reasonable to assume that the reaction, and therefore the swelling, will be less than 22% even if the failure occurs at the high burnup levels. Therefore, sodium-fuel-fission product reactions may increase the extent

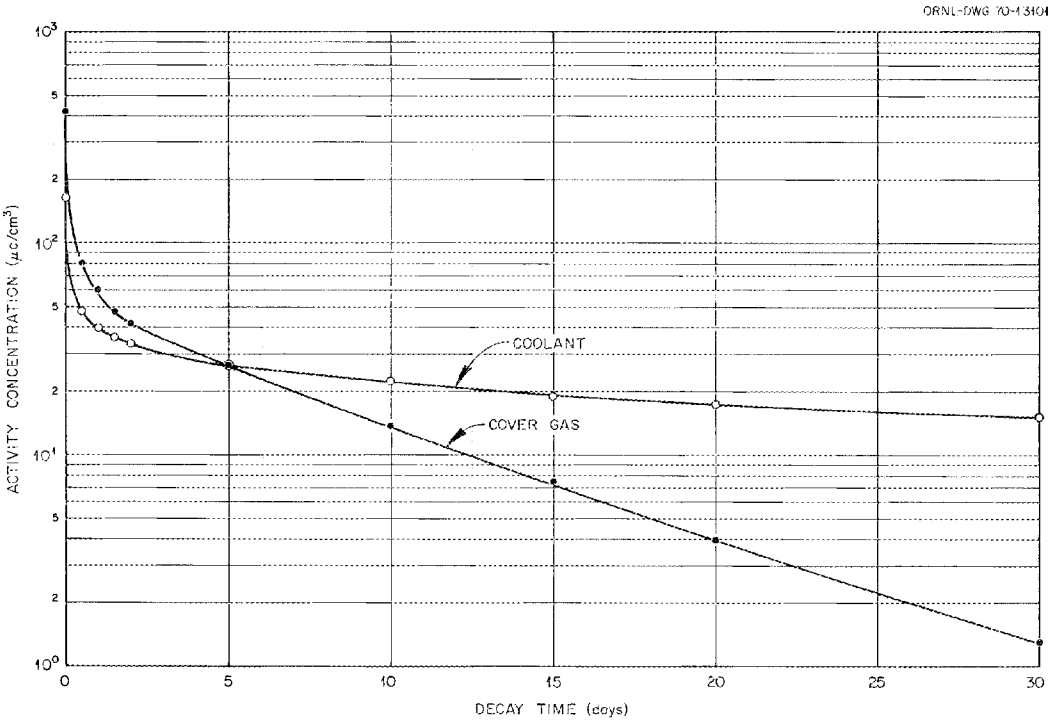

Fig. 16. Reactor Coolant and Cover Gas Contamination Following Rupture of 85% Smear Density Pin after 600 Effective Full Power Days of Operation.

of the original failure but will not lead to additional failures in the subassembly.

Should the initial pin failure go undetected or the wrong subassembly be removed after detection of a failure, both highly unlikely since all pins have an identifying xenon tag, sodium could enter the fuel pin during the reactor shutdown period. This condition, sodium logging, could cause gross rupture of the pin on the subsequent return to power and the washout of fuel particles into the coolant stream. Although this would lead to additional contamination of the primary reactor coolant, it should not result in failure propagation or damage to the subassembly hex can. The additional release of contamination will readily be detected and the subassembly containing the failed fuel pin removed from the reactor.

Sodium Removal from Failed Pin

The consequences of subjecting the failed fuel element to the normal sodium removal process will depend on the location and extent of the failure. Reactions between the fuel and the cleaning agents will be insignificant. However, reactions between the moist air or water and trapped sodium or sodium-fuel-fission product reaction layers are to be expected. Such reactions will undoubtedly lead to contamination of the inter-building-coffin and the effluent cleaning gas and liquid. Such reactions will not significantly add to the failure, but will cause changes in the cladding reactions and reaction products which will make determination of the cause of failure more difficult. However, we do not have a suggestion for an alternate practical cleaning procedure which would eliminate this difficulty.

Subassembly Criticality Analysis

The k_{eff} was calculated for this subassembly under the conditions of water flooding. A number of conservative approximations were used in making this calculation. The assembly was assumed to be infinite in length and surrounded by an infinite water reflector. No self-shielding was assumed for ^{235}U and ^{239}Pu, and the ^{238}U resonances were not shielded. Despite these positive approximations, the calculated multiplication constant was 0.46, well below the limit of 0.60 set by safety requirements.

Criteria for Reinsertion of Pins

Interim examinations of the pins in this subassembly which go to full burnup are required at the levels of burnup requested for removal and replacement of pins defined in this data package. The interim examination requirements are detailed in the section on Designed Out-of-Reactor Services.

When evaluating the data on these pins for reinsertion, the following limitations are to apply:

1. No pin which shows a diameter increase in excess of 1.5% at 250 effective full power days of exposure or 3% at 390 effective full power days of exposure is to be reinserted. These limits reflect the primary uncertainties in the swelling calculations as a function of neutron fluence and temperature and so are larger than the predicted changes given in Table A-9. The limit applies to the maximum diameter change at any axial location.

2. No pins with broken wire wraps shall be reinserted.

3. All pins which show unusual evidence of fretting attack in the cladding region, or evidence of localized mechanical damage to the cladding, shall be removed from testing.

4. Evidence from the neutron radiographs of gross fuel redistribution such as slumping shall be cause for rejection for further testing.

QUALITY ASSURANCE DESCRIPTIONS AND AS-BUILT INFORMATION

Both ORNL and B & W used essentially identical requirements for hardware components and fabrication procedures to assure the highest quality in producing pins for this experimental subassembly. However, the exact procedures for fabrication, inspection, and analysis did vary in detail.

Copies of all reference procedures or methods have been supplied separately to the EBR-II Project and are on file at the respective fabrication site. Also, in accordance with Revision 3 of the Guide[7] the following materials, samples, and information were supplied under separate cover to the appropriate EBR-II Project personnel: (1) three each full size drawings; (2) two each sample weld assemblies with complete closure assemblies on each end of a 12-in. length of cladding; (3) duplicate x-ray films of all welds and assembled fuel pins; and (4) two each xenon tagged dummy elements from each fabrication site.

In the following two sections of this report, one for each fabrication site, we have provided a brief description of the fabrication procedures and the specific as-built information as required under Sections VI-F and VIII-A of Revision 3 of the Guide.

Fabrication and Inspection of ORNL Pins

Fabrication and Quality Assurance Procedures

The ORNL EBR-II Series II fuel pins were fabricated to the design shown in Fig. 3, p. 11, in accordance with MET-FCT-FQ-1 and the other specifications and procedures listed in Appendix B.

The quality assurance program for the fuel pins includes the following:

1. certified analyses on all metallic components,
2. ultrasonic inspection of all cladding material in both transverse and longitudinal modes. All tubing containing flaw indications in excess of the reference notches 0.001 in. deep × 0.030 in. long is rejected,
3. the wall thickness of all cladding material is measured ultrasonically and recorded, and any tube with a wall thickness measurement outside a tolerance range of $\pm^{0.0015}_{0.0010}$ in. is rejected,
4. eddy current and profilometer measurements of the inside diameter recorded for all cladding used,
5. dye-penetrant inspection of all cladding tubes for surface-connected defects,
6. outer diameter dimensions measured at 6-in. intervals along cladding tube length,
7. dye-penetrant and radiographic inspection of top and bottom end plugs and top end cap for surface-connected and internal defects,
8. dye-penetrant, radiographic, and helium leak testing of all closure welds; mass spectrometer leak test equipment to a sensitivity of 1×10^{-9} cm^3/sec is used,
9. final dimensional inspection of finished fuel pins at 1/2-in. intervals for outer diameter to an accuracy of 0.0002 in., inspection for TIR over length of cladding, and measurement of final length to an accuracy of 0.002 in.,
10. radiography of completed fuel pin to confirm proper fuel and component positions and dimensions, and
11. inspection of fuel column in finished pin by gamma-ray densitometer with density variations recorded along the total length of the fuel column.

Fuel Pin Assembly

A general description of the fuel pin assembly process follows.

After machining, each metallic component was cleaned, weighed, and dimensionally and nondestructively tested as required. The bottom end plugs were assembled to the cladding tube and welded and inspected to closure weld requirements. The assembly was weighed, cleaned, and transferred to the alpha facility for fuel loading and final weld closures. The blanket pellets (UO_2) were loaded, a 1/16-in.-thick Fiberfrax pad was placed in the column, followed by loading of two thoria insulator pellets. Glove box loading of the $(U,Pu)O_2$ fuel either as pellets or microspheres followed. Two thoria insulator pellets were loaded and a Fiberfrax pad was placed on top of the column. The nickel rod was next inserted, followed by the spring with the two spring seats attached.

After decontamination of the weld zone, the fuel pins were transferred to the welding box. After evacuation to 10^{-2} torr and backfilling with helium, the spacer rod was inserted compressing the spring and the top end plug inserted. The top end plug was welded to the cladding tube. This was followed by xenon tagging, plug welding of the capillary tube end, insertion of the top end cap into the top end plug, and final closure welding of top end plug to top end cap. The rod was then transferred from the alpha facility for final nondestructive inspection which included visual inspection, radiograph of top end plug, capillary, top end cap welds, and overall rod, helium leak check of rod, dye-penetrant inspection of top end plug, top end cap welds, and adjacent areas. A gamma densitometer inspection of the rod was performed, followed by weighing, final dimensioning, marking of the rod identification number, cleaning, and packaging in the shipping container.

A summary of the nondestructive testing reports pertaining to inspections performed on the fuel pins and fuel pin components is given in Tables 22 and 23. Copies of these reports are on file at ORNL.

Table 22. Nondestructive Testing Summary — EBR-II Components

Pin Number	Cladding Tube			Top Cap		Top Plug		Bottom Cap		Cladding Number
	Dye Check	Ultrasonic Wall Thickness	Ultrasonic Defects	Dye Check	Radiograph	Dye Check	Radiograph	Dye Check	Radiograph	
OS-6	IR-10863	IR-10863	IR-10854	Not performed before welding to top end plug	IR-10868	M&C Form 117, dated 3/9/70	IR-10868	Not performed before welding of bottom cap to tube. See pin data on Weld W-1.		19-52A
OS-7	IR-10863	IR-10863	IR-10854							19-23A
OS-8	IR-10863	IR-10863	M&C Rept. 19-7, dated 10/69							19-7A
OS-9	IR-10863	IR-10863	IR-10854							19-60A
OS-10	IR-10863	IR-10863	M&C Rept. 19-6, dated 10/69							19-6C
OS-2	IR-10863	IR-10863	IR-10854							19-37A
OS-1	IR-10863	IR-10863	IR-10854							19-26A
OS-3	IR-10863	IR-10863	IR-10854							19-60B
OS-4	IR-10863	IR-10863	IR-10854							19-53B
OS-5	IR-10872	IR-10869	IR-10854							19-53A

Table 22. continued

Pin Number	Cladding Tube			Top Cap		Top Plug		Bottom Cap		Cladding Number
	Dye Check	Ultrasonic Wall Thickness	Ultrasonic Defects	Dye Check	Radiograph	Dye Check	Radiograph	Dye Check	Radiograph	
OS-11	IR-10863	IR-10863	IR-10854	Not performed before welding to top end plug	IR-10858	M& C Form 117, dated 3/9/70	IR-10868	Not performed before welding of bottom cap to tube. See pin data on Weld W-1.		19-35A
OS-12	IR-10872	IR-10869	IR-10854							19-49A
OS-13	IR-10863	IR-10863	M &C Rept. 19-8, dated 10/69							19-8A
OP-1	IR-10863	IR-10863	IR-10854							19-66B
OP-2	IR-10872	IR-10869	IR-10854							19-54A
OP-4	IR-10872	IR-10869	IR-10854							19-49B
OP-6	IR-10863	IR-10863	IR-10854							19-66A
OP-7	IR-10863	IR-10863	M&C Rept. 19-10, dated 10/69							19-10B
OP-3	IR-10863	IR-10863	IR-10854							19-55A
OP-5	IR-10872	IR-10869	IR-10854							19-76A

Table 23. Nondestructive Testing Summary, EBR-II Series II Fuel Pins

Pin Number	Cladding Number	Radiography, Helium Leak Test, Dye-Penetrant Test					Finished Overall Radiography	Pin Helium Leak Test
		Weld W-1	Weld W-2[a]	Weld W-3	Weld W-4[b]	Weld W-5		
OS-[illegible]	1[illegible]-52-A	Inspection Engineering letter dated 4/21/70	IR-11467	Req. 158	Req. 158	Req. 158	ok	Req. 158
OS-[illegible]	1[illegible]-23-A	Inspection Engineering letter dated 4/21/70	IR-11467	IR-11083	IR-11083	IR-11083	ok	IR-11083
OS-[illegible]	1[illegible]-7-A	Inspection Engineering letter dated 4/29/70	IR-11467	IR-11005	IR-11005	IR-11005	ok	IR-11037 IR-11005
OS-[illegible]	1[illegible]-[illegible]-A	Inspection Engineering letter dated 4/21/70	IR-11467	IR-11005	IR-11005	IR-11005	ok	IR-11005 IR-11037
OS-1	1[illegible]-[illegible]-C	Inspection Engineering letter dated 4/21/70	IR-11467	IR-11082	IR-11082	IR-11082	ok	IR-11082
OS-[illegible]	1[illegible]-3[illegible]-A	Req. 153	IR-11469	IR-11077	IR-11077	IR-11077	ok	IR-11077
OS-1	1[illegible]-2[illegible]-A	Inspection Engineering letter dated 4/21/70	IR-11467	IR-11005	IR-11005	IR-11005	ok	IR-11037 IR-11005
OS-3	1[illegible]-[illegible]-B	Inspection Engineering letter dated 4/21/70	IR-11467	IR-11005	IR-11005	IR-11005	ok	IR-11005 IR-11037
OS-4	1[illegible]-59-B	Inspection Engineering letter dated 4/29/70	IR-11467	IR-11010	IR-11010	IR-11010	ok	IR-11010
OS-[illegible]	1[illegible]-[illegible]-A	Inspection Engineering letter dated 4/29/70	IR-11467	IR-11010	IR-11007	IR-11007	ok	IR-11007
OS-11	1[illegible]-35-A	Inspection Engineering letter dated 4/21/70	IR-11467	IR-11087	IR-11087	IR-11087	ok	IR-11087
OS-12	1[illegible]-4[illegible]-A	Inspection Engineering letter dated 4/29/70	IR-11467	IR-11087	IR-11087	IR-11087	ok	IR-11082
OS-13	1[illegible]-8-A	Inspection Engineering letter dated 4/21/70	IR-11467	IR-11082	IR-11082	IR-11082	ok	IR-11082
OP-1	1[illegible]-66-B	Inspection Engineering letter dated 4/29/70	IR-11469	IR-11006	IR-11006	IR-11006	ok	IR-11006
OP-2	1[illegible]-64-A	Inspection Engineering letter dated 4/29/70	IR-11469	IR-11008	IR-11008	IR-11008	ok	IR-11008
OP-4	1[illegible]-4[illegible]-B	Inspection Engineering letter dated 4/29/70	IR-11469	IR-11009	IR-11009	IR-11009	ok	IR-11009
OP-6	1[illegible]-66A	Inspection Engineering letter dated 4/29/70	IR-11469	IR-11007	IR-11007	IR-11007	ok	IR-11007
OP-7	1[illegible]-10B	Inspection Engineering letter dated 4/29/70	IR-11469	IR-11008	IR-11008	IR-11008	ok	IR-11008
OP-3	1[illegible]-55A	IR-11076	IR-11467	IR-11116	IR-11116	IR-11116	ok	IR-11116
OP-5	1[illegible]-76A	IR-11076	IR-11467	IR-11081	IR-11081	IR-11081	ok	IR-11081

[a]Dye-penetrant - M & C Inspection Form 117, dated 3/7/70.

[b]Not dye-penetrant inspected.

As-Fabricated Data

Complete Pin Data. — The "as-built" data for each of the fuel pins fabricated to date are presented in Table 24. This includes all of the information required by the Guide for Items 1, 5–11, 13, 14, and 18 in Section VI-F. Additional dimensional data on the cladding before and after assembly into the fuel pins are presented in Table 25.

Fuel Data. — The various fuel compositions are given in Tables 26 and 27, and this includes all of the information requested by the Guide for Items 2 and 3 for Section VI-F. Item 4 of this Guide section requests the date of last chemical separation of the fuel. The plutonium in these fuels was prepared from seven equal batches, three of which were separated in February 1967. The remainder were separated in May 1968.

Items 12, 15, 16, and 17 of Section VI-F of the Guide apply to capsules and not to this type of test pin.

Additional Component Data. — Additional chemical analyses on the nonfuel components are summarized in the following tables: UO_2 blanket pellets and ThO_2 insulator pellets in Tables 28 and 29; Fiberfrax in Table 30; and all metallic components in Table 31.

Quality Assurance Certifications

In accordance with the requirements of Section VIII of Revision 3 of the Guide,[7] we are including the following item-by-item certification for the various materials. Table 32 lists the specification and inspection certification for each of the metallic components. Additional information in accordance with Guide requirements follows.

Table 24. Fuel Pin Data Summary for ORNL EBR-II Series II Experiment

Fuel pin number			OS-13	OS-2	OS-1	OS-4	OS-5	OS-6	OS-7
Cladding equivalent number			19-9-A	19-37-A	19-20-A	19-53-B	19-53-A	19-52-A	19-23-A
Fuel batch number			SP80C SPF	SP85C SPF	SP85C SPF	SP 80/85 SPLF	SPL 80/85 SPLF	SP85C SPF	SP85C SPF
Fuel length, in.			13.30	13.35	13.35	13.54	13.45	13.34	13.48
Fuel diameter, in.			NA	NA	NA	NA	NA	NA	NA
Fuel weight, g									
Coarse			53.508	53.609	54.012	54.785	54.898	54.278	54.382
Fines			19.164	19.524	18.638	18.704	19.742	19.655	19.701
TOTAL			72.672	73.133	72.650	73.489	74.640	73.933	74.083
Fuel smear density, % of theoretical			82.0	82.4	81.9	81.6	83.8	83.1	82.4
Fuel Pin Components									
Item	Batch or Composition								
23 UO_2 blanket pellets	ORNL R-1	Average outer diameter, in.	0.2084	0.2080	0.2046	0.2080	0.2080	0.2080	0.2081
		SL, in.	5.875	5.890	5.88[a]	5.88	5.88	5.890	5.890
		ΣW, g	32.7434	33.2626	32.275	33.400	33.600	33.303	33.291
Fiberfrax pad, ~ 0.05 in. thick	MAT 8-H134	Weight, g	0.035	0.031	0.035	0.035	0.032	0.035	0.030
2 lower ThO_2 insulator pellets	ORNL I-1	Average outer diameter, in.	0.2077	0.2080	0.2087	0.2076	0.2074	0.2077	0.2086
		SL, in.	0.5064	0.5082	0.5092	0.5069	0.5071	0.5095	0.5098
		ΣW, g	2.5573	2.5631	2.6138	2.550	2.552	2.5653	2.6186
2 upper ThO_2 insulator pellets	ORNL I-1	Average outer diameter, in.	0.2078	0.2077	0.2089	0.2078	0.2075	0.2081	0.2090
		SL, in.	0.5081	0.5047	0.5090	0.5063	0.5062	0.5078	0.5156
		ΣW, g	2.5667	2.5588	2.6177	2.5635	2.540	2.5612	2.6182
Fiberfrax pad, ~ 0.05 in. thick	MAT 8-H134	Weight, g	0.031	0.035	0.032	0.030	0.034	0.032	0.034
Nickel shielding rod, outer diameter = 0.212 ± 0.001 in.	MAT 37	Length, in. (±1/64)	2 7/32	2 7/32	2 7/32	2 7/32	2 7/32	2 7/32	2 7/32
		Weight, g	11.43	11.31	11.35	11.37	11.35	11.44	11.32
Retainer spring and end seats	Spring, MAT 38 Seats, MAT 20	Length under 4-lb load, in.	1.59	1.53	1.75	1.61	1.75	1.67	1.69
		Spring weight, g	1.93	1.94	1.95	1.94	1.97	1.96	1.94
		Σ seat weight, g	1.15	1.14	1.15	1.15	1.15	1.16	1.13
Spacer tube, outer diameter = 0.188 inner diameter = 0.148	MAT 16	Length, in.	13.12	13.12	12.93	12.90	12.81	13.04	12.98
		Weight, g	17.130	17.257	17.017	17.220	16.910	17.200	17.040
Fuel cladding, end plugs and end caps[b]	Type 316 stainless steel Cladding, MAT 19 Plugs and caps, MAT 20	Σ weight, g	70.246	70.829	70.486	70.260	70.281	70.101	70.462
		Average cladding outer diameter,[b] in.	0.2494	0.2495	0.2497	0.2496	0.2496	0.2498	0.2498
		Average cladding inner diameter,[b] in.	0.2178	0.2174	0.2180	0.2178	0.2177	0.2176	0.2178
Loaded rod[c]									
Total weight, g			212.175	213.645		213.100	213.935	213.545	213.455
Overall length, in.			39.997	39.984	39.988	40.030	39.983	39.972	39.997
Center of gravity from bottom of rod, in.			16 9/16	16 13/32	16 17/32	16 5/8	16 19/32	16 9/16	16 13/32
Gas used in rod assembly, 1 cm^3 Xe + He balance, TOTAL -			8.524	8.469	8.504	8.510	8.389	8.500	8.734
Total free void volume, cm^3			8.524	8.469	8.504	8.510	8.389	8.500	8.734
Approximate activity at 1 ft, gamma mr/hr			3	3	3	3	3	3	3
neutron			Nil	Nil	Nil	Nil	Nil	Nil	Nil

Table 24. continued

Fuel pin number			OS-10	OS-9	OS-8	OS-11	OS-13	OP-1	OP-2
Cladding equivalent number			19-6-C	19-60-A	19-7-A	19-35-A	19-49-A	19-66-B	19-54-A
Fuel batch number			SP80C SPF	SP85C SPF	SP85C SPF	SPL 80/85 SPLF	SPL 80/85 SPLF	PEL 85 S156 and S157	PEL 90 S142 and S143
Fuel length, in.			13.28	13.36	13.24	13.56	13.44	13.44	13.43
Fuel diameter, in.			NA	NA	NA	NA	NA	0.2139	0.2101
Fuel weight, g									
Coarse			53.478	54.234	53.339	54.102	54.528		
Fines			19.823	19.743	18.740	19.407	19.748		
TOTAL			73.301	73.977	72.079	73.509	74.276	77.065	80.96
Fuel smear density, % of theoretical			82.8	83.2	81.7	81.9	83.1	86.1	90.8
Fuel Pin Components									
Item	Batch or Composition								
23 UO_2 blanket pellets	ORNL B-1	Average outer diameter, in.	0.2082	0.2079	0.2045	0.2080	0.2080	0.2081	0.2078
		ΣL, in.	5.875	5.886	5.88	5.88	5.88	5.886	
		ΣW, g	33.312	33.233	32.300[a]	33.200	33.200	33.153	33.1481
Fiberfrax pad, ~ 0.05 in. thick	MAT 8-H134	Weight, g	0.034	0.035	0.035	0.033	0.035	0.035	0.033
2 lower ThO_2 insulator pellets	ORNL I-1	Average outer diameter, in.	0.2087	0.2075	0.2077	0.2077	0.2076	0.2077	0.2076
		ΣL, in.	0.5059	0.5076	0.5073	0.5063	0.5071	0.5061	0.5064
		ΣW, g	2.5892	2.5606	2.5626	2.5581	2.546	2.5590	2.5571
2 upper ThO_2 insulator pellets	ORNL I-1	Average outer diameter, in.	0.2075	0.2076	0.2072	0.2073	0.2079	0.2094	0.2078
		ΣL, in.	0.5074	0.5059	0.5070	0.5066	0.5058	0.5093	0.5067
		ΣW, g	2.5669	2.5592	2.5614	2.5585	2.5589	2.6224	2.5609
Fiberfrax pad, ~ 0.05 in. thick	MAT 8-H134	Weight, g	0.031	0.030	0.033	0.031	0.033	0.033	0.035
Nickel shielding rod, outer diameter = 0.212 ± 0.001 in.	MAT 37	Length, in. (±1/64)	2 7/32	2 7/32	2 7/32	2 7/32	2 7/32	2 7/32	2 7/32
		Weight, g	11.40	11.35	11.32	11.30	11.32	11.34	11.35
Retainer spring and end seats	Spring, MAT 38 Seats, MAT 20	Length under 4-lb load, in.	1.74	1.80	1.67	1.74	1.83	1.81	1.76
		Spring weight, g	1.92	1.96	1.97	1.95	1.99	1.96	1.96
		Σ seat weight, g	1.12	1.15	1.13	1.17	1.15	1.13	1.14
Spacer tube, outer diameter = 0.188 inner diameter = 0.148	MAT 16	Length, in.	12.99	12.81	12.97	12.81	12.74	12.77	12.88
		Weight, g	17.250	16.846	17.055	17.050	16.900	16.882	17.010
Fuel cladding, end plugs and end caps[b]	Type 316 stainless steel Cladding, MAT 19 Plugs and caps, MAT 20	Σ weight, g	70.194	70.356	71.030	71.020	70.240	70.472	70.552
		Average cladding outer diameter,[b] in.	0.2495	0.2496	0.2496	0.2498	0.2494	0.2497	0.2498
		Average cladding inner diameter,[b] in.	0.2177	0.2175	0.2177	0.2177	0.2182	0.2177	0.2179
Loaded rod[c]									
Total weight, g			213.045	213.305	213.285	212.615	213.275	217.155	220.635
Overall length, in.			39.996	39.993	39.992	39.984	39.992	39.946	39.916
Center of gravity from bottom of rod, in.			16 17/32	16 29/32	16 1/2	16 19/32	16 21/32	16 9/16	16 17/32
Gas used in rod assembly, 1 cm^3 Xe + He balance; TOTAL =			8.449	8.419	8.729	8.509	8.379	7.609	7.739
Total free void volume, cm^3			8.449	8.419	8.729	8.509	8.379	7.609	7.739
Approximate activity at 1 ft, gamma mr/hr			3	3	3	3	3	3	2.5
neutron			Nil	Nil	Nil	Nil	Nil	Nil	Nil

Table 24. continued

Fuel pin number			OP-3	OP-4	OP-5	OP-6	OP-7	OS-3
Cladding equivalent number			19-55-A	19-49-B	19-76-A	19-66-A	19-10-B	19-60-B
Fuel batch number			PELL 80 S122, S123 S124/H142	PELL 85 S153, S158 H144	PEL 85 S151, S154 S155	PEL 90 S144, S145	PELL 80 S192, S195 H162	SP85C SPF
Fuel length, in.			13.48	13.54	13.57	13.47	13.60	13.28
Fuel diameter, in.			0.2099	0.2102	0.2140	0.2101	0.2099	NA
Fuel weight, g								
Coarse								53.965
Fines								19.528
TOTAL			72.102	75.627	78.038	80.845	71.623	73.492
Fuel smear density, % of theoretical			80.4	84.3	86.5	90.4	79.6	83.2
Fuel Pin Components								
Item	Batch or Composition							
23 UO_2 blanket pellets	ORNL R-1	Average outer diameter, in.	0.2080	0.2080	0.2081	0.2080	0.2079	0.2077
		ΣL, in.	5.88	5.88	5.886	5.88	5.885	5.885
		ΣW, g	32.950	33.100	33.153	33.206	33.1424	33.3331
Fiberfrax pad, ~ 0.05 in. thick	MAT 8-H134	Weight, g	0.031	0.030	0.030	0.032	0.030	0.032
2 lower ThO_2 insulator pellets	ORNL I-1	Average outer diameter, in.	0.2076	0.2086	0.2078	0.2077	0.2081	0.2075
		ΣL, in.	0.5064	0.5109	0.5063	0.5063	0.5072	0.5077
		ΣW, g	2.5611	2.6181	2.5623	2.5618	2.5611	2.5579
2 upper ThO_2 insulator pellets	ORNL I-1	Average outer diameter, in.	0.2079	0.2086	0.2085	0.2077	0.2076	0.2077
		ΣL, in.	0.5064	0.5094	0.5095	0.5072	0.5068	0.5062
		ΣW, g	2.5568	2.6120	2.6233	2.5623	2.5589	2.5602
Fiberfrax pad, ~ 0.05 in. thick	MAT 8-H134	Weight, g	0.032	0.034	0.030	0.035	0.031	0.035
Nickel shielding rod, outer diameter = 0.212 + 0.001 in.	MAT 37	Length, in. (+1/64)	2 7/32	2 7/32	2 7/32	2 7/32	2 7/32	2 7/32
		Weight, g	11.34	11.41	11.38	11.18	11.38	11.36
Retainer spring and end seats	Spring, MAT 38 Seats, MAT 20	Length under 4-lb load, in.	1.63	1.69	1.77	1.67	1.55	1.72
		Spring weight, g	1.95	1.92	1.94	1.90	1.91	1.96
		Σ seat weight, g	1.15	1.13	1.14	1.14	1.15	1.12
Spacer tube, outer diameter = 0.188, inner diameter = 0.148	MAT 16	Length, in.	12.85	12.79	12.72	12.94	12.937	13.02
		Weight, g	17.160	16.840	16.722	17.28	17.05	17.174
Fuel cladding, end plugs and end caps[b]	Type 316 stainless steel Cladding, MAT 19 Plugs and caps, MAT 20	Σ weight, g	70.334	70.230	70.500	70.460	70.544	70.308
		Average cladding outer diameter,[b] in.	0.2496	0.2495	0.2497	0.2496	0.2497	0.2494
		Average cladding inner diameter,[b] in.	0.2177	0.2179	0.2178	0.2176	0.2177	0.2175
Loaded rod[c]								
Total weight, g			211.815	214.785	217.975	220.330	211.265	213.512
Overall length, in.			39.996	39.974	39.984	39.880	39.988	39.990
Center of gravity from bottom of rod, in.			16 5/8	16 19/32	16 9/16	16 1/2	16 5/8	16 9/16
Gas used in rod assembly, 1 cm^3 Xe + He balance, TOTAL			8.549	7.759	7.414	7.724	8.679	8.479
Total free void volume, cm^3			8.549	7.759	7.414	7.724	8.679	8.479
Approximate activity at 1 ft, gamma mr/hr			3	4	3	3	3	3
neutron			Nil	Nil	Nil	Nil	Nil	Nil

[a] 2.[illegible]3 g fine UO_2 microspheres (batch UF-1) around blanket pellets.

[b] 2.[illegible]2 g fine UO_2 microspheres (Batch UF-1) around blanket pellets.

[c] See Table 2[illegible] for detailed dimensional measurements of claddings and fuel pins.

Table 25. Dimensions (in Inches) of ORNL EBR-II Series II Fuel Pins

	Cladding Equivalent Number				
	19-37-A	19-60-B	19-26-A	19-59-B	19-53-A
Inner diameter over length,					
max	0.218	0.2182	0.2186	0.2188	0.2184
min	0.2168	0.2167	0.2174	0.2167	0.2170
Inner diameter ovality over length,					
max	0.0005	0.0004	0.001	0.0006	0.0008
Mean inner diameter over fuel length	0.2177	0.2178	0.2181	0.2182	0.2178
Inner diameter ovality over fuel length					
max	0.0005	0.0004	0.0004	0.0006	0.0008
Wall thickness over length,					
max	0.0161	0.0157	0.0156	0.0155	0.0167
min	0.0150	0.0148	0.0148	0.0149	0.0153
Wall thickness over fuel length,					
max	0.0160	0.0156	0.0156	0.0155	0.0166
min	0.0150	0.0149	0.0148	0.0149	0.0153
	Fuel Pin Number				
	OS-2	OS-3	OS-1	OS-4	OS-5
Outer diameter over cladding length,					
max	0.2499	0.2499	0.2501	0.2500	0.2502
min	0.2492	0.2490	0.2494	0.2492	0.2491
Outer diameter ovality over length,					
max	0.0005	0.0009	0.0006	0.00045	0.001
Outer diameter over fuel length,					
max	0.2499	0.2495	0.2499	0.2497	0.2497
min	0.2494	0.2494	0.2496	0.2495	0.2496
Outer diameter ovality over fuel length,					
max	0.0003	0.0001	0.0003	0.00015	0.0001
TIR,					
max	0.002	0.003	0.003	0.003	0.003
Overall length	39.984	39.990	39.988	40.030	39.983
Envelope diameter,					
max	0.2515	0.2515	0.2515	0.2515	0.2515

Table 25. continued

	Cladding Equivalent Number				
	19-52-A	19-23-A	19-7-A	19-60-A	19-6-C
Inner diameter over length,					
max	0.2185	0.2183	0.2182	0.2183	0.2181
min	0.2167	0.2173	0.2172	0.2168	0.2172
Inner diameter ovality over length,					
max	0.0007	0.0009	0.0006	0.0009	0.0007
Mean inner diameter over fuel length	0.2181	0.2180	0.2180	0.2178	0.2178
Inner diameter ovality over fuel length,					
max	0.0004	0.0004	0.0005	0.0005	0.0006
Wall thickness over length,					
max	0.0157	0.0159	0.0159	0.0156	0.0156
min	0.0148	0.0146	0.0153	0.0150	0.0148

	Fuel Pin Number				
	OS-6	OS-7	OS-8	OS-9	OS-10
Outer diameter over cladding length,					
max	0.2500	0.2502	0.2500	0.2501	0.2500
min	0.2496	0.2493	0.2493	0.2492	0.2491
Outer diameter ovality over length,					
max	0.0006	0.001	0.0004	0.0003	0.0009
Outer diameter over fuel length,					
max	0.2498	0.2497	0.2498	0.2497	0.2496
min	0.2496	0.2494	0.2495	0.2494	0.2493
Outer diameter ovality over fuel length,					
max	0.00015	0.0001	0.0002	0.0002	0.0002
TIR,					
max	0.005	0.005	0.006	0.003	0.007
Overall length	39.972	39.997	39.992	39.993	39.996
Envelope diameter,					
max	0.2515	0.2515	0.2515	0.2515	0.2515

Table 25. continued

	Cladding Equivalent Number				
	19-35-A	19-49-A	19-8-A	19-66-B	19-54-A
Inner diameter over length,					
max	0.2183	0.2185	0.2184	0.2182	0.2186
min	0.2172	0.2179	0.2172	0.2172	0.2172
Inner diameter ovality over length,					
max	0.0009	0.0004	0.0007	0.0009	0.0007
Mean inner diameter over fuel length	0.2177	0.2182	0.2178	0.2179	0.2177
Inner diameter ovality over fuel length,					
max	0.0005	0.0002	0.0006	0.0007	0.0006
Wall thickness over length,					
max	0.0163	0.0164	0.0162	0.0157	0.0167
min	0.0149	0.0151	0.0152	0.0150	0.0155
Wall thickness over fuel length,					
max	0.0162	0.0163	0.0160	0.0156	0.0165
min	0.0150	0.0152	0.0153	0.0150	0.0157
	Fuel Pin Number				
	OS-11	OS-12	OS-13	OP-1	OP-2
Outer diameter over cladding length,					
max	0.2508	0.2499	0.2497	0.2499	0.2503
min	0.2489	0.2489	0.2491	0.2495	0.2494
Outer diameter ovality over length,					
max	0.0019	0.0008	0.0002	0.0002	0.0005
Outer diameter over fuel length,					
max	0.2503	0.2498	0.2496	0.2496	0.2497
min	0.2494	0.2494	0.2494	0.2495	0.2495
Outer diameter ovality over fuel length,					
max	0.0008	0.0002	0.0001	0.0001	0.00015
TIR,					
max	0.003	0.005	0.007	0.005	0.005
Overall length	39.984	39.992	39.997	39.946	39.916
Envelope diameter,					
max	0.2515	0.2515	0.2515	0.2515	0.2515

Table 25. continued

	Cladding Equivalent Number				
	19-55-A	19-49-B	19-76-A	19-66-A	19-10-B
Inner diameter over length,					
max	0.2184	0.2182	0.2182	0.2183	0.2181
min	0.2170	0.2176	0.2175	0.2170	0.2172
Inner diameter ovality over length,					
max	0.0007	0.0006	0.0006	0.0009	0.0005
Mean inner diameter over fuel length	0.2178	0.2179	0.2176	0.2177	0.2178
Inner diameter ovality over fuel length,					
max	0.0007	0.0004	0.0004	0.0009	0.0004
Wall thickness over length,					
max	0.0157	0.0163	0.0165	0.0157	0.0156
min	0.0150	0.0153	0.0154	0.0149	0.0148
Wall thickness over fuel length,					
max	0.0156	0.0163	0.0165	0.0156	0.0156
min	0.0150	0.0153	0.0154	0.0149	0.0148
	Fuel Pin Number				
	OP-3	OP-4	OP-5	OP-6	OP-7
Outer diameter over cladding length,					
max	0.2500	0.2500	0.2501	0.2500	0.2502
min	0.2492	0.2490	0.2493	0.2492	0.2492
Outer diameter ovality over length,					
max	0.0006	0.0009	0.0005	0.0006	0.0008
Outer diameter over fuel length,					
max	0.2497	0.2495	0.2497	0.2497	0.2497
min	0.2495	0.2493	0.2493	0.2495	0.2496
Outer diameter ovality over fuel length,					
max	0.0001	0.0001	0.0003	0.0002	0.0001
TIR,					
max	0.005	0.004	0.006	0.005	0.005
Overall length	39.996	39.974	39.984	39.880	39.988
Envelope diameter,					
max	0.2515	0.2515	0.2515	0.2515	0.2515

Table 26. ORNL EBR-II Series II Fuel Chemical and Isotopic Composition

	PEL 90	PEL 85	SP85C	SPF	PELL 80	PELL 85	SPL 80/85	SPLF	SP80C
Uranium, wt %	70.32	70.39	70.40	68.97	70.58	70.43	69.86	69.60	69.35
Plutonium, wt %	17.93	17.67	17.72	17.46	17.51	17.68	18.22	17.86	17.93
Pu/U + Pu, wt %	20.32	20.07	20.11	20.20	19.88	20.07	20.69	20.42	20.54
Oxygen-to-metal ratio	1.970	1.980	1.976	1.988	OP-3, 1.957; OP-7, 1.961	1.955	1.961	1.965	1.985
Moisture, ppm	< 5	36	3	19	19	8	5	< 6	7
Gas release, cm^3/g	0.035	0.014	0.02	0.13	0.04	< 0.01	0.045	0.14	0.01
Density, % of theoretical			99.0	NM			93.7		NM
Nitrogen, ppm	130	16	30	20	45		83		
Carbon, ppm	24	< 15	44	93	< 20	< 20	< 20	a	b
Chloride, ppm	12	14	28	28	29		25		
Fluoride, ppm	5	20	14	21	20	25	15		
Uranium Isotopic									
233	≤ 0.001	< 0.0005	0.004	0.0004	< 0.0006	< 0.0005	< 0.0003	a	b
234	1.005	0.999	1.004	1.006	1.009	1.007	1.006		
235	92.75	92.76	93.02	92.93	93.04	92.75	93.16		
236	0.465	0.469	0.511	0.507	0.452	0.466	0.513		
237	5.78	5.77	5.46	5.56	5.50	5.78	5.32		
Plutonium Isotopic									
238	≤ 0.04	≤ 0.04	≤ 0.04		≤ 0.032	≤ 0.04	≤ 0.03	a	b
239	88.76	88.73	88.70	88.74	88.59	88.69	88.74		
240	9.96	9.98	10.00	9.94	10.10	10.02	9.98		
241	1.182	1.190	1.197	1.216	1.203	1.185	1.18		
242	0.101	0.102	0.103	0.101	0.107	0.102	0.103		
244	< 0.0005	< 0.0005	< 0.001	< 0.003	< 0.0005	< 0.0005	< 0.0002		
Oxygen-to-metal ratio	1.970	1.980	1.976	1.988	19-10-B, 1.961; 19-55-A, 1.957	1.955	1.961	1.965	1.985

[a]SPF analyses are representative of this material.

[b]SPL 80/85 analyses are representative of this material.

Table 27. Trace Metallic Impurities in ORNL EBR-II, Series II Fuel Pellets and Microspheres[a]

Element	Batch Identity														
	SP-85C		SPL 90/85	SPF		PEL-85		PEL-90					PEL-85	PELL-80	
	Sample 1[b]	Sample 2		Sample 1[c]	Sample 2	Sample 1[c]	Sample 2	Sample 1[c]	Sample 2	Sample 3	Sample 4	Sample 5[d]		Sample 1	Sample 2[d]
Al	> 1000	15	20	> 1000	1500	[illegible]	200	< 13	200	500	50	SNF	300	200	SNF
Be	NR	NR	NR	NR	NR		NR		NR				NR	NR	
Bi	NR	NR	< 1	NR	NR		< 1		< 1				< 1	< 1	
B	> 100	0.2	< 0.1	> 100	1	SNF[f]	0.7	SNF	0.2			SNF	0.2	0.2	SNF
Cd	NR	1	NR	NR	NR		NR		NR				NR	NR	
Ca	> 1000	30	20	> 1000	80		200		70				200	70	
Cr	70	15	1	70	300	130	100	< 7	300	120	120	60	300	100	< 10
Cu	10	2	2	8	6	VFT[g]	20	SNF	200				100	20	
Fe	1000	150	100	300	300	1900	300	< 13	≈ 5000	450	1400	270	1500	1000	< 200
Pb	NR	1	20	NR	25	SNF	70		70			SNF	200	10	SNF
Li	NR	NR	NR	NR	NR		NR		NR				NR	NR	
Mg	1000	2	5	> 1000	500		50		20				150	150	
Mn	5	NR	0.3	4	10	SNF	10	< 1.3	3	3	10	SNF	30	0.5	SNF
Mo	NR	2	20	NR	2	50	10	< 3	20			SNF	20	30	SNF
Ni	NR	25	50	NR	50	2200	500	< 7	~ 5000	380	1100	100	1000	~ 1500	110
Si	> 1000	40	20	> 1000	300	SNF	1000		3000	1000	> 3000	SNF	500	200	SNF
Ag	NR	NR	NR	20	NR		NR		NR				NR	NR	
Na	NR	0.2	< 0.5	NR	10		2		< 0.5				NR	< 0.5	
Sn	NR	NR	NR	NR	NR	SNF	NR	< 15	NR			SNF	NR	NR	SNF
Ti	NR	7	20	NR	30	40	20	< 2	20			VFT	100	500	VFT
V	NR	NR	0.3	NR	1		1	SNF	1			SNF	1	1	SNF
Zn	90	5	3	40	1000		50		5				100	70	

[a]Analysis by spark source mass spectrometer unless otherwise indicated.
[b]B, Ca, Mg, Si probably high due to contamination during dissolution.
[c]Emission spectrographic.
[d]Whole pellet dissolved – emission spectrographic.
[e]Not reported (generally < 1 ppm).
[f]Sought, not found.
[g]Very faint trace.

Table 28. ORNL EBR-II, Series II Blanket and Insulator Pellet and Fine UO_2 Microsphere Characterization

Material Type Batch Number	UO_2 Blanket Pellets ORNL B-1	ThO_2 Insulator Pellets ORNL I-1	Fine UO_2 Microspheres UF-1
Oxygen-to-metal ratio	2.002	NM[a]	2.005
Moisture, ppm	8	31	20
Gas release, cm^3/g	0.02	0.014	0.04
Nitrogen, ppm	19	4	15
Carbon, ppm	8	4	7
Chloride, ppm	14	13	2
Fluoride, ppm	< 2	12	6.5

[a]NM — Not measured because of the known characteristics of this material in attaining an oxygen-to-metal ratio of 2.00.

Table 29. Trace Metallic Impurities in ORNL EBR-II, Series II Blanket and Insulator Pellets and Fine UO_2 Microspheres

Material Type Batch Number	UO_2 Blanket Pellets ORNL B-1	ThO_2 Insulator Pellets ORNL I-1	Fine UO_2 Microspheres UF-1
Al	100	50	50
Bi	NR[a]	NR	NR
B	0.4	30	2
Cd	NR	NR	NR
Ca	100	950	50
Cr	20	5	10
Cu	0.3	9	20
Fe	200	30	100
Pb	NR	NR	3
Li	NR	NR	NR
Mg	8	4	5
Mn	0.6	2	1
Mo	NR	2.5	NR
Ni	7	7	3
Si	20	50	100
Ag	NR	NR	NR
Na	< 0.3	4.5	100
Sn	NR	NR	< 0.4
V	2	0.3	NR
Zn	NR	8	30

[a]NR — Not reported (probable value < 1 ppm).

Table 30. Characterization of Fiberfrax Used in ORNL EBR-II, Series II

Batch MAT8-H134		
Spectrographic Analysis, %		
B	0.3	
Na	0.2	
Gas release, cm^3/g		0.536

Table 31. Chemical Analyses of Metallic Components of ORNL EBR-II, Series II Fuel Pins

Material Use and Identification	Cladding Tube MAT-19			End Plugs, End Caps, Spring Seats MAT-20		
Requirement[a] Material Type	Specified	Vendor's Report Type 316 Stainless Steel	ORNL Check	Specified	Vendor's Report Type 316 Stainless Steel	ORNL Check
C	0.08 max	0.054	0.061	0.08 max	0.04	0.038
Si	0.75 max	0.47	0.53	1.00 max	0.47	0.44
Mn	2.0 max	1.44	1.42	2.0 max	1.59	1.31
Cr	16.0–18.0	16.5	16.0	16.0–18.0	16.5	16.4
Ni	12.0–14.0	13.3	13.4	10.0–14.0	13.1	12.9
Mo	2.0–3.0	2.4	2.11	2.0–3.0	2.68	2.48
P	0.03 max	0.013	0.008	0.045 max	0.011	0.006
S	0.03 max	0.006	0.004	0.030 max	0.010	0.007
Nb						
Ti						
Al						
V		B < 0.001			B < 0.0001	
Co		0.04				
Cu		0.05			0.03	
Fe						
Tensile strength, KIPS						
Ultimate	75 min	89.8		90	90.4	
0.2%	30 min	41.1		45	73.5	
Elongation, %	35 min	47.5		35	39.5	
Reduction in area, %				45	77	
Hardness		63 R/B			95/97 R/B	

Table 31. continued

Material Use and Identification	Spacer Tube MAT-16			Capillary Tubing MAT-41		
Requirement[a] Material Type	Specified	Vendor's Report Type 304 Stainless Steel	ORNL Check	Specified	Vendor's Report Type 304 Stainless Steel	ORNL Check
C	0.08 max	0.059	0.049	0.08 max	0.05	0.081
Si	0.75 max	0.57	0.52	1.00 max	0.50	0.47
Mn	2.00 max		1.60	2.00 max	1.64	1.60
Cr	18.0–20.0	18.3	18.1	18.0–20.0	18.7	18.8
Ni	8.0–11.0	9.9	9.6	8.0–12.0	9.8	9.8
Mo		0.33		0.5 max	0.28	
P	0.04 max	0.024	0.011	0.030 max	0.024	0.014
S	0.03 max	0.011	0.013	0.030 max	0.025	0.022
Nb						
Ti						
Al						
V						
Co						
Cu					0.19	
Fe						
Tensile strength, KIPS						
Ultimate				115 max	112.8	
0.2%		42.2		30 min	56.4	
Elongation, %		64		35 min	55.0	
Reduction in area, %						
Hardness						

	Shielding Rod MAT-37			Spring MAT-38		
	Specified	Vendor's Report Nickel	ORNL Check	Specified	Vendor's Report Inconel X-750	ORNL Check
C	0.15 max		0.12	0.08 max		0.01
Si	0.35 max		0.03	0.5 max		
Mn	0.35 max		0.25	1.0 max		0.2
Cr			0.005	14.0–17.0		15.3
Ni	99.0 min		99.46 by difference	70 min		72.35
Mo	0.01 max		0.01			0.2
P						
S	0.01 max		0.004	0.015		0.012
Nb				0.7–1.2 (Cb+Ta)		0.85
Ti				2.25–2.75		2.1
Al				0.4–1.0		0.66
V						0.02
Co			0.03	1.0 max		0.10
Cu	0.25 max		0.03	0.5 max		0.20
Fe	0.40 max		0.05	5–9		7.92
Tensile strength, KIPS						
Ultimate				140		
0.2%				90		
Elongation, %				8		
Reduction in area, %						
Hardness, BHN				262 min		

[a]Chemical analyses in weight percent.

Table 32. Metallic Component Certification[a]

MAT-19	Stainless steel tubing, ASTM A213, type 316, 0.250-in.-OD, 218-in.-ID, solution annealed and straightened. Chemistry: (ASTM E59) ladle and check analyses; mechanical properties ASTM A213, dye-penetrant inspection; MET-NDT-4 ultrasonic inspection; RDT-F3-8T, MET-FR-4. Use: clad tube.
MAT-16	Stainless steel tubing, ASTM A269, type 304, 3/16-in.-OD × 0.020-in. wall. Chemistry: (ASTM E59) ladle and check analyses; mechanical properties (no requirement on ASTM A269). Use: spacer tube.
MAT-20	Stainless steel rod, ASTM A276, type 316, 1/4-in.-diam, solution annealed, cold drawn, bright annealed. Chemistry: (ASTM E59) ladle and check analyses; mechanical properties ASTM A276. Use: bottom end plug, top end plug, top end cap, spring seats.
MAT-41	Stainless steel capillary tubing, MIL-T-8504, type 304, 0.062-in.-diam × 0.10-in. wall. Chemistry: ASTM E59. Use: capillary tube.
MAT-37	High-purity metal rod, ASTM B160, 1/4-in.-diam rod. Chemistry: ASTM E59. Use: shielding rod.
MAT-38	Inconel X-750 wire, MET-FR-3, RDT M8-1T, 1/32-in.-diam. Chemistry: ASTM E59. Use: spring.

[a]It is certified that all materials listed in the table met the listed specifications and inspection.

Tubing for Cladding (MAT-19). — We certify that the inspection and testing procedures described in Section VIII.A.1(b) of the Guide were followed with satisfactory results. Chemical analyses performed by the vendor and by ORNL are summarized in Table 31. Results of mechanical properties tests are also given in Table 31. Metallography of the tubing is provided in Appendix B.

We certify that archive samples of the tubing (MAT-19) are available for the EBR-II Project.

End Fittings (MAT-20). — We certify that the inspection and testing procedures described in Section VIII.A.2(b) of the Guide were followed with satisfactory results. Chemical analyses performed by the vendor and by ORNL are summarized in Table 31; results of mechanical properties tests are also given in Table 31. Metallography of the material used for end fittings is provided in Appendix B.

We certify that archive samples of the end fitting materials (MAT-20) are available for the EBR-II Project.

Welds of End Fittings to Cladding Tube. – We certify the welding procedure described in Section VIII.A.3(a) was followed on the welds and (b) that the welds meet the acceptance critera of Section VIII.A.3 of the Guide. Photomicrographs showing the appearance of qualification welds on W-1, W-2, W-3, W-4, and W-5 are provided in Appendix B.

Representative sample welds (two each of top and bottom closure welds) have been shipped under separate cover to the Irradiation Coordinator. A summary of all weld repair is given in Appendix B.

Radiographs of closure welds for each fuel pin (OS-1 through OS-13, and OP-1 through OP-7) have been shipped to the Irradiation Coordinator under separate cover:

With use of shape correction form, 0 and 90° orientations of welds W-1, W-3, and W-5, and

Without use of shape correction form, 0, 60, and 120° orientations of welds W-1, W-3, and W-5.

Each radiograph is identified by use of lead numbers and letters during exposure as to cladding equivalent number, weld number, orientation, and date of exposure. These welds were radiographed per ORNL Inspection Engineering Standards, Section 3, and ASTM Technical Publication No. 223 (Symposium on Nondestructive Testing in the Field of Nuclear Energy). A duplicate set of these radiographs is filed at ORNL.

Helium Leak Testing. – A leak test was performed in accordance with ORNL Inspection Engineering Standards, Section 7, on each fuel pin. The results of these tests are given in Table 33. No detectable leaks were found. The sensitivity of the leak test system was at least 2×10^{-9} cm^3/sec. Test data showing the system sensitivity on each day that fuel pins were tested are given in Table 33.

Xenon Tag Insertion. – We certify that the requirement of 1 ± 0.25 cm^3 special isotopic mixture xenon gas insertion in each fuel pin void space has been accomplished as required in Section IX of the Guide.

The procedures for inserting the xenon tags were submitted to the EBR-II Project on January 9, 1970.

The initial xenon tagging operation was observed by W. J. Larson on June 2, 1970.

Table 33. EBR-II, Series II Fuel Pins Helium Leak Test Results[a]

Fuel Pin Numbers	Date of Test	System Sensitivity (cm^3/sec)	Measured Leak Rate (cm^3/sec)
	Bottom Closure Welds		
OS-13, OS-7, OS-1, OS-11	4/14/70	3.4×10^{-10}	$< 3.4 \times 10^{-10}$
OS-2, OS-6, OS-9	4/14/70	3.4×10^{-10}	$< 3.4 \times 10^{-10}$
OS-3, OS-10	4/14/70	3.4×10^{-10}	$< 3.4 \times 10^{-10}$
OS-8, OS-12, OS-5, OP-2	4/27/70	1.5×10^{-10}	$< 1.5 \times 10^{-10}$
OP-3, OP-6, OP-5, OP-7	4/27/70	1.5×10^{-10}	$< 1.5 \times 10^{-10}$
OP-4, OS-4, OP-1	4/27/70	1.5×10^{-10}	$< 1.5 \times 10^{-10}$
	Finished Pins		
OS-2	6/4/70	4.0×10^{-10}	$< 4.0 \times 10^{-10}$
OS-6	6/8/70	1.6×10^{-10}	$< 1.6 \times 10^{-10}$
OP-5	7/15/70	9.0×10^{-10}	$< 9.0 \times 10^{-10}$
OP-1	7/21/70	6.0×10^{-10}	$< 6.0 \times 10^{-10}$
OS-10, OS-13	7/22/70	4.0×10^{-10}	$< 4.0 \times 10^{-10}$
OS-7	7/23/70	6.0×10^{-10}	$< 6.0 \times 10^{-10}$
OP-3	7/28/70	4.5×10^{-10}	$< 4.5 \times 10^{-10}$
OP-7, OP-2	7/29/70	5.1×10^{-10}	$< 5.1 \times 10^{-10}$
OP-4	7/31/70	6.0×10^{-10}	$< 6.0 \times 10^{-10}$
OS-4	8/4/70	6.0×10^{-10}	$< 6.0 \times 10^{-10}$
OP-6, OS-5	8/5/70	1.0×10^{-9}	$< 1.0 \times 10^{-9}$
OS-11, OS-12	8/6/70	2.0×10^{-10}	$< 2.0 \times 10^{-10}$
OS-1, OS-3, OS-8, OS-9	9/22/70	2.0×10^{-10}	$< 2.0 \times 10^{-10}$

[a]As per MET-FCT-OP-9, paragraph 4.

Two tagged dummy elements have been shipped under separate cover (are being shipped with fuel pins) to the Irradiation Coordinator. One of these was filled just prior to tagging the first fuel pin. The other was filled just following the tagging of the last fuel pin.

Bond Tests (Sodium-Bonded Fuel Elements). — Does not apply.

Spacer Wire Attachment. — Spacer wires will be attached by the EBR-II Project.

Dimensional Inspections. — The dimensional inspection procedures, descriptions of gages, and requirements for gage calibration are referenced in Appendix B.

As-built dimensional data on the fuel pins are given in Tables 24 and 25, pp. 58–60.

Fuel Element Weights. — The procedure used for calibrating the balances is referenced in Appendix B.

The weight of each as-built fuel pin is given in Table 24.

Fuel Element Assembly Radiographs (by the Experimenter). — Radiographs of each fuel pin showing the arrangement and condition of internal parts were made in accordance with ORNL Inspection Engineering Standards, Section 3. Copies of these radiographs have been sent under separate cover to the Irradiation Coordinator. Duplicate films are on file at ORNL.

Fabrication and Testing of B&W Unencapsulated Fuel Pins

Description of Fuel Pin

The Babcock & Wilcox fuel pin is similar in design to the ORNL fuel pin described in this document. Detailed features and dimensions of these pins are described in Drawing NDC 1730 D-1. A reproduced copy of this drawing is included as Fig. 2, p. 10. The "as-built" data for each fuel pin are presented in Table 34. Design values common to all fuel pins are summarized as follows:

Fuel form	Sphere-Pac, Vi-Pac, or sintered pellet
Fuel composition, wt %	80 UO_2–20 PuO_2
Enrichment, wt %	93 ^{235}U in U
Fuel diameter	0.218-in. OD, Sphere-Pac and Vi-Pac 0.205-in. OD, pellet
Fuel column length, in.	13.5
Average fuel smear density, % of theoretical	80 ± 2
Blanket material	Depleted UO_2 pellets
Reflector material	Nickel
Spring material	Type 302 stainless steel
Plenum tube material	Type 316 stainless steel

Table 34. As-Built Description of Each Babcock & Wilcox EBR-II Fuel Pin

Fuel Pin Identification Number	D-2	D-4	D-5	D-9	D-10	D-12
Fuel	$(U,Pu)O_2$	$(U,Pu)O_2$	$(U,Pu)O_2$	$(U,Pu)O_2$	$(U,Pu)O_2$	$(U,Pu)O_2$
Fabrication	Sphere-Pac	Pellet	Vi-Pac	Pellet	Sphere-Pac	Pellet
Pu/(U+Pu), wt %	19.96	20.20	20.10	20.20	19.96	20.20
$^{235}U/U$	92.68	92.68	92.68	92.68	92.68	92.68
$(^{239}Pu+^{241}Pu)/Pu$	91.53	91.53	91.53	91.53	91.53	91.53
Length, in.	13.55	13.458	13.518	13.494	13.51	13.483
Diameter, in.	0.218	0.205	0.218	0.205	0.218	0.205
Weight, g	71.19	74.82	70.98	75.01	71.10	75.00
Smear density, % of theoretical	78.26	82.50	78.18	82.78	78.40	82.73
Distance from top of fuel column to top of tube, in.	17 5/16	17 5/8	17 7/16	17 19/32	17 3/8	17 5/8
Blanket Material	UO_2	UO_2	UO_2	UO_2	UO_2	UO_2
Fabrication	Pellet	Pellet	Pellet	Pellet	Pellet	Pellet
Length, in.	6.104	6.059	5.965	6.059	6.058	6.060
Diameter, in.	0.214	0.214	0.214	0.214	0.214	0.214
Weight, g	36.96	37.055	36.993	37.054	37.18	37.082
Length of Bottom Fiberfrax Pad, in.	1/4	1/16	1/4	1/16	1/4	1/16
Bottom Insulators	UO_2	UO_2	UO_2	UO_2	UO_2	UO_2
Fabrication	Pellets	Pellets	Pellets	Pellets	Pellets	Pellets
Length, in.	0.508	0.507	0.506	0.501	0.486	0.490
Diameter, in.	0.214	0.214	0.214	0.214	0.214	0.214
Weight, g	3.056	3.095	3.046	3.116	3.000	2.982
Top Insulators	UO_2	UO_2	UO_2	UO_2	UO_2	UO_2
Fabrication	Pellets	Pellets	Pellets	Pellets	Pellets	Pellets
Length, in.	0.495	0.501	0.494	0.500	0.508	0.505
Diameter, in.	0.214	0.214	0.214	0.214	0.214	0.214
Weight, g	3.017	3.095	3.043	3.078	3.067	3.104
Length of Top Fiberfrax Pad, in.	3/32	1/16	1/16	1/16	3/32	1/16
Nickel Reflector						
Length, in.	2.221	2.221	2.218	2.219	2.219	2.220
Diameter, in.	0.210	0.210	0.211	0.211	0.210	0.210
Weight, g	10.18	10.17	10.20	10.20	10.1[illegible]	10.20
Spring						
Free length, in.	4.500	4.475	4.500	4.525	4.525	4.525
Diameter, in.	0.208	0.209	0.208	0.207	0.209	0.207
Weight, g	3.30	3.28	3.24	3.27	3.31	3.29
Plenum Tube						
Length, in.	10.497	10.497	10.505	10.496	10.499	10.501
Diameter, in.	0.187	0.187	0.187	0.187	0.187	0.187
Weight, g	11.23	11.29	11.26	11.23	11.30	11.27
Clad Tube						
Length, in.	37.866	37.862	37.863	37.864	37.859	37.864
Maximum deviation from nominal 0.250 in. OD, in.	−0.0004	−0.0006	−0.0006	−0.0009	−0.0008	−0.0007
Maximum deviation from nominal 0.218 in. ID, in.	+0.0003	+0.0004	+0.0004	−0.0003	+0.0006	−0.0002
Minimum wall thickness, in.	0.0155	0.0152	0.0150	0.0150	0.0151	0.0150
Fuel Pin						
Length, in.	39.978	39.967	39.979	39.972	39.957	39.967
Maximum outside diameter, in.	0.2497	0.2495	0.2497	0.2502	0.2497	0.2500
Minimum outside diameter, in.	0.2491	0.2490	0.2490	0.2492	0.2491	0.2492
Straightness, TIR, in.	0.0025	0.003	0.007	0.004	0.005	0.004

Table 34. continued

Fuel Pin (continued)						
Total weight of fuel pin, g	211.0	214.1	208.8	214.8	210.2	214.7
Smearable alpha activity, dpm/100 cm^2	29	< 10	< 10	< 10	< 10	< 10
Fuel Pin Identification Number	D-14	D-17	D-18	D-19	D-20	D-21
Fuel	$(U,Pu)O_2$	$(U,Pu)O_2$	$(U,Pu)O_2$	$(U,Pu)O_2$	$(U,Pu)O_2$	$(U,Pu)O_2$
Fabrication	Pellet	Pellet	Vi-Pac	Sphere-Pac	Vi-Pac	Vi-Pac
Pu/(U+Pu), wt %	20.20	20.20	20.10	19.96	20.10	20.10
$^{235}U/U$	92.68	92.68	92.68	92.68	92.68	92.68
$(^{239}Pu+^{241}Pu)/Pu$	91.53	91.53	91.53	91.53	91.53	91.53
Fuel						
Length, in.	13.458	13.457	13.541	13.55	13.490	13.482
Diameter, in.	0.205	0.205	0.218	0.218	0.218	0.218
Weight, g	74.74	74.76	71.07	71.14	70.58	70.66
Smear density, % of theoretical	82.92	82.79	78.15	78.21	77.90	78.03
Distance from top of fuel column to top of tube, in.	17 19/32	17 9/16	17 3/8	17 9/32	17 15/32	17 13/32
Blanket Material	UO_2	UO_2	UO_2	UO_2	UO_2	UO_2
Fabrication	Pellet	Pellet	Pellet	Pellet	Pellet	Pellet
Length, in.	6.060	6.060	6.058	6.047	6.049	6.058
Diameter, in.	0.214	0.214	0.214	0.214	0.214	0.214
Weight, g	37.144	37.164	37.149	36.97	37.230	37.034
Length of bottom Fiberfrax pad, in.	1/16	1/16	1/4	1/4	1/4	1/4
Bottom Insulators	UO_2	UO_2	UO_2	UO_2	UO_2	UO_2
Fabrication	Pellet	Pellet	Pellet	Pellet	Pellet	Pellet
Length, in.	0.501	0.499	0.500	0.500	0.505	0.496
Diameter, in.	0.214	0.214	0.214	0.214	0.214	0.214
Weight, g	3.113	3.086	3.078	3.100	3.074	3.058
Top Insulators	UO_2	UO_2	UO_2	UO_2	UO_2	UO_2
Fabrication	Pellets	Pellets	Pellets	Pellets	Pellets	Pellets
Length, in.	0.502	0.496	0.504	0.500	0.494	0.500
Diameter, in.	0.214	0.214	0.214	0.214	0.214	0.214
Weight, g	3.100	3.076	3.063	3.106	3.054	3.114
Length of top Fiberfrax pad, in.	1/16	1/16	1/16	3/32	1/16	1/16
Nickel Reflector						
Length, in.	2.218	2.220	2.220	2.219	2.221	2.221
Diameter, in.	0.211	0.210	0.211	0.210	0.210	0.210
Weight, g	10.18	10.19	10.20	10.18	10.18	10.19
Spring						
Free length, in.	4.500	4.525	4.500	4.475	4.525	4.475
Diameter, in.	0.206	0.204	0.208	0.208	0.207	0.209
Weight, g	3.23	3.21	3.23	3.20	3.29	3.25
Plenum Tube						
Length, in.	10.500	10.498	10.503	10.500	10.497	10.497
Diameter, in.	0.187	0.187	0.187	0.187	0.187	0.187
Weight, g	11.24	11.24	11.27	11.26	11.23	11.25
Clad Tube						
Length, in.	37.863	37.862	37.863	37.863	37.865	37.864
Maximum deviation from nominal 0.250 in. OD, in.	−0.001	−0.0005	−0.0005	−0.0002	−0.0006	−0.0005
Maximum deviation from nominal 0.218 in. ID, in.	−0.0003	−0.0003	+0.0002	+0.0008	+0.0002	+0.0009
Minimum wall thickness, in.	0.0152	0.0151	0.0154	0.0151	0.0151	0.0150
Fuel Pin						
Length, in.	39.959	39.971	39.976	39.965	39.965	39.974
Maximum outside diameter, in.	0.2500	0.2506	0.2496	0.2502	0.2500	0.2500

Table 34. continued

Fuel Pin (continued)						
Minimum outside diameter, in.	0.2485	0.2495	0.2491	0.2490	0.2490	0.2493
Straightness, TIR, in.	0.005	0.005	0.0035	0.0025	0.0055	0.0065
Total weight, g	214.1	214.5	210.7	210.2	210.0	209.6
Smearable alpha activity, dpm/100 cm^2	25	< 10	17	41	< 10	< 10
Fuel Pin Identification Number	D-22	D-25	D-27	D-29	D-30	D-31
Fuel	$(U,Pu)O_2$	$(U,Pu)O_2$	$(U,Pu)O_2$	$(U,Pu)O_2$	$(U,Pu)O_2$	$(U,Pu)O_2$
Fabrication	Vi-Pac	Vi-Pac	Sphere-Pac	Sphere-Pac	Sphere-Pac	Sphere-Pac
Pu/(U+Pu), wt %	20.10	20.10	19.96	19.95	19.96	19.96
$^{235}U/U$	92.68	92.68	92.68	92.68	92.68	92.68
$(^{239}Pu+^{241}Pu)/Pu$	91.53	91.53	91.53	91.53	91.53	91.53
Fuel						
Length, in.	13.554	13.501	13.49	13.48	13.59	13.53
Diameter, in.	0.218	0.218	0.218	0.218	0.218	0.218
Weight, g	71.00	68.96	71.19	70.87	71.20	71.17
Smear density, % of theoretical	77.99	76.05	78.61	78.32	78.28	78.36
Distance from top of fuel column to top of tube, in.	17 11/32	17 15/32	17 3/8	17 3/8	17 11/32	17 3/8
Blanket Material	UO_2	UO_2	UO_2	UO_2	UO_2	UO_2
Fabrication	Pellet	Pellet	Pellet	Pellet	Pellet	Pellet
Length, in.	6.044	6.056	6.053	6.058	6.056	6.043
Diameter, in.	0.214	0.214	0.214	0.214	0.214	0.214
Weight, g	36.93	37.100	37.17	37.07	37.16	37.15
Length of bottom Fiberfrax pad, in.	1/4	1/4	1/4	1/4	1/4	1/4
Bottom Insulators	UO_2	UO_2	UO_2	UO_2	UO_2	UO_2
Fabrication	Pellet	Pellet	Pellet	Pellet	Pellet	Pellet
Length, in.	0.499	0.482	0.500	0.514	0.499	0.501
Diameter, in.	0.214	0.214	0.214	0.214	0.214	0.214
Weight, g	3.096	3.002	3.084	3.040	3.112	3.109
Top Insulators	UO_2	UO_2	UO_2	UO_2	UO_2	UO_2
Fabrication	Pellet	Pellet	Pellet	Pellet	Pellet	Pellet
Length, in.	0.500	0.496	0.509	0.507	0.510	0.499
Diameter, in.	0.214	0.214	0.214	0.214	0.214	0.214
Weight, g	3.074	3.084	3.063	3.088	3.130	[illegible]
Length of top Fiberfrax pad, in.	1/16	1/16	3/32	3/32	3/32	3/32
Nickel Reflector						
Length, in.	2.221	2.220	2.221	2.220	2.222	[illegible]
Diameter, in.	0.210	0.210	0.211	0.210	0.210	0.211
Weight, g	10.19	10.18	10.20	10.18	10.20	10.20
Spring						
Free length, in.	4.450	4.500	4.500	4.525	4.500	4.500
Diameter, in.	0.207	0.208	0.209	0.207	0.208	0.207
Weight, g	3.24	3.24	3.30	3.27	3.27	3.24
Plenum Tube						
Length, in.	10.499	10.500	10.497	10.498	10.501	10.49[illegible]
Diameter, in.	0.187	0.187	0.187	0.187	0.187	0.187
Weight, g	11.26	11.23	11.23	11.25	11.26	11.26
Cladding Tube – Type 316 Stainless Steel						
Length, in.	37.864	37.864	37.865	37.865	37.865	37.864
Maximum deviation from nominal 0.250 in. OD, in.	−0.0005	−0.0006	−0.0003	−0.0009	−0.0005	−0.0003
Maximum deviation from nominal 0.214 in. ID, in.	+0.0005	+0.0003	+0.0007	+0.0002	+0.0008	+0.0008
Minimum wall thickness, in.	0.0151	0.015	0.002	0.0155	0.0152	0.0152
Fuel Pin						
Length, in.	39.977	39.964	39.976	39.983	39.977	39.972
Maximum outside diameter, in.	0.2500	0.2498	0.2502	0.2498	0.2500	0.2495
Minimum outside diameter, in.	0.2492	0.2490	0.2492	0.2490	0.2492	0.2480
Straightness, TIR, in.	0.003	0.005	0.002	0.002	0.003	0.005
Total weight, g	209.9	208.3	210.9	210.5	211.2	210.6
Smearable alpha activity, dpm/100 cm^2	25	< 10	< 10	< 10	17	17

End cap material	Type 316 stainless steel ASTM-276-67 and ASTM 484-65
Cladding material	Type 316 stainless steel ASTM A213 except tolerances
Cladding dimensions	0.250 in. OD × 0.218 in. ID
Gas volume at room temperature	7.8 cm^3, Sphere-Pac and Vi-Pac 8.2 cm^3, pellet
Gas pressure at room temperature, atm	1.1

Fuel Material

The fuel consists of hypostoichiometric UO_2–20% PuO_2 fabricated by three different processes. These fabrication processes are: (1) Sphere-Pac pins made from sol-gel-derived microspheres; (2) Vi-Pac pins made from angular particles prepared from coprecipitated oxide powder; and (3) pellet pins containing sintered pellets made from coprecipitated oxide powders. For each fuel form the UO_2 is fully enriched in ^{235}U. The isotopic composition of the fuels is presented in Table 35. Complete chemical characterization data for both the fuel and blanket material are presented in Tables 36, 37, 38, and 39. The blanket and insulator material in all fuel pins consist of depleted UO_2 pellets.

Table 35. Isotopic Compositions of B&W EBR-II Fuel

Plutonium[a]	
^{238}Pu, wt %	0.047
^{239}Pu, wt %	90.497
^{240}Pu, wt %	8.344
^{241}Pu, wt %	1.033
^{242}Pu, wt %	0.079
Uranium[b]	
^{234}U, wt %	0.99 + 0.01
^{235}U, wt %	92.68 ± 0.05
^{236}U, wt %	0.38 ± 0.01
^{238}U, wt %	5.95 ± 0.03

[a]Analysis performed on June 21, 1968.

[b]Analysis performed on July 10, 1968.

Table 36. EBR-II Fuel Characterization

Analysis	Fully Enriched $(U,Pu)O_2$[a]			
	Pellets	Shards (Vi-Pac)	Microspheres	
			Coarse 420–590 μm	Fine < 44 μm
Pu/(Pu+U), wt %	20.20 ± 0.04	20.10 ± 0.15	20.51 ± 0.05	19.16 ± 0.06
^{235}U content, wt %	92.68[b]	92.68[b]	92.68[b]	92.68[b]
Oxygen to metal atom ratio	1.983 ± 0.003	1.980 ± 0.005	1.992 ± 0.006	1.993 ± 0.004
Moisture, ppm oxide	2.4 ± 1.0	42.5 ± 12.9	53.5 ± 9.2	88.2 ± 2.0
Sorbed gas, cm^3/g	0.0053	0.045	0.033[c]	0.033[c]
Density, % of theoretical	93.0 ± 2.0	91.0	91.5	NM
Nitrogen, ppm metal	23.8 ± 2.7	35.2 ± 9.2	10.5 ± 5.8	6.5 ± 0.9
Carbon, ppm metal	17.2 ± 6.8	70.5 ± 11.5	6.8 ± 0.8	14.0 ± 3.9
Chloride, ppm metal	16.2 ± 3.7	12.7 ± 0.6	2.6 ± 0.8	4.7 ± 0.7
Fluoride, ppm metal	13.0 ± 4.3	6.6 ± 1.9	0.9 ± 0.2	2.6 ± 0.6

[a]Errors are for 95% confidence limits on the mean.

[b]^{235}U content determined by AVCO.

[c]Sorbed gas analysis was performed on a mixture of 73 wt % coarse and 27 wt % fine microspheres in order to simulate the fuel composition in a pin.

Table 37. Trace Metallic Impurities in EBR-II Fuel[a]

Element	Fully Enriched $(U,Pu)O_2$			
	Pellets	Shards (Vi-Pac)	Microspheres	
			Coarse 420–590 μm	Fine < 44 μm
Aluminum	300	330	320	320
Beryllium	< 0.5	< 0.5	< 0.5	< 0.5
Bismuth	< 1	< 1	< 0.5	< 0.5
Boron	< 0.3	< 0.3	1.0	< 0.5
Cadmium	< 0.5	< 0.5	3	< 0.5
Calcium	120	120	50	22
Chromium	12	18	45	330
Copper	75	19	10	< 5
Iron	65	80	260	140
Lead	< 2	< 2	2	1
Lithium	< 1	< 1	1	1
Magnesium	6	15	9	16
Manganese	< 4	< 4	8	32
Nickel	< 10	< 10	< 50	< 50
Silicon	150	450	125	230
Silver	< 0.5	< 0.5	< 0.5	< 0.5
Sodium	< 10	< 10	80	320
Tin	< 2	< 2	< 2	< 2
Titanium	9	27	6	17
Vanadium	< 2	< 2	< 5	< 5
Zinc	< 50	< 50	< 30	< 30

[a]Errors are for 95% confidence limits on the mean.

Table 38. EBR-II Blanket and Insulator Pellet Characterization[a]

^{235}U content, wt %	0.7[b]	0.7[b]	0.7[b]
Oxygen to metal atom ratio	2.007 ± 0.000	2.007 ± 0.000	2.007 ± 0.000
Moisture, ppm oxide	10.3 ± 2.2	3.2 ± 0.7	1.1 ± 0.6
Sorbed gas, cm^3/g	0.004	0.005	0.005
Nitrogen, ppm metal	24.0 ± 11.7	23.8 ± 4.4	23.7 ± 3.9
Carbon, ppm metal	13.8 ± 11.4	12.2 ± 9.1	10.5 ± 5.3
Chloride, ppm metal	2.6 ± 0.9	6.3 ± 2.0	6.8 ± 2.4
Fluoride, ppm metal	0.5 ± 0.3	0.7 ± 0.4	2.6 ± 1.2

[a]Errors are for 95% confidence limits on the mean.

[b]^{235}U content was not determined, but should be less than normal.

Table 39. Trace Metallic Impurities in EBR-II Blanket and Insulator Pellets[a]

Element	Firing 1	Firing 2	Firing 3
Aluminum	< 15	< 15	< 15
Bismuth	< 2	< 2	< 2
Boron	0.5	0.4	0.3
Cadmium	< 0.3	< 0.3	< 0.3
Calcium	55	40	40
Chromium	100	47	26
Copper	4	3	< 2
Iron	130	150	67
Lead	< 2	< 2	< 2
Lithium	< 2	< 2	< 2
Magnesium	< 3	< 3	7
Manganese	< 6	< 6	< 6
Molybdenum	21	16	< 3
Nickel	< 10	< 10	< 10
Silicon	15	16	26
Silver	< 0.25	< 0.25	< 0.25
Sodium	15	19	59
Tin	22	15	6
Vanadium	< 3	< 3	< 3
Zinc	< 50	< 50	< 50

[a]Values given are in parts per million of metal and are the mean of four determinations.

Tubing for Cladding

Procurement Specifications. — Cladding for these fuel pins is type 316 stainless steel tubing which is 0.250 ± 0.001-in. OD with a 0.016 ± 0.001-in.-thick wall. This tubing was obtained from BNWL and is from the same lot as that used by ORNL for their fuel pin cladding. This material was purchased by BNWL from Carpenter Steel Company to ASTM Specification A213 (except tolerances) and BNWL purchase order number B9S-777-47372. All tubing was fabricated from Carpenter Steel Company heat 87210. Results of an independent chemical analysis performed by National Spectrographic Laboratories are presented in Table 40. Independent tensile data on the tubing is presented in Table 41.

Table 40. Alloy Composition of Type 316 Stainless Steel Cladding and Type 316 Stainless Steel End Plug Material

Element	Type 316 Stainless Steel Cladding Composition, wt %		Type 316 Stainless Steel End Plug Composition, wt %	
	Specification Limits	Independent[a] Analysis	Specification Limits	Independent[a] Analysis
Carbon	0.04 to 0.06	0.054	0.08 max	0.048
Magnanese	1.00 to 2.00	1.51	1.00 to 2.00	1.30
Phosphorus	0.03 max	0.013	0.03 max	0.013
Sulfur	0.03 max	0.006	0.03 max	0.006
Silicon	0.75 max	0.46	0.75 max	0.45
Nickel	12.0 to 14.0	13.29	12.0 to 14.0	13.18
Chromium	16.0 to 18.0	16.81	16.0 to 18.0	16.70
Molybdenum	2.00 to 3.00	2.46	2.00 to 3.00	2.49
Copper	0.20 max	0.07	0.50 max	0.04
Boron	0.0010 max	0.0006	0.002 max	0.0006
Nitrogen	0.02 to 0.03	0.0074	0.06 max	0.0072
Cobalt		0.045		0.026
Iron	Balance	Balance	Balance	Balance

[a]Analyzed by National Spectrographic Laboratories, Inc.

Table 41. Tensile Test Data[a,b] on Cladding Material

Tube Number	Temperature	Strength, psi		Total Elongation (%)
		Yield 0.2% Offset	Ultimate	
16	Room	37,600	88,900	56
35	Room	35,700	84,100	59
53	Room	36,300	85,500	57

[a]Tensile tests performed by the Babcock & Wilcox Company, Nuclear Development Center.

[b]All tests performed on tubing from Carpenter Steel Company, mill release Nos. 83594, 83613, and 83619.

Inspection and Testing. — Fabrication tolerances on the tubing were specified in the BNWL purchase order. The tubing was 100% ultrasonically inspected by Wolverine Tube Company to ensure that no tubes showing defects greater than the standard (0.001 in. deep × 0.030 in. long × 0.005 in. wide) would be accepted. Copies of the procedure and of the individual traces are available upon request.

Inside and outside diameters of all tubes were measured to a precision of ±0.0001 in. with an air plug and air-ring gage in accordance with the procedure for Dimensional Inspection of Metallic Components and Finished EBR-II Fuel Pins.

Archive samples of the tubing are available at B&W and will be supplied to EBR-II personnel upon request.

End Fittings

End caps for these fuel pins were made from type 316 stainless steel bar stock. This material was obtained from BNWL. This material was purchased by BNWL from Crucible Steel Company to ASTM Specifications A-276-67 and A-484-65 and BNWL purchase order B9-S-777-47376. Results of an independent chemical analysis performed by National Spectrographic Laboratories are presented in Table 40.

Archive samples of end cap material are available at B&W and will be supplied to EBR-II personnel upon request.

Reflector, Spring, and Plenum Tube

The bar stock for the nickel reflector was obtained from BNWL. This material was purchased by BNWL to ASTM Specification B-160061 and BNWL purchase order No. B9S-777-47368. Independent chemical analyses are presented in Table 42.

The type 302 stainless steel plenum springs were obtained from BNWL. These springs were purchased to the specifications in BNWL purchase order No. B9S-777-55818. Independent chemical analyses are presented in Table 42.

The type 316 stainless steel plenum tubing was obtained from BNWL. This material was purchased by BNWL from Carpenter Steel Company to ASTM Specification A-269 and BNWL purchase order No. B9S-777-47370. Independent chemical analyses are presented in Table 42.

Fiberfrax Pad

Chemical analyses of the Fiberfrax material used for the top and bottom pad are presented in Table 43.

Table 42. Alloy Composition of Nickel Reflector, Type 302 Stainless Steel Plenum Spring, and Type 316 Stainless Steel Plenum Tube

Element	Nickel Reflector[a] (wt %)	Type 302 Stainless Steel Plenum[a] Spring (wt %)	Type 316 Stainless Steel Plenum[a] Tube (wt %)
Carbon	0.048	0.065	0.065
Manganese	0.21	0.95	1.51
Sulfur	0.008	0.020	0.007
Phosphorus		0.018	0.012
Silicon	0.016	0.95	0.48
Nickel	99.4	7.83	13.47
Molybdenum			2.47
Chromium		17.94	16.73
Copper	0.032		0.06
Cobalt	0.060		0.048
Iron	0.20	Balance	Balance
Boron			0.0005
Nitrogen			0.010

[a]Analyzed by National Spectrographic Laboratories, Inc.

Table 43. Wet Chemical and Spectrographic Semiquantitative Analysis of Fiberfrax[a]

Element[b] or Compound	Weight Percent
Si as SiO_2[c]	48.3
Al as Al_2O_3[c]	50.2
Fe as Fe_2O_3	0.3
Cu as Cu_2O	< 0.1
B as B_2O_3	1.2

[a]Analyzed by Babcock & Wilcox Alliance Research center.

[b]All the elements are reported as the oxides. This does not necessarily imply their presence as such. The elements Ti, Mg, Ni, Cr, Mo, V, Co, Mn, Zn, Pb, Sn, and Zr were not detected in this sample. The limit of detectability for these elements by the semiquantitative technique is approximately 0.05%.

[c]Wet chemical analysis.

Fuel Pin Assembly and Quality Control

Before assembly all metallic components were inspected in accordance with the procedure for Dimensional Inspection of Metallic Components and Finished EBR-II Fuel Pins. Bottom end caps were welded to the clad tube in accordance with the "Procedure for Welding End Plugs." After welding, each bottom closure weld was helium leak tested in accordance with the procedure for Helium Leak Testing of Welded End Plugs, Method HL-2. The helium leak test results are presented in Table 44. Radiographs in accordance with Section 8.A.3.F of the "Guide for Irradiation Experiments in EBR-II" were obtained for each bottom closure weld. Any closure weld which did not meet the weld acceptance criteria was rejected. Room temperature burst tests performed on closure welds using the same welding procedure and cladding and end caps from the same lot all failed outside the weld and heat-affected zones. Any oversized weld was polished to size prior to radiography and helium leak testing.

After the bottom closure weld was established as acceptable, the fuel and internal pin hardware were loaded into each fuel pin. The top

Table 44. Helium Leak Test Results

Fuel Pin Number	Date of Test	System Sensitivity (cm^3/sec)	Measured Leak Rate (cm^3/sec)
		$\times 10^{-10}$	$\times 10^{-10}$
	Bottom Closure Welds		
D-2	May 5, 1970	4.7	
D-4	April 6, 1970	5.1	< 5.1
D-5	May 5, 1970	4.7	9.2
D-6	April 6, 1970	5.1	< 5.1
D-9	April 6, 1970	5.1	< 5.1
D-10	May 5, 1970	4.7	< 4.7
D-12	April 6, 1970	5.1	< 5.1
D-14	April 6, 1970	5.1	< 5.1
D-16	April 6, 1970	5.1	7.6
D-17	April 6, 1970	5.1	< 5.1
D-18	May 5, 1970	4.7	< 4.7
D-19	May 5, 1970	4.7	< 4.7
D-20	May 5, 1970	4.7	4.7
D-21	April 6, 1970	5.1	< 5.1
D-22	May 5, 1970	4.7	< 4.7
D-24	May 5, 1970	4.7	< 4.7
D-25	May 5, 1970	4.7	< 4.7
D-27	June 25, 1970	2.1	< 2.1
D-29	June 25, 1970	2.1	< 2.1
D-30	June 25, 1970	2.1	< 2.1
D-31	June 25, 1970	2.1	< 2.1
	Welded Fuel Pin[a] (both end plugs welded in place)		
Group Number			
1[b]	July 21, 1970	9.3	< 9.3
2[c]	July 21, 1970	9.3	< 9.3
3[d]	July 21, 1970	9.3	< 9.3

[a]The fuel pins were divided into three groups, each group consisting of seven fuel pins.

[b]Group 1 – D-4, D-6, D-12, D-14, D-15, D-17.

[c]Group 2 – D-5, D-18, D-20, D-21, D-22, D-24, D-25.

[d]Group 3 – D-2, D-10, D-19, D-27, D-29, D-30, D-31.

end cap was welded in place after a mixture of helium plus 1 cm^3 of xenon was introduced into the fuel pin. The gas mixture was at 1.1 atm pressure (at room temperature). All closure welds were considered to have met the acceptance criteria.

Final dimensional inspections of the finished fuel pins were made in accordance with the "Procedure for Dimensional Inspection of Metallic Components and Finished EBR-II Fuel Pin."

Quality Assurance Certifications

In accordance with the requirements of the "Guide for Irradiation Experiments in EBR-II, Revision 3," we submit the following certification statements.

1. We certify that the inspection and testing procedures for tubing procurement described in Section VIII-A-1-(b) of the "Guide for Irradiation Experiments in EBR-II" were followed with satisfactory results. Metallography of the claddings is presented in Fig. 17.

2. We certify that archive samples of the tubing are available to the EBR-II Project.

3. We certify that the inspection and testing procedures for end fitting procurement described in Section VIII-A-2-(b) of the "Guide for Irradiation Experiments in EBR-II" were followed with satisfactory results.

4. We certify that archive samples of the end fitting materials are available to the EBR-II Project.

5. We certify that the welding procedure, "Welding of End Fittings to Cladding Tube for EBR-II Fuel Pins," written by E. N. Harbinson in August 1970, was followed and that the welds meet the acceptance criteria of Section VIII-A-3-(b) of the "Guide for Irradiation Experiments in EBR-II." Metallography of a typical weld is presented in Fig. 18.

6. We certify that a leak test was performed in accordance with the procedure, "Helium Leak Test of EBR-II Fuel Pins," written by E. N. Harbinson in August 1970, on each fuel element to be irradiated and that the leak test disclosed no detectable leaks in the elements submitted for irradiation.

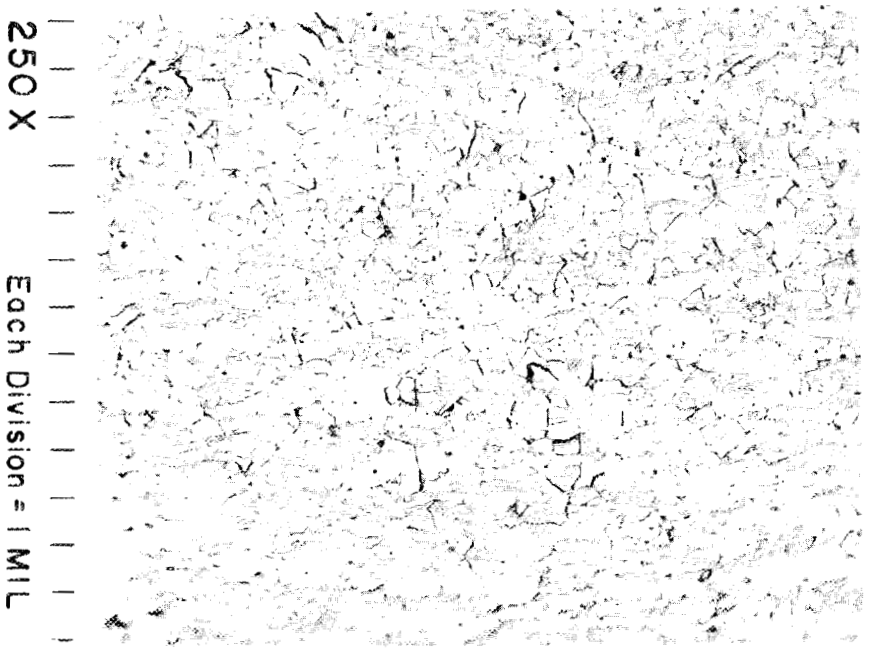

Fig. 17. Microstructure of Type 316 Stainless Steel Used for EBR-II Fuel Pin Cladding. Babcock & Wilcox photograph.

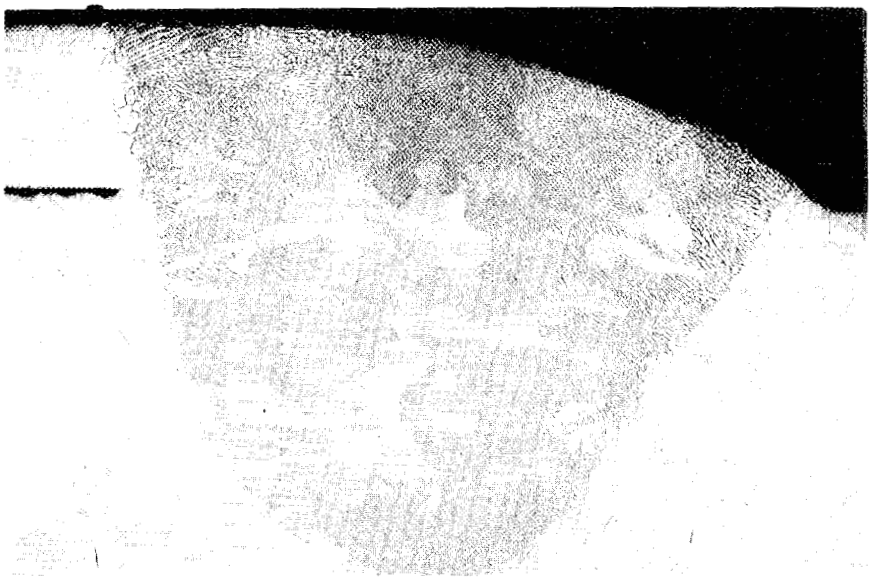

Fig. 18. Typical End Closure Weld for EBR-II Fuel Pin. Babcock & Wilcox photograph.

ACKNOWLEDGMENTS

We would like to take this opportunity to thank those persons of the EBR-II Project who assisted us so willingly in the initiation and planning of these experiments, particularly J. H. Kittel and O. M. Seim who recognized our needs and provided the subassembly designs and engineering information and W. J. Larson for his advice and assistance on the xenon tagging procedure.

In addition, we want to express our appreciation to J. C. Tverberg and R. J. Lobsinger of the Pacific Northwest Laboratories for their assistance in procuring the stainless steel tubing and rod used in these pins.

We would also like to thank: J. D. Jenkins of the ORNL Reactor Division for his assistance with physics analyses; M. J. Bell of the ORNL Chemical Engineering Division for the modification and operation of the ØRIGEN code; W. D. Turner of the Mathematics Division for the temperature transient calculations with the HEATING code; W. H. Bridges for ths assistance in the stress-strain analyses; C. M. Cox, T. N. Washburn, and A. L. Lotts for their consultation during the planning of the tests and the review of this document; and all of the individuals at both ORNL and B&W who contributed toward the development of the procedures and to the precise, although sometimes tedious, efforts involved in fabricating these tests and collecting and maintaining the necessary detailed records on each pin.

REFERENCES

1. "Series I EBR-II Irradiation Tests Proposal," sent to Dr. S. Lawroski by A. R. Olsen on March 28, 1968.

2. "Experiment Proposal for EBR-II Irradiations," sent to Dr. S. Lawroski by E. N. Harbinson of the Babcock & Wilcox Company on May 1, 1968.

3. Letter from Dr. S. Lawroski to A. R. Olsen, dated May 24, 1968.

4. Letter from Dr. S. Lawroski to E. N. Harbinson, dated May 24, 1968.

5. "Preliminary Proposal for Approval-in-Principle of a 37-Pin EBR-II Subassembly," A. R. Olsen and C. J. Baroch, letter to Milton Shaw from F. L. Culler, Jr., dated Aug. 22, 1969.

6. Letter to Assistant Director (RDT) ORNL, from E. E. Sinclair on Nov. 7, 1969.

7. "Guide for Irradiation Experiments in EBR-II, Revision 3, 1969," prepared by the EBR-II Project, Argonne National Laboratory, July 1969 and subsequent revisions through Aug. 1, 1970.

8. Babcock & Wilcox Company 189-A Contract AT(30-1)-3714, "The Gel Addition Process for Production of Plutonia-Urania Fuels," (April 24, 1969).

9. Oak Ridge National Laboratory 189-A No. 10090, "Development of LMFBR Oxide Fuels," (April 1, 1969).

10. Letter to J. H. Kittel from A. R. Olsen, dated July 22, 1969.

11. Letter to J. H. Kittel from A. R. Olsen, dated Nov. 7, 1969.

12. Letter to A. R. Olsen from J. H. Kittel, dated March 30, 1970.

13. Letter to J. H. Kittel from A. R. Olsen, dated June 15, 1970.

14. Letter from J. H. Kittel to A. R. Olsen, dated July 8, 1970.

15. Telephone request by R. Neidner to T. N. Washburn on July 14, 1970.

16. Telephone conversation between J. H. Kittel and A. R. Olsen on Aug. 5, 1970.

17. J. H. Kittel, transmittal of May 11, 1970, of "Meeting on Effects of Sodium Cleaning on Stainless Steel."

18. Telephone discussion of sodium removal procedures between M. J. Feldman and A. R. Olsen on Aug. 14, 1970.

19. Letter to Mr. Lee Love from A. R. Olsen, with copy to J. C. Case of EBR-II, dated June 16, 1970.

20. A. R. Olsen, Experiment Description and Hazards Evaluation for the Series I ORNL Oxide Fuels Irradiation in EBR-II, ORNL-TM-2635 (April 1970).

21. A. R. Olsen, C. M. Cox, and R. B. Fitts, "Low Burnup Irradiation Tests of Sphere-Pac Sol-Gel $(U,Pu)O_2$ Fuels," Trans. Am. Nucl. Soc. 12(2), 605–606 (1969).

22. A. R. Olsen, "Intermediate Burnup Irradiation Tests of Sphere-Pac Sol-Gel Fuels," Trans. Am. Nucl. Soc. 13(1), 32–36 (1970).

23. D. E. Lew and A. E. Miller to Sherman Greenberg, 71 LMEC-398 (March 16, 1971).

24. W. Milich and E. C. King, Sodium Reactivity Tests – Fiberfrax Insulation, NP-7401 (March 1955).

25. Stephen Lawroski et al., Chemical Engineering Division Summary Reports, ANL-6145 (1960), pp. 32–33; ANL-6183 (1960), pp. 32–33.

26. Telephone conversation between J. H. Kittel and A. R. Olsen on June 4, 1970.

27. Letter from J. H. Kittel to A. R. Olsen on March 30, 1970.

28. D. A. Dyslin, Little MAMU – A Radial Steady-State Heat Transfer Computer Program (in preparation).

29. C. M. Cox and F. J. Homan, PRØFIL – A One-Dimensional FØRTRAN IV Program for Computing Steady-State Temperature Distributions in Cylindrical Ceramic Fuels, ORNL-TM-2443 (March 1969).

30. W. E. Bailey, C. N. Craig, and E. L. Zebroski, "Effect of Diametral Gap Size on the In-Pile Performance of Fast Ceramic Reactor Mixed Oxide Fuel," Trans. Am. Nucl. Soc. 9(1), 40–41 (1966).

31. L. J. Koch, W. B. Loewenstein, and H. O. Manson, Addendum to Hazards Summary Report, Experimental Reactor II (EBR-II), ANL-5719 (Addendum), (January 1964), pp. 56–59.

32. Letter to J. H. Kittel from A. R. Olsen, dated June 15, 1970.

33. "Guide for Irradiation Experiments in EBR-II," p. 67.

34. C. M. Cox and F. J. Homan, "Performance Analysis of a Mixed Oxide LMFBR Fuel Pin," Nucl. Appl. Technol. 9(3), 317–325 (September 1970).

35. W. H. Bridges, Physical and Tensile Properties of Type 316 Stainless Steel, ORNL-TM-3037 (in press).

36. K. J. Perry, G. F. Melde, and R. N. Duncan, "Fuel-Clad Reactions Observed in Stainless-Steel-Clad Mixed-Oxide Fuel Pin Irradiation," Trans. Am. Nucl. Soc. 14, 17–18, Suppl. 1 (April 1970).

37. Telephone conversation between J. H. Kittel and A. R. Olsen, June 4, 1970.

38. C. M. Cox, E. J. Manthos, and D. R. Cuneo, "Transient Performance of Sol-Gel $(U,Pu)O_2$ Sphere-Pac and Pellet Fuels," Trans. Am. Nucl. Soc. 13(2), 653–654 (November 1970).

39. E. O. Ballard and L. A. Pember, Proposal to Irradiate Unencapsulated Pins in the EBR-II – Subassemblies PNL-6, PNL-7, and PNL-8, BNWL-1103, UC-25 (June 1970).

40. W. D. Turner and J. S. Crowell, Notes on HEATING — An IBM/360 Heat Conduction Program, CTC-INF-980 and Addendum 1 (Nov. 21, 1969).

41. A. J. Brook, Temperatures Associated with Local Blockages in the Prototype Fast Reactor, UKAEA AHSB(S) M-153 (March 1966). Limited distribution.

42. M. J. Bell, ØRIGEN, The ORNL Isotope Generation and Depletion Code, ORNL-4628 (in preparation).

43. "Sodium-Cooled Reactors," Fast Ceramics Reactor Development Program 30th Quart. Rept., January 1969 to April 1969, GEAP-10028.

APPENDIX A

SAMPLE CALCULATIONS

The following examples show calculations for the heat rates, fission gas production, pin and subassembly thermal analyses. All calculations, with the exception of the revised gas pressure data, were based on the design densities for the fuel pin. In these examples we have chosen a pin with 85% smear density. The composition of the fuel used is:

U	699.1 mg/g
Pu	182.5 mg/g
O_2	118.4 mg/g
Theoretical density	10.90 g/cm^3

The isotopic analysis used is:

U		Pu	
^{234}U	0.996%	^{239}Pu	88.65%
^{235}U	93.16%	^{240}Pu	10.00%
^{236}U	0.514%	^{241}Pu	1.25%
^{238}U	5.33%	^{242}Pu	0.10%

Heat Generation in Fuel

Fission rates from Table C-1 for grid locations 6-N3 or 6-N4.

Location	Isotope	Fission Rates (fissions/g-sec $\times 10^{-13}$) 50 Mw	62.5 Mw
Peak	^{235}U	0.655	0.8188
	^{238}U	0.0414	0.0518
	$^{239}Pu + {}^{241}Pu$	0.774	0.9675
	^{240}Pu	0.281	0.3513
Average	^{235}U	0.603	0.7538
	^{238}U	0.036	0.045
	$^{239}Pu + {}^{241}Pu$	0.711	0.8888
	^{240}Pu	0.240	0.3000
Minimum	^{235}U	0.549	0.6863
	^{238}U	0.0283	0.0354
	$^{239}Pu + {}^{241}Pu$	0.639	0.7988
	^{240}Pu	0.187	0.2338

Volume of fuel:

$$\left(\frac{\pi}{4}\right)(0.218 \text{ in.} \times 2.54 \text{ cm/in.})^2 \ (1 \text{ cm}) = 0.240808 \text{ cm}^3/\text{cm}$$

$$(0.240808)\ (13.5 \text{ in.})\ (2.54 \text{ cm/in.}) = 8.2573 \text{ cm}^3/\text{pin}$$

Weight of fuel per cm of pin at theoretical density:

$$0.240808 \text{ cm}^3\ (10.90 \text{ g/cm}^3) = 2.62481 \text{ g/cm}$$

Grams of fissile isotope/cm³ at theoretical density:

$$^{235}U\ 10.90 \text{ g/cm } (0.6991 \text{ g/g})\ (0.9316) = 7.099 \text{ g/cm}^3$$

Fission rate per cm at peak axial location and

85% of theoretical density:

$$^{235}U\ \ 7.099\ (0.240808)\ (0.85 \text{ T.D.})\ (0.8188 \times 10^{13}) =$$

$$1.1897 \times 10^{13} \text{ fissions/cm-sec.}$$

Fission Rates for 85% Dense Fuel Position 6-N3 or 6-N4

Isotope	Weight (g/cm)	Fission Rate (fissions/cm-sec × 10^{-13})		
		Max.	Avg.	Min.
^{235}U	1.4531	1.1897	1.0953	0.9972
^{238}U	0.0831	0.0043	0.0037	0.0029
^{239}Pu	0.3610	0.3492	0.3208	0.2883
^{240}Pu	0.0407	0.0143	0.0122	0.0095
^{241}Pu	0.0051	0.0049	0.0045	0.0041
TOTALS	1.9430	1.5625	1.4365	1.3020

At 192 Mev/fission, there are 3.07×10^{-11} w-sec/fission. The peak fission heat rates then are:

Maximum $(1.5625 \times 10^{13}$ fissions/cm-sec$)$ $(3.07 \times 10^{-11}$ w-sec/fission$)$ = 479.7 w/cm

Average $(1.4365 \times 10^{13}$ fissions/cm-sec$)$ $(3.07 \times 10^{-11}$ w-sec/fission$)$ = 441.0 w/cm

Minimum $(1.3020 \times 10^{13}$ fissions/cm-sec$)$ $(3.07 \times 10^{-11}$ w-sec/fission$)$ = 399.7 w/cm

The peak-to-average fission rate is 1.12:1.

Thus, a fuel pin with 85% smear density fuel located at the average subassembly location will generate the following total fission heat.

$$\left(\frac{1}{1.12}\right) \left(\frac{441.0 \text{ w/cm}}{1000 \text{ w/kw}}\right) \quad (13.5 \text{ in.}) \ (2.54 \text{ cm/in.}) = 13.5 \text{ kw} .$$

The actual heat generation for each subassembly location is calculated on the basis of the design fuel density for the pin in that location and the fission rate proportioned as shown in Fig. 4 of the text.

Calculations of Flow Rate and Flow Area

Three different flow channels were derived from the geometric arrangements shown below and the flow distribution for an H-37 subassembly published in Table D-II of the Guide.

These are shown graphically below.

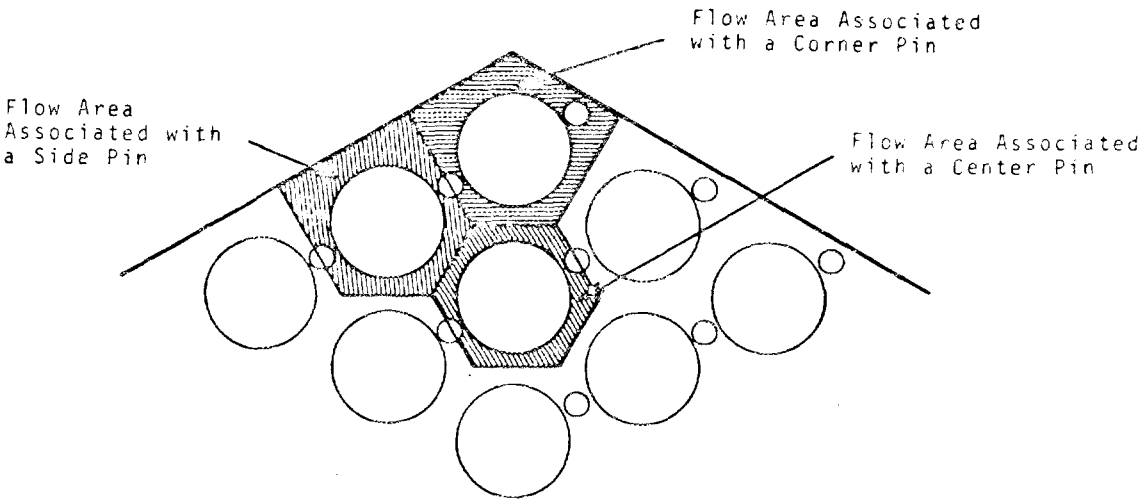

Two conditions were calculated; (1) the initial flow area and velocity for start-of-irradiation, and (2) a final flow area and velocity for end-of-life, assuming a constant change in diameter to 103.84% of original pin diameter. Thus, a circular flow channel was defined with an equivalent diameter (D_e) based on a flow area (A_n) equal to the nonsymmetric areas for each of the three locations. In the following calculations the terms are:

D_n = pin diameter, in.

A_n = flow area, in.^{2} = geometric area − pin area − wire area

ρ = density of Na at 911°F = 51.95 lb/ft^3

w = Na flow, lb/hr

The values of the subscript n are 1 for initial conditions and 2 for end-of-life.

V = Na flow, ft/hr $= w/\rho A)$ (144 in.^{2}/ft^2)

P_w = Wetted perimeter, in.

Center Pin $D_1 = 0.250$ in. $D_2 = 0.2596$

Total region is a hexagon with 0.290 in. across flats.

$A_1 = 0.07283 - 0.04909 - 0.00126 = 0.02249$ in.^{2}

W_1 = 384.35 lb/hr determined by iterative calculations to obtain maximum cladding temperature desired.

V_1 = 47,375 ft/hr or 13.16 ft/sec

$$D_{e_1} = \frac{4\ A_1}{P_w} = \frac{4(0.02249)}{\pi(0.250)} = 0.11453$$

$A_2 = 0.07283 - 0.05293 - 0.00127 = 0.01865$ in.^{2}

$$De_2 = \frac{4(0.01865)}{\pi(0.2596)} = 0.09147 .$$

Because of the difficulties in defining other pressure drops in the subassembly, we assumed the pressure drop (h) was constant at the beginning and end-of-life, i.e. $h_1 = h_2$. We also assumed that only 80% of the calculated reduction in flow occurred as a result of pin swelling because 20% of the pressure drop is unaffected in the remaining subassembly components.

$$h = f \frac{1}{D_e} \left(\frac{V^2}{2\ g}\right) ,$$

where

f, the friction factor,

L, the length of the channel, and

g, gravity are constant for both h_1 and h_2.

Thus,

$$V_2 = \left(\frac{D_{e_2}}{D_{e_1}} V_1^2\right)^{1/2}$$

$$V_2 = \left[\left(\frac{0.09147}{0.11453}\right) (47,375)^2\right]^{1/2} = 42,333 \text{ ft/hr}$$

$$W_2 = \frac{V_2 \ A_2 \ \rho}{144} = 284.8 \text{ lb/hr}$$

Since we have assumed an 80% factor, then W_2 actual is:

$$W_2 \text{ (actual)} = W_1 - (0.80) \ (W_1 - W_2) = 304.68.$$

Edge Pin

$$\text{Geometric area} = 1/2 \text{ hex area} + \text{rectangular area}$$

$$= 0.036416 + (0.165) \ (0.29)$$

$$= 0.036416 + 0.04785$$

$$= 0.084266 \text{ in.}^2$$

$$A_1 = 0.084266 - 0.04909 - 1.5 \ (0.00126)$$

$$= 0.033285 \text{ in.}^2$$

$$De_1 = \frac{4(0.0332937)}{\pi \ (0.25)} = 0.1695$$

$$\rho = 52.7 \text{ lb/ft}^3 \text{ at } 820°\text{F}$$

$$W_1 = 638.02 \text{ lb/hr}$$

$$V_1 = 52,363 \text{ ft/hr or } 14.5 \text{ ft/sec}$$

$$A_2 = 0.0294514 \text{ in.}^2$$

$$De_2 = 0.144446$$

$$V_2 = 48,330 \text{ ft/hr}$$

$$W_2 = 570.92 \text{ lb/hr}$$

$$W_2 \text{ (actual)} = 544.34 \text{ lb/hr}$$

Corner Pin

Geometric area = 1/3 hex area + rectangular areas + triangular areas

$$= 0.02427745 + 2(0.145)\ (0.165) + \frac{2(0.165)\ (0.09526)}{2}$$

$$= 0.02427745\ \ 0.04785 + 0.0157179$$

$$= 0.0878454 \text{ in.}^2$$

$$A_1 = 0.08785 - 0.04909 - 1.5\ (0.00126)$$

$$= 0.03687 \text{ in.}^2$$

$$De_1 = 0.187794$$

$$\rho = 52.8 \text{ lb/ft}^3 \text{ at } 813°F$$

$$W_1 = 687.35 \text{ lb/hr}$$

$$V_1 = 50{,}838 \text{ ft/hr or } 14.12 \text{ ft/sec}$$

$$A_2 = 0.03303104 \text{ in.}^2$$

$$De_2 = 0.162004$$

$$V_2 = 47{,}218 \text{ ft/hr}$$

$$W_2 = 571.88 \text{ lb/hr}$$

$$W_2 \text{ (actual)} = 594.97 \text{ lb/hr}$$

These values were then used to establish the input for the computer code MAMU. The code assumes that all heat is transferred radially through the pin. The program then sums the heat produced, both fission and gamma, in predetermined axial increments, calculates the heat flow and radial temperature distribution, and prints out these quantities. Tables A1 and A2 are copies of the computer output sheets for calculations on a pin located at the maximum temperature position in the subassembly (Position 7).

Table A-1. Temperature Distribution, Subassembly Position 7

Pin Axial Position	T-C	T-0	T-1	T-2
1	700.0	700.1	700.6	701.1
2	700.5	701.5	704.1	775.6
3	701.6	702.8	705.9	789.5
4	702.9	704.3	707.8	804.0
5	704.3	705.9	710.0	819.3
6	706.0	707.8	712.4	836.6
7	708.0	710.0	715.4	858.8
8	709.2	709.8	711.5	755.4
9	716.1	742.0	811.1	1174.6
10	729.8	756.6	827.2	1201.4
11	743.9	771.6	843.9	1229.3
12	758.4	787.2	861.5	1259.8
13	773.4	803.2	879.4	1289.8
14	788.9	819.5	897.2	1317.9
15	804.7	836.2	915.1	1345.4
16	820.8	853.0	932.8	1370.8
17	837.2	870.0	950.5	1395.0
18	853.8	887.1	968.0	1417.1
19	870.5	904.2	985.2	1437.4
20	887.3	921.3	1002.1	1455.9
21	904.2	938.4	1018.7	1472.5
22	921.0	955.2	1034.7	1486.5
23	937.7	971.9	1050.5	1499.6
24	954.3	988.2	1065.6	1509.9
25	970.7	1004.3	1080.3	1518.9
26	986.8	1020.0	1094.3	1525.2
27	1002.7	1035.4	1107.9	1530.5
28	1018.2	1050.3	1120.8	1533.7
29	1033.3	1064.8	1133.3	1536.0
30	1048.1	1078.8	1145.1	1536.4
31	1062.4	1092.2	1156.1	1534.9
32	1076.2	1105.2	1166.9	1533.9
33	1089.7	1117.9	1177.6	1533.9
34	1102.7	1130.4	1188.3	1535.4
35	1115.5	1142.9	1199.7	1541.8
36	1122.0	1122.8	1124.1	1159.8
37	1122.3	1122.5	1123.0	1127.6
38	1122.4	1122.6	1123.1	1126.0
39	1122.5	1122.6	1123.1	1124.7
40	1122.5	1122.7	1123.2	1124.4
41	1122.6	1122.7	1123.2	1124.2
42	1122.6	1122.7	1123.2	1124.7
43	1122.6	1122.7	1123.2	1124.4
44	1122.7	1122.8	1123.3	1124.2
45	1122.7	1122.8	1123.3	1124.0
46	1122.7	1122.8	1123.3	1123.9
47	1122.7	1122.8	1123.3	1123.8
48	1122.7	1122.8	1123.3	1123.8

T-C = temperature of coolant, °F; T-0 = temperature of outside surface of clad, °F; T-1 = temperature of inside surface of clad, °F; T-2 = temperature of outer surface of fuel, °F.

Table A-2. Calculated Heat Transfer, Subassembly Position 7

Pin Axial Position	QF	HTC	QIC	QIS	QT	QTX
1	0.1750	22142.2	4	4	2	2
2	0.2050	22136.1	116	116	62	62
3	0.2500	22128.7	136	136	187	188
4	0.3150	22120.3	157	158	334	335
5	0.4063	22110.6	180	181	503	504
6	0.5625	22099.5	207	207	697	698
7	0.8875	22086.6	242	243	921	924
8	1.4400	22083.3	39	39	1061	1065
9	2.4013	21961.7	1566	1567	1864	1868
10	2.4710	21873.7	1611	1612	3452	3458
11	2.5449	21783.1	1659	1661	5087	5094
12	2.6304	21689.3	1715	1716	6774	6783
13	2.7107	21592.8	1767	1769	8516	8525
14	2.7790	21493.8	1812	1813	10305	10316
15	2.8420	21392.9	1853	1855	12138	12150
16	2.8929	21290.3	1886	1888	14008	14022
17	2.9357	21186.3	1914	1916	15908	15923
18	2.9665	21081.5	1934	1936	17832	17849
19	2.9866	20976.1	1947	1949	19773	19791
20	2.9973	20870.5	1954	1956	21724	21744
21	2.9973	20765.1	1954	1956	23678	23700
22	2.9839	20660.4	1946	1947	25628	25651
23	2.9665	20556.4	1934	1936	27568	27593
24	2.9344	20454.0	1913	1915	29492	29518
25	2.8969	20352.8	1889	1890	31393	31421
26	2.8460	20253.6	1856	1857	33265	33294
27	2.7911	20156.5	1820	1821	35103	35134
28	2.7268	20061.9	1778	1779	36902	36934
29	2.6598	19969.6	1734	1736	38658	38691
30	2.5848	19880.2	1685	1687	40368	40403
31	2.5018	19793.9	1631	1633	42026	42062
32	2.4241	19710.2	1581	1582	43632	43669
33	2.3531	19628.9	1534	1536	45189	45228
34	2.2929	19549.5	1495	1496	46704	46744
35	2.2594	19470.8	1473	1474	48188	48229
36	1.3500	19513.1	36	37	48943	48985
37	0.8250	19513.2	19	20	48970	49013
38	0.5125	19512.5	12	12	48986	49029
39	0.3688	19512.1	7	7	48995	49039
40	0.2913	19511.8	6	6	49001	49045
41	0.2375	19511.6	4	5	49006	49051
42	0.2000	19511.4	2	2	49009	59054
43	0.1625	19511.3	3	4	49012	49057
44	0.1250	19511.1	2	3	49015	59060
45	0.1063	19511.0	2	2	49017	49063
46	0.0875	19510.9	2	2	49019	49065
47	0.0650	19510.8	1	1	49020	49066
48	0.0475	19510.7	1	1	49022	49068

QF = unperturbed heating rate, w/g; QCH = heat generated in the coolant, Btu/hr; HTC = heat transfer coefficient, Btu ft^{-2} $°F^{-1}$; QIC = sum of heat in all regions excluding coolant, Btu/hr; QT = total heat in all regions (excluding coolant) in all capsules above midplane, Btu/hr; QIS = sum of heat in all regions including coolant, Btu/hr; QTX = total heat in regions (including coolant) in all capsules above capsule midplane, Btu/hr.

The entire pin was subdivided into 48 increments with lengths that depended upon the contents at various axial locations. For the fuel region, Positions 9 through 35, the increments were 0.5 in. The fuel surface temperature and the heat rating for a specific fueled increment were then input into our PRØFIL code to calculate the fuel centerline temperatures. Since the initial fuel will restructure under the conditions of these irradiations, we have reported the fuel center temperatures after restructuring. A typical computer printout for the axial midplane fuel section is shown in Table A3. To determine the effects of uncertainties on the various temperatures, we used the format and factors described in the Addendum to Hazard Summary Report, Experimental Breeder Reactor II (EBR-II), ANL-5719, Addendum, pp. 58-59.

Additional analyses of fuel performance characteristics were calculated with common assumptions and equations as follows:

Gas Pressure

1. Preliminary Analysis

Gas pressure buildup in pin located in Subassembly Position 7.

The average fission rate for this pin is:

$$\frac{450 \text{ w/cm}}{1.12 \text{ pk/avg}} \left(\frac{1}{192 \text{ Mev/fission}}\right) \left(\frac{1}{1.603 \times 10^{-13} \text{ w-sec/Mev}}\right)$$

$$\frac{401.78 \text{ avg w/cm}}{307.776 \times 10^{13} \text{ w-sec/fission}} = 1.3054 \times 10^{13} \text{ fissions/sec-cm}$$

The total fission rate for 13.5 in. of fuel is:

$$1.3054 \times 10^{13} \text{ (13.5 in.) (2.54 cm/in.)} = 4.4762 \times 10^{14} \text{ fissions/sec}$$

Table A-3. Typical Profile Calculation Results for Pin in Position 7

EBR Series II fuel region heat section of MAMU
Mev/fission = 192.0
Initial void diameter = 0 cm
Initial fuel density = 0.830 T.D. 10.902 g/cm^3
Profile with K = 0.0110 + 1/((0.4848 = 0.4465 = D) + T
The next output is for densified fuel.

Radius (cm)	Temperature (°C)	K (w/cm = C)	KT (w/cm)	S (w/cm^3)	Density
0.0	2274	0.0	0.0	0	0.0
0.0	2274	0.0	0.0	0	0.0
0.0807	2274	0.0195	0.0	0	0.970
0.0876	2271	0.0195	7.88	-734	0.970
0.1011	2253	0.0196	25.30	-2033	0.970
0.1130	2222	0.0197	42.71	-3052	0.970
0.1238	2185	0.0199	60.12	-3893	0.970
0.1337	2142	0.0200	77.54	-4607	0.970
0.1430	2097	0.0202	94.95	-5226	0.970
0.1516	2049	0.0204	112.37	-5770	0.970
0.1598	2000	0.0207	129.78	-6251	0.970
0.1676	1949	0.0209	147.19	-6679	0.970
0.1751	1898	0.0212	164.61	-7060	0.970
0.1823	1846	0.0211	182.02	-7542	0.965
0.1891	1794	0.0185	199.35	-9052	0.920
0.1958	1732	0.0188	215.87	-9336	0.920
0.2022	1672	0.0191	232.38	-9586	0.920
0.2084	1611	0.0194	248.90	-9806	0.920
0.2145	1552	0.0197	265.41	-9995	0.920
0.2203	1492	0.0189	281.93	-10785	0.895
0.2261	1430	0.0171	297.57	-12236	0.830
0.2316	1362	0.0174	312.48	-12318	0.830
0.2371	1294	0.0178	327.38	-12371	0.830
0.2424	1228	0.0181	342.28	-12396	0.830
0.2476	1184	0.0185	357.18	-12393	0.830
0.2527	1101	0.0180	372.08	-12361	0.830
0.2577	1039	0.0194	386.98	-12299	0.830
0.2627	979	0.0199	401.88	-12208	0.830
0.2675	920	0.0205	416.78	-12088	0.830
0.2722	863	0.0211	431.67	-11937	0.830
0.2769	808	0.0218	446.57	-11757	0.830

13.61 kw/ft heat generation
0.081 cm void diameter

Columnar grains of density 0.97 assumed for T greater than 1800.0
Equiaxed grains of density 0.92 assumed for T greater than 1450.0
Equiaxed grains start at 0.2245 cm radius
Columnar grains start at 0.1885 cm radius

The fission gas production rate per effective full power day is:

4.4762×10^{14} fissions/sec (0.26 gas atoms/fission) (8.64×10^{4} sec/day) $= 1.0055 \times 10^{19}$ gas atoms per day.

At standard pressure and temperature, this is:

$$\left(\frac{1.0055 \times 10^{19} \text{ atoms/day}}{6.023 \times 10^{23} \text{ atoms/mole}}\right) \quad (22{,}400 \text{ cm}^3\text{/mole}) = 0.374 \text{ cm}^3\text{/day.}$$

Since the initial gas loading of the fuel pin is assumed to be 8.5 cm^3, the total gas content at the end-of-life is:

$8.5 \text{ cm}^3 + 0.374 \text{ cm}^3\text{/day} \times 592.5$ effective full power days $=$ 230.08 cm^3

The effective plenum volume, excluding all available porosity in the fuel and neglecting any diametral changes in the cladding due to thermal expansion or irradiation-induced density changes, is 6.82 cm^3. From MAMU computer calculations, the average gas plenum temperature is 607°C (880°K). Therefore, the end-of-life gas pressure is:

$$\frac{230.08 \text{ cm}^3}{6.82 \text{ cm}^3} \left(\frac{880°\text{K}}{273°\text{K}}\right) \quad (15 \text{ psi}) = 1630 \text{ psi} .$$

2. Revised Analysis

Following fabrication of the pins and in keeping with new EBR-II requirements, we revised our gas analysis to more precisely predict the actual fission gas production in each pin and to include the amount of sorbed gas in each pin component plus any moisture.

To obtain a more precise estimate of the initial gas content in each fuel pin, we obtained the amount of absorbed gas for each pin component by multiplying the weight of the component by the measured gas content in cm^3/g. To this we added a H_2O contribution by multiplying the component weight by the measured H_2O content in ppm and the conversion factor.

Pin OS-12 in Position 7 is given here as an example.

Pin Contents:	Fuel	54.5 g SPL 80/85
		19.7 g SPLL
	Blanket	33.2 g UO_2 (B1)
	Insulators	5.1 g ThO_2
	Fiberfrax	0.07 g

Partial Analysis of Contents:

	SPL 80/85	SPLF	UO_2	ThO_2	Fiberfrax
Gas release, cm/g	0.045	0.14	0.02	0.014	0.536
H_2O, ppm	5	< 6	8	31	——

$$H_2O\text{-to-gas conversion} \quad \frac{1(\text{ppm } H_2O)\ (2.24 \times 10^4\ cm^3/\text{mole})}{18\ \text{g/mole}\ (10^6\ \text{ppm/g})}$$

$$= 0.001244\ cm^3/\text{ppm}\ .$$

Thus, for the fuel:

$$54.5\ (0.045) + 19.7\ (0.14) + 176.3\ (5)\ (0.001244) = 6.30\ cm^3$$

For the Blanket

$$33.2\ [0.02 + 8(0.001244)] = 1.00\ cm^3$$

For the Insulators

$$5.1\ [0.014 + 31(0.001244)] = 0.27\ cm^3$$

For the Fiberfrax

$$0.02\ (0.536) = 0.08\ cm^3$$

To this it is necessary to add the amount of helium and xenon tag gas in the pin, which can be obtained from Table 26 as $8.38\ cm^3 \times \frac{273}{293} = 7.80\ cm^3$ STP. This yields an as-fabricated gas content of $15.4\ cm^3$ at STP. These data, together with similar data for all 37 pins, are presented in Table A-4.

To obtain the plenum volume outside of the fuel region, because of our assumption that fuel porosity would be completely filled by fuel swelling, we subtracted the fuel void volume associated with the fuel from the measured free volume in each pin. The fuel void volume was calculated as:

$$\left(\frac{8.2573\ cm^3}{13.5\ \text{in. of cladding}}\right)\left(1 - \text{fractional fuel density}\right).$$

Thus, for Pin OS-12,

$$8.379 - 8.2573\ (1 - 0.831) = 6.98\ cm^3 \text{ plenum volume.}$$

Thus, the beginning-of-life plenum pressure can be calculated using the plenum temperature calculated by the MAMU code.

$$\frac{15.4\ cm^3 \text{ of gas}}{6.98\ cm^3 \text{ of plenum}}\ (14.7) \qquad \left(\frac{880°K}{273°K}\right) = 104 \text{ psia}.$$

To obtain the end-of-life pressures and all other gas pressures, a depletion calculation was made using the DEPLETE code to obtain the peak burnup in each pin. The average burnup for each pin was then obtained by using the peak-to-average ratio of 1.12 from the Guide. Then the moles of fission gas production at 26% of all fission product pairs can be obtained.

Table A-4. Gas Content and Pressure Calculations for As-Fabricated Pins

Subassembly Position	Pin Identity	Start-of-Life: Fuel Weight (g)	Fuel Gas and H_2O (cm^3)	Blanket Weight (g)	Blanket Gas and H_2O (cm^3)	Insulators Weight (g)	Insulators Gas and H_2O (cm^3)	Tagged Helium (cm^3)	Total[a] Gas (cm^3)	Plenum Volume (cm^3)	Plenum Temp (°K)	Plenum Pressure (psia)	End-of-Life: Average Burnup (% FIMA)	Fission Gas (cm^3)	Total Gas (cm^3)	Plenum Pressure (psia)
1	D-2	71.19	7.95	36.96	0.66	6.07	0.11	8.58	17.3	7.8	777	93	7.74	119.9	137.2	740
2	OP-7	71.62	4.56	33.14	0.99	5.12	0.27	8.68	14.5	7.0	785	88	11.25	175.1	189.6	1140
3	OS-4	73.49	5.67	33.40	1.00	5.11	0.27	8.51	15.4	7.0	783	93	5.27	84.0	99.5	600
4	OS-9	73.98	4.35	33.23	1.00	5.12	0.27	8.42	14.0	7.0	778	84	10.94	175.1	189.2	1130
5	D-30	71.20	7.95	37.16	0.66	6.24	0.11	8.58	17.3	7.8	785	94	11.25	174.2	191.5	1040
6	OS-8	72.08	1.33	35.86[b]	1.16	5.12	0.27	8.73	11.5	7.2	876	75	11.09	171.7	183.2	1200
7	OS-12	74.28	5.73	33.20	1.00	5.11	0.27	8.38	15.4	7.0	880	104	10.94	176.1	191.5	1300
8	D-9	75.01	0.62	37.05	0.66	6.07	0.11	9.02	10.4	8.2	877	60	7.34	119.8	130.2	750
9	OP-5	78.04	4.51	33.15	0.99	5.18	0.27	7.41	13.2	6.8	786	82	10.63	180.3	193.5	1200
10	OP-3	72.10	4.59	32.95	0.99	5.12	0.27	8.55	14.4	7.1	783	86	5.27	82.6	97.0	580
11	D-20	70.58	6.91	37.23	0.66	6.14	0.11	8.58	16.3	7.8	880	99	10.94	168.0	184.3	1120
12	D-10	71.10	7.94	37.18	0.66	6.07	0.11	8.58	17.3	7.8	877	105	5.13	79.3	96.6	580
13	OS-2	73.13	4.30	33.26	1.00	5.12	0.27	8.47	14.0	7.0	880	95	5.05	80.0	94.0	630
14	OS-6	73.93	4.35	33.30	1.00	5.13	0.27	8.51	14.1	7.1	876	94	7.13	114.1	128.2	850
15	D-22	71.00	6.95	36.93	0.66	6.17	0.11	8.58	16.3	7.8	779	88	7.02	108.5	124.8	670
16	OS-11	73.51	5.67	33.20	1.00	5.16	0.27	8.51	15.4	7.0	777	92	10.94	174.5	189.9	1130
17	D-21	70.66	6.92	37.03	0.66	6.17	0.11	8.58	16.3	7.8	877	99	7.34	112.8	129.2	780
18	D-31	71.17	6.97	37.15	0.66	6.19	0.11	8.58	16.4	7.8	880	100	10.63	164.7	181.1	1100
19	OS-7	74.08	4.35	33.29	1.00	5.23	0.28	7.73	13.4	7.0	876	91	7.13	114.3	127.7	860
20	D-17	74.76	0.62	37.16	0.66	6.16	0.11	9.02	10.5	8.2	868	60	7.02	114.2	124.7	710
21	OS-1	72.65	1.36	34.97[b]	1.14	5.23	0.28	8.50	11.4	6.8	864	77	4.84	75.5	86.9	590
22	OS-13	72.67	1.36	32.74	0.98	5.13	0.27	8.52	11.2	7.0	768	66	4.76	74.3	85.5	500
23	OS-10	73.30	4.31	33.31	1.00	5.17	0.27	8.45	14.1	7.0	786	85	10.63	168.6	182.8	1100
24	D-12	75.00	0.62	37.08	0.66	6.09	0.11	9.02	10.5	8.2	871	60	10.49	171.1	181.6	1040
25	D-19	71.14	7.94	36.97	0.66	6.21	0.11	8.58	17.4	7.8	868	104	7.02	108.7	126.1	750
26	D-18	71.07	6.96	37.15	0.66	6.14	0.11	8.58	16.4	7.8	864	98	4.84	74.8	91.2	540
27	OS-3	73.49	4.32	33.33	1.00	5.12	0.27	8.48	14.1	7.1	866	93	4.76	75.7	89.9	590
28	D-14	74.74	0.62	37.14	0.66	6.21	0.11	9.02	10.5	8.2	772	60	9.87	160.5	171.0	870
29	D-27	71.19	7.95	37.17	0.66	6.15	0.11	8.58	17.4	7.8	779	93	7.02	108.8	126.1	680
30	D-4	74.82	0.62	37.06	0.66	6.19	0.11	9.02	10.5	8.2	864	60	4.84	78.7	89.2	510
31	OS-5	74.64	5.76	33.60	1.01	5.09	0.27	8.39	15.5	7.0	866	103	4.76	77.1	92.6	610
32	D-25	68.96	6.75	37.10	0.66	6.09	0.11	8.58	16.2	7.8	857	96	9.87	148.1	164.3	970
33	OP-2	80.96	3.34	33.15	0.99	5.11	0.27	7.74	12.4	6.8	781	77	4.62	81.4	93.8	580
34	OP-1	77.06	4.45	33.15	0.99	5.18	0.27	7.61	13.4	6.8	768	81	4.76	79.7	93.1	560
35	D-29	70.87	7.91	37.07	0.66	6.24	0.11	8.58	17.3	7.8	772	92	9.87	152.2	169.5	900
36	OP-6	80.84	3.33	33.21	1.00	5.12	0.27	7.72	12.4	7.1	781	73	9.71	171.0	183.4	1080
37	D-5	70.98	6.95	36.99	0.66	6.09	0.11	8.58	16.4	7.8	760	86	9.54	147.3	163.7	860

[a]Including 0.08 cm^3 for gas sorbed in Fiberfrax pads.

[b]Including UO_2 fines in blanket area.

$$\text{Moles of fission gas produced} = \left(\frac{\text{Wt of fuel} \times \text{wt \% of actinides}}{\text{MW [the isotopic average molecular wt]}}\right) \left(\frac{\%\ \text{FIMA}}{100}\right) (0.26)$$

This can be reduced to cm^3 at STP and added to the initial gas content to obtain the end-of life gas content.

For example, for OS-12

$$\frac{54.5\ (0.8808) + 19.7\ (0.8746)}{235.975} \left(\frac{10.94}{100}\right) (0.26)\ (22{,}400) + 15.4 = 191.5\ cm^3 .$$

The end-of-life pressure then is:

$$\frac{191.5}{6.98} \left(\frac{880}{273}\right) (14.7) = 1300 \text{ psia} .$$

Since OS-12 in Position 7 has the highest gas pressure of all the pins throughout the life of these tests, we calculated the gas pressure for this pin as a function of irradiation time. These pressures as a function of effective full power days of reactor operation, together with the average burnup level, are given in Table A-5.

Stress and Strain Analysis

Details of the stress and strain analyses are given in Ref. 32, and the mechanical normal properties used are presented in Table 10. The creep formula and the constants used are presented below for completeness. Thermal creep:

$$\dot{\epsilon} = A \exp(-Q/RT) \sinh(C\sigma/T)^N ,$$

where, for annealed type 316 stainless steel, we used:

Table A-5. Gas Pressure in Pin OS-12, Position 7
As a Function of Irradiation Time

Irradiation Time (EFPD)[a]	Average Burnup (% FIMA)	Fission Gas Produced (cm^3)	Total Gas (cm^3)	Plenum Pressure[b] (psia)
25	0.57	9.2	24.6	167
50	1.13	18.2	33.6	228
75	1.68	27.0	42.4	288
100	2.21	35.7	51.1	347
125	2.74	44.1	59.5	404
150	3.25	52.4	67.8	460
175	3.76	60.6	75.9	515
200	4.25	68.5	83.9	570
225	4.74	76.3	91.7	623
250	5.21	84.0	99.3	674
275	5.68	91.5	106.8	725
300	6.13	98.8	114.2	775
325	6.58	106.0	121.4	824
350	7.01	113.0	128.4	872
375	7.44	120.0	135.3	919
400	7.86	126.7	142.1	965
425	8.28	133.4	148.8	1010
450	8.68	139.9	155.2	1054
475	9.08	146.3	161.6	1097
500	8.46	152.5	167.9	1140
525	9.84	158.6	174.0	1181
550	10.22	164.7	180.0	1222
575	10.58	170.6	185.9	1262
600	10.94	176.3	191.5	1300

[a]EFPD = Effective Full Power Days of Reactor Operation = $\frac{MWd}{62.5}$.

[b]Assuming a constant plenum volume of 6.98 cm^3 and plenum temperature of 880°K (607°C).

$A = 2.95 \times 10^{24}$

$Q = 110,935$

$C = 0.02$

$N = 6.371$

R = gas constant, 1.986 cal/g-mole-°C .

σ = psi.

The form of the flux enhanced creep equation[1] is:

$\dot{\epsilon} = A \sigma \Phi \alpha$,

$\dot{\epsilon} = hr^{-1}$,

Φ = neutrons/cm^2-sec,

σ = psi,

$\alpha = e^{(1.405 - 0.0027\ T)}$,

T = °K,

$A = 6.732 \times 10^{-27}$ for annealed cladding, and

$A = 6.948 \times 10^{-27}$ for cold-worked cladding.

All other sample calculations have been presented in the text.

Preliminary Stress-Strain Analysis

Since no fuel-cladding mechanical interaction was assumed, we reduced the 0.016-in. wall to 0.0133 in. by increasing the inner radius from 0.109 to 0.1117 in. and retaining the outer radius of 0.125 in.

The stress-strain-time relationships were investigated for the two highest heat rate pins (subassembly locations 4 and 7) by calculations using the DEFØRM subroutine of the FMØDEL code. The

---

[1]T. T. Claudson, Irradiation Induced Swelling and Creep in Fast Reactor Materials, BNWL-SA-3283 (May 21, 1970).

total effective full power operating time requested is only 592 days. However, we chose to extend the operating period for stress analysis to 675 days to account for additional time at less than full power, but when temperatures and stress are high enough to affect creep deformation. The 675 days were subdivided into five full power increments of 135 days each; and a zero power period of 25 days was inserted between each full power increment, with an assumed reactor coolant temperature of 371°C (700°F). A final increment of 25 days at 20°C was assumed for subassembly dismantling, etc. before fuel cladding deformation can be measured. The actual incremental conditions used are summarized in Table A-6. The cladding radial temperature differentials are listed in Table A-7 for the three axial locations investigated on each pin. These sections are taken from the three extremes of temperature and temperature gradient.

Table A-6. DEFØRM Input Pressure Data

Cycles	Power Level	Position 7 Plenum		
		Temp (°C)	Pressure (psi) Initial	Pressure (psi) Final
1	Full	607	60	418
2	Zero	371	306	306
3	Full	607	418	776
4	Zero	371	568	568
5	Full	607	776	1134
6	Zero	371	830	830
7	Full	607	1134	1490
8	Zero	371	1090	1090
9	Full	607	1490	1850
10	Zero	20	616	616

Table A-7. Pin 7 Cladding Temperatures Used in Calculations

Section Location	Temperature		Temperature Differential (°C)
	Inner Surface (°C)	Outer Surface (°C)	
Bottom of fuel	433	394	39
Peak heat rate	548	504	44
Top of fuel	649	617	32

The results of the DEFØRM calculations without fuel cladding mechanical interaction or flux enhanced cladding creep, but with the abnormally high assumed gas pressure, are presented in Table A-8.

These calculations do not include dimensional changes in the cladding from fast flux exposure. These were calculated independently for each pin at discrete axial locations.

Effects of Fast Flux on Cladding Volume Changes

The primary source of cladding dimensional changes will be the volume changes in the cladding material as a result of fast neutron exposure. To determine these at 1/2-in. intervals along the axial length of the fuel, we used the following swelling formula:

$$\% \frac{\Delta V}{V} = 4.90 \times 10^{-49} \, (\Phi t)^{1.71} \quad 10^{\left[\frac{1.549 \times 10^4}{T} - \frac{5.988 \times 10^6}{T^2}\right]} .$$

The temperature (T) at each interval was the mean temperature of the cladding for that interval, as determined by the MAMU heat transfer analysis. The axial flux distribution was based on Fig. C5 of the

Table A-8. Stress-Strain Analysis with no Allowance for Fabrication and Corrosion Effects

Pin Number	Cycle	Integrated Time of Test (hr)	Bottom of Fuel				Peak Heat Rate				Top of Fuel			
			Inner Surface		Outer Surface		Inner Surface		Outer Surface		Inner Surface		Outer Surface	
			Radius (in.)[a]	Stress (psi)[b]	Radius (in.)[a]	Stress (psi)	Radius (in.)	Stress (psi)	Radius (in.)	Stress (psi)	Radius (in.)	Stress (psi)	Radius (in.)	Stress (psi)
4	1	3,240	0.10977	-13,350	0.12588	14,610	0.10990	-16,500	0.12605	16,860	0.11004	-12,880	0.12621	14,130
4	2	3,840	0.10968	1,650	0.12578	1,420	0.10966	1,650	0.12528	1,420	0.10967	1,650	0.12578	1,420
4	3	7,080	0.10977	-11,450	0.12589	16,300	0.10990	-14,590	0.12607	18,550	0.11005	-11,000	0.12622	15,810
4	4	7,680	0.10968	3,500	0.12578	3,012	0.10966	3,490	0.12579	3,000	0.10967	3,490	0.12579	3,010
4	5	10,920	0.10978	-9,250	0.12589	18,250	0.10990	-12,410	0.12609	20,490	0.11005	-8,810	0.12624	17,730
4	6	11,520	0.10969	5,340	0.12579	4,610	0.10966	5,330	0.12581	4,590	0.10963	5,330	0.12580	4,600
4	7	14,760	0.10879	-7,051	0.12591	20,200	0.10991	-10,250	0.12612	22,410	0.11006	-6,630	0.12626	19,640
4	8	15,360	0.10970	7,190	0.12580	6,200	0.10967	7,160	0.12584	6,170	0.10968	7,170	0.12583	6,180
4	9	18,600	0.10980	-4,370	0.12593	22,130	0.10992	-8,100	0.12616	24,310	0.11007	-4,450	0.12630	21,510
4	10	19,200	0.10905	3,830	0.12507	3,300	0.10902	3,810	0.12513	3,280	0.10903	3,820	0.12511	3,290
Measurable Δ radius (in.)					0.00007				0.00013				0.00011	
Strain (%)					0.06				0.10				0.08	
7	1	3,240	0.10977	-12,490	0.12588	14,840	0.11002	-16,120	0.12623	17,940	0.11019	-8,150	0.12653	11,190
7	2	3,840	0.10968	1,750	0.12578	1,500	0.10963	1,740	0.12579	1,490	0.10956	1,730	0.12582	1,480
7	3	7,080	0.10978	-9,900	0.12589	17,140	0.11001	-13,840	0.12626	20,220	0.11016	-6,560	0.12663	12,340
7	4	7,680	0.10969	3,670	0.12579	3,160	0.10961	3,640	0.12581	3,140	0.10953	3,600	0.12593	3,090
7	5	10,920	0.10979	-7,310	0.12590	19,430	0.11001	-11,420	0.12630	22,430	0.11017	-3,800	0.12682	13,190
7	6	11,520	0.10969	5,590	0.12579	4,320	0.10961	5,540	0.12585	4,770	0.10953	5,430	0.12612	4,660
7	7	14,760	0.10980	-4,730	0.12592	21,720	0.11002	-8,930	0.12636	24,570	0.11019	-10	0.12712	13,980
7	8	15,360	0.10970	7,510	0.12581	6,480	0.10962	7,430	0.12591	6,390	0.10954	7,180	0.12642	6,150
7	9	18,600	0.10981	-2,160	0.12595	24,000	0.11003	-6,410	0.12644	26,620	0.11023	4,560	0.12756	14,900
7	10	19,200	0.10905	4,010	0.12508	3,460	0.10897	4,010	0.12523	3,450	0.10891	3,760	0.12611	3,210
Measurable Δ radius (in.)					0.00008				0.00023				0.00111	
Strain (%)					0.06				0.18				0.88	

[a]At room temperature the initial radii are: inner surface – 0.109 in. outer surface – 0.125 in.

[b]The stress values are for tangential stress in the increment adjacent to the surface identified. Positive values are tensile, and negative (–) values are compressive. The cladding thickness was divided into five radial increments for this analysis.

Guide. The peak fast flux for a pin in subassembly Position 1 was calculated as follows:

From the Guide: Peak fission rate for ^{239}Pu = 0.774×10^{13} fissions/g-sec at 50 MW.

Therefore, at 62.5 MW the peak rate is $0.774 \times 10^{13} \times 1.25$ = 0.9675×10^{13} fissions/g-sec.

From a physics analysis of the EBR-II, we had determined an effective fission cross section for ^{239}Pu in Row 6 of 1.77 barns, thus setting:

$$\Phi = \frac{\text{fission rate}}{n\,\sigma_f}$$

$$\Phi = 0.9675 \times 10^{13} \; \frac{239 \text{ g/mole}}{6.023 \times 10^{23} \text{ atoms/mole}} \; \frac{1}{1.77 \times 10^{-24}}$$

$$\Phi = 2.1685 \times 10^{15}$$

Since the flux with energy greater than 0.1 Mev is reportedly[34] 87%, we used a peak flux of 1.887×10^{15} for the pin in subassembly Position 1. This agrees well with the curves on pages 60 and 61 of the Guide.

The flux at all other pin locations was ratioed in accordance with the fission rate decrease in going from Position 1 to Position 37 approximately 17%.

The results of the cladding volume change calculations are given in Table A-9. The maximum change in diameter from the change in cladding density is 3.4% in the peak flux regions. To this must be added the 0.4% for creep deformation calculated by the preliminary stress analysis to yield a peak measurable change in diameter of 3.8% for the peak flux position of pins irradiated to the maximum burnup level.

Table A-9

The following tables are the computer output for each pin showing the calculated end-of-life volume and diameter changes for the cladding material as a result of fast neutron fluence. Each position is a one-half-inch length of cladding beginning at the bottom of the fueled section (9) and terminating at the top of the fuel column (35).

PIN NO IS 1 TIME IN DAYS = 381. PEAK FLUX IS 0.88660E 15

POSI	T(IN) DEG C	T(OUT) DEG C	DEL T DEG C	T(M) DEG C	FLUX	FLUENCE	PERC V	PERC D
9	433.4	394.8	38.6	414.1	0.151E 16	0.497E 23	2.30	0.77
10	439.2	399.7	39.5	419.4	0.155E 16	0.512E 23	2.53	0.84
11	445.2	404.7	40.6	424.9	0.160E 16	0.527E 23	2.79	0.93
12	451.7	409.9	41.8	430.8	0.165E 16	0.545E 23	3.08	1.03
13	458.1	415.2	42.8	436.6	0.170E 16	0.561E 23	3.38	1.13
14	464.3	420.6	43.8	442.4	0.175E 16	0.575E 23	3.65	1.22
15	470.5	426.0	44.6	448.3	0.179E 16	0.588E 23	3.91	1.30
16	476.7	431.2	45.6	453.9	0.182E 16	0.599E 23	4.13	1.38
17	482.7	436.9	45.7	459.8	0.185E 16	0.608E 23	4.34	1.45
18	488.4	442.4	46.1	465.4	0.187E 16	0.614E 23	4.50	1.50
19	494.0	447.8	46.2	470.9	0.188E 16	0.618E 23	4.63	1.54
20	499.3	453.1	46.2	476.2	0.188E 16	0.620E 23	4.71	1.57
21	504.4	458.4	46.1	481.4	0.188E 16	0.620E 23	4.75	1.58
22	509.3	463.6	45.7	486.4	0.188E 16	0.618E 23	4.75	1.58
23	513.9	468.7	45.3	491.3	0.187E 16	0.614E 23	4.72	1.57
24	518.3	473.6	44.7	495.9	0.185E 16	0.607E 23	4.65	1.55
25	522.4	478.4	44.0	500.4	0.182E 16	0.600E 23	4.55	1.52
26	526.2	483.1	43.1	504.6	0.179E 16	0.589E 23	4.41	1.47
27	529.7	487.6	42.2	508.6	0.176E 16	0.578E 23	4.26	1.42
28	533.0	491.9	41.1	512.4	0.171E 16	0.564E 23	4.08	1.36
29	536.1	495.6	40.6	515.8	0.167E 16	0.551E 23	3.90	1.30
30	538.9	500.1	38.8	519.5	0.163E 16	0.535E 23	3.69	1.23
31	541.3	503.9	37.4	522.6	0.157E 16	0.518E 23	3.48	1.16
32	543.8	507.6	36.3	525.7	0.152E 16	0.502E 23	3.28	1.09
33	546.3	511.2	35.1	528.7	0.148E 16	0.487E 23	3.10	1.03
34	548.9	514.7	34.2	531.8	0.144E 16	0.475E 23	2.94	0.98
35	552.1	518.4	33.6	535.2	0.142E 16	0.468E 23	2.85	0.95

T(IN) = TEMP OF INNER CLAD SURFACE. TOUT = TEMP OF OUTER CLAD SURFACE
DEL T = T(IN) - T(OUT) T(M) = CLAD MEAN TEMP.
PERC V = PERCENT CLAD VOLUME CHANGE. PERC D = PERCENT CLAD DIAMETER CHANGE.

PIN NO IS 2 TIME IN DAYS = 590. PEAK FLUX IS 1.86020E 15

POSI	T(IN) DEG C	T(OUT) DEG C	DEL T DEG C	T(M) DEG C	FLUX	FLUENCE	PERC V	PERC D
9	431.6	393.5	38.1	412.5	0.149E 16	0.759E 23	4.67	1.56
10	437.6	398.6	39.0	418.1	0.153E 16	0.781E 23	5.16	1.72
11	443.8	403.8	40.0	423.8	0.156E 16	0.804E 23	5.70	1.90
12	450.4	409.2	41.2	429.8	0.163E 16	0.831E 23	6.31	2.10
13	457.1	414.8	42.3	435.9	0.168E 16	0.857E 23	6.93	2.31
14	463.6	420.4	43.2	442.0	0.172E 16	0.878E 23	7.50	2.50
15	470.1	426.1	44.0	448.1	0.176E 16	0.898E 23	8.05	2.68
16	476.5	431.8	44.7	454.2	0.179E 16	0.914E 23	8.53	2.84
17	482.7	437.6	45.1	460.2	0.182E 16	0.928E 23	8.96	2.99
18	488.8	443.3	45.4	466.1	0.184E 16	0.938E 23	9.30	3.10
19	494.6	449.1	45.6	471.8	0.185E 16	0.944E 23	9.56	3.19
20	500.3	454.7	45.6	477.5	0.186E 16	0.947E 23	9.74	3.25
21	505.8	460.3	45.4	483.1	0.186E 16	0.947E 23	9.83	3.28
22	510.9	465.8	45.1	488.4	0.185E 16	0.943E 23	9.81	3.27
23	515.9	471.3	44.7	493.6	0.184E 16	0.938E 23	9.75	3.25
24	520.5	476.6	44.1	498.6	0.182E 16	0.928E 23	9.59	3.20
25	525.1	481.7	43.3	503.4	0.180E 16	0.916E 23	9.38	3.13
26	529.2	486.7	42.4	507.9	0.176E 16	0.900E 23	9.08	3.03
27	533.1	491.6	41.5	512.4	0.173E 16	0.882E 23	8.75	2.92
28	536.7	496.3	40.4	516.5	0.169E 16	0.862E 23	8.38	2.79
29	540.2	500.8	39.3	520.5	0.165E 16	0.841E 23	7.98	2.66
30	543.3	505.2	38.2	524.2	0.160E 16	0.817E 23	7.56	2.52
31	546.2	509.3	36.9	527.7	0.155E 16	0.791E 23	7.10	2.37
32	548.9	513.3	35.7	531.1	0.150E 16	0.766E 23	6.68	2.23
33	551.8	517.2	34.6	534.5	0.146E 16	0.744E 23	6.31	2.10
34	554.7	521.1	33.6	537.9	0.142E 16	0.725E 23	5.98	1.99
35	558.1	525.1	33.0	541.6	0.140E 16	0.714E 23	5.78	1.93

T(IN) = TEMP OF INNER CLAD SURFACE. TOUT = TEMP OF OUTER CLAD SURFACE.
DEL T = T(IN) - T(OUT) T(M) = CLAD MEAN TEMP.
PERC V = PERCENT CLAD VOLUME CHANGE. PERC D = PERCENT CLAD DIAMETER CHANGE.

PIN NO IS 3 TIME IN DAYS = 254. PEAK FLUX IS 1.83190E 15

POSI	T(IN) DEG C	T(OUT) DEG C	DEL T DEG C	T(M) DEG C	FLUX	FLUENCE	PERC V	PERC D
9	430.8	393.3	37.6	412.1	0.147E 16	0.322E 23	1.07	0.36
10	436.7	398.2	38.5	417.5	0.151E 16	0.331E 23	1.18	0.39
11	442.9	403.4	39.5	423.1	0.155E 16	0.341E 23	1.31	0.44
12	449.4	408.7	40.7	429.1	0.161E 16	0.352E 23	1.45	0.48
13	456.0	414.2	41.8	435.1	0.166E 16	0.363E 23	1.59	0.53
14	462.4	419.8	42.7	441.1	0.170E 16	0.372E 23	1.72	0.57
15	468.9	425.4	43.5	447.1	0.174E 16	0.381E 23	1.85	0.62
16	475.1	431.1	44.1	453.1	0.177E 16	0.388E 23	1.96	0.65
17	481.3	436.7	44.6	459.0	0.179E 16	0.393E 23	2.06	0.69
18	487.3	440.7	46.6	464.0	0.181E 16	0.398E 23	2.13	0.71
19	493.1	448.1	45.0	470.6	0.182E 16	0.400E 23	2.20	0.73
20	498.7	453.7	45.0	476.2	0.183E 16	0.402E 23	2.24	0.75
21	504.0	459.2	44.8	481.6	0.183E 16	0.402E 23	2.26	0.75
22	509.1	464.6	44.5	486.9	0.182E 16	0.400E 23	2.26	0.75
23	514.1	469.9	44.1	492.0	0.181E 16	0.398E 23	2.25	0.75
24	518.7	475.2	43.5	496.9	0.179E 16	0.393E 23	2.21	0.74
25	523.1	480.3	42.8	501.7	0.177E 16	0.388E 23	2.16	0.72
26	527.2	485.2	41.9	506.2	0.174E 16	0.381E 23	2.10	0.70
27	531.1	490.0	41.1	510.5	0.170E 16	0.374E 23	2.02	0.67
28	534.6	494.6	40.0	514.6	0.167E 16	0.365E 23	1.93	0.64
29	538.0	499.1	38.9	518.6	0.162E 16	0.356E 23	1.85	0.62
30	541.1	503.4	37.7	522.2	0.156E 16	0.346E 23	1.75	0.58
31	543.9	507.4	36.4	525.7	0.153E 16	0.335E 23	1.64	0.55
32	546.6	511.4	35.2	529.0	0.148E 16	0.325E 23	1.55	0.52
33	549.4	515.3	34.1	532.3	0.144E 16	0.315E 23	1.46	0.49
34	552.3	519.1	33.2	535.7	0.140E 16	0.307E 23	1.39	0.46
35	555.7	523.1	32.6	539.4	0.138E 16	0.303E 23	1.34	0.45

T(IN) = TEMP OF INNER CLAD SURFACE.
DEL T = T(IN) - T(OUT)
PERC V = PERCENT CLAD VOLUME CHANGE.

TOUT = TEMP OF OUTER CLAD SURFACE.
T(M) = CLAD MEAN TEMP.
PERC D = PERCENT CLAD DIAMETER CHANGE.

PIN NO IS 4 TIME IN DAYS = 590. PEAK FLUX IS 1.80550E 15

POSI	T(IN) DEG C	T(OUT) DEG C	DEL T DEG C	T(M) DEG C	FLUX	FLUENCE	PERC V	PERC D
9	434.6	395.3	39.3	414.9	0.145E 16	0.737E 23	4.54	1.51
10	440.4	400.2	40.2	420.3	0.149E 16	0.758E 23	5.00	1.67
11	446.6	405.3	41.3	425.9	0.153E 16	0.781E 23	5.51	1.84
12	453.2	410.6	42.6	431.9	0.158E 16	0.807E 23	6.09	2.03
13	459.7	416.1	43.7	437.9	0.163E 16	0.832E 23	6.67	2.22
14	466.1	421.5	44.6	443.8	0.167E 16	0.853E 23	7.20	2.40
15	472.5	427.1	45.4	449.3	0.171E 16	0.872E 23	7.71	2.57
16	478.7	432.6	46.1	455.7	0.174E 16	0.888E 23	8.16	2.72
17	484.3	438.2	46.6	461.5	0.177E 16	0.901E 23	8.55	2.85
18	490.7	443.7	46.9	467.2	0.179E 16	0.910E 23	8.87	2.96
19	496.3	449.2	47.1	472.8	0.180E 16	0.916E 23	9.10	3.03
20	501.8	454.7	47.1	478.2	0.180E 16	0.920E 23	9.27	3.09
21	507.0	460.1	46.9	483.5	0.180E 16	0.920E 23	9.35	3.12
22	511.9	465.3	46.6	488.6	0.180E 16	0.915E 23	9.33	3.11
23	516.7	470.6	46.1	493.6	0.179E 16	0.910E 23	9.27	3.09
24	521.1	475.6	45.6	498.3	0.177E 16	0.900E 23	9.11	3.04
25	525.3	480.5	44.8	502.9	0.174E 16	0.889E 23	8.91	2.97
26	529.1	485.2	43.9	507.2	0.171E 16	0.873E 23	8.63	2.88
27	532.8	489.8	43.9	511.3	0.168E 16	0.856E 23	8.33	2.78
28	536.1	494.2	41.9	515.2	0.164E 16	0.837E 23	7.97	2.66
29	539.3	498.5	40.8	518.9	0.160E 16	0.816E 23	7.60	2.53
30	542.1	502.6	39.5	522.4	0.156E 16	0.793E 23	7.21	2.40
31	544.6	506.4	38.2	525.5	0.151E 16	0.768E 23	6.78	2.26
32	547.2	510.2	36.9	528.7	0.146E 16	0.744E 23	6.38	2.13
33	549.7	513.9	35.8	531.8	0.142E 16	0.722E 23	6.03	2.01
34	552.3	517.6	34.8	534.9	0.138E 16	0.704E 23	5.73	1.91
35	555.6	521.3	34.2	538.4	0.136E 16	0.693E 23	5.54	1.85

T(IN) = TEMP OF INNER CLAD SURFACE.
DEL T = T(IN) - T(OUT)
PERC V = PERCENT CLAD VOLUME CHANGE.

TOUT = TEMP OF OUTER CLAD SURFACS.
T(M) = CLAD MEAN TEMP.
PERC D = PERCENT CLAD DIAMETER CHANGE.

PIN NO IS 5 TIME IN DAYS = 590. PEAK FLUX IS 1.86020E 15

POS I	T(IN) DEG C	T(OUT) DEG C	DEL T DEG C	T(M) DEG C	FLUX	FLUENCE	PERC V	PERC D
9	431.6	393.5	38.1	412.5	0.149E 16	0.759E 23	4.67	1.56
10	437.6	398.6	39.0	418.1	0.153E 16	0.781E 23	5.16	1.72
11	443.8	403.8	40.0	423.8	0.158E 16	0.804E 23	5.70	1.90
12	450.4	409.2	41.2	429.8	0.163E 16	0.831E 23	6.31	2.10
13	457.1	414.8	42.3	435.9	0.168E 16	0.857E 23	6.93	2.31
14	463.6	420.4	43.2	442.0	0.172E 16	0.878E 23	7.50	2.50
15	470.1	426.1	44.0	448.1	0.176E 16	0.898E 23	8.05	2.68
16	476.5	431.8	44.7	454.2	0.179E 16	0.914E 23	8.53	2.84
17	482.7	437.6	45.1	460.2	0.182E 16	0.928E 23	8.96	2.99
18	488.8	443.3	45.4	466.1	0.184E 16	0.938E 23	9.30	3.10
19	494.6	449.1	45.6	471.8	0.185E 16	0.944E 23	9.56	3.19
20	500.3	454.7	45.6	477.5	0.186E 16	0.947E 23	9.74	3.25
21	505.8	460.3	45.4	483.1	0.186E 16	0.947E 23	9.83	3.28
22	510.9	465.8	45.1	488.4	0.185E 16	0.943E 23	9.81	3.27
23	515.9	471.3	44.7	493.6	0.184E 16	0.938E 23	9.75	3.25
24	520.6	476.6	44.1	498.6	0.182E 16	0.928E 23	9.59	3.20
25	525.1	481.7	43.3	503.4	0.180E 16	0.916E 23	9.38	3.13
26	529.2	486.7	42.4	507.9	0.176E 16	0.900E 23	9.08	3.03
27	533.1	491.6	41.5	512.4	0.173E 16	0.882E 23	8.75	2.92
28	536.7	496.2	40.4	516.5	0.169E 16	0.862E 23	8.38	2.79
29	540.2	500.8	39.3	520.5	0.165E 16	0.841E 23	7.98	2.66
30	543.3	505.2	38.2	524.2	0.160E 16	0.817E 23	7.56	2.52
31	546.2	509.3	36.9	527.7	0.155E 16	0.791E 23	7.10	2.37
32	548.9	513.3	35.7	531.1	0.150E 16	0.766E 23	6.68	2.23
33	551.8	517.2	34.6	534.5	0.146E 16	0.744E 23	6.31	2.10
34	554.7	521.1	33.6	537.9	0.142E 16	0.725E 23	5.98	1.99
35	558.1	525.1	33.0	541.6	0.140E 16	0.714E 23	5.78	1.93

T(IN) = TEMP OF INNER CLAD SURFACE. TOUT = TEMP OF OUTER CLAD SURFACE
DEL T = T(IN) - T(OUT) T(M) = CLAD MEAN TEMP.
PERC V = PERCENT CLAD VOLUME CHANGE. PERC D = PERCENT CLAD DIAMETER CHANGE

PIN NO IS 6 TIME IN DAYS = 590. PEAK FLUX IS 1.31900E 15

POSI	T(IN) DEG C	T(OUT) DEG C	DEL T DEG C	T(M) DEG C	FLUX	FLUENCE	PERC V	PERC D
9	432.8	394.4	38.4	413.6	0.106E 16	0.538E 23	2.62	0.87
10	441.8	402.6	39.2	422.2	0.109E 16	0.554E 23	2.97	0.99
11	451.1	410.9	40.2	431.0	0.112E 16	0.570E 23	3.34	1.11
12	460.8	419.6	41.3	440.2	0.116E 16	0.590E 23	3.75	1.25
13	470.8	428.4	42.3	449.6	0.119E 16	0.608E 23	4.16	1.39
14	480.7	437.5	43.2	459.1	0.122E 16	0.623E 23	4.51	1.50
15	490.6	446.8	43.8	468.7	0.125E 16	0.637E 23	4.84	1.61
16	500.4	456.1	44.3	478.3	0.127E 16	0.648E 23	5.10	1.70
17	510.3	465.6	44.7	487.9	0.129E 16	0.658E 23	5.30	1.77
18	520.0	475.1	44.9	497.5	0.130E 16	0.665E 23	5.43	1.81
19	529.6	484.6	45.0	507.1	0.131E 16	0.669E 23	5.48	1.83
20	538.9	494.1	44.9	516.5	0.132E 16	0.672E 23	5.47	1.82
21	548.2	503.6	44.6	525.9	0.132E 16	0.672E 23	5.39	1.80
22	557.1	512.9	44.2	535.0	0.131E 16	0.669E 23	5.25	1.75
23	565.8	522.2	43.7	544.0	0.130E 16	0.665E 23	5.08	1.69
24	574.2	531.2	43.0	552.7	0.129E 16	0.658E 23	4.85	1.62
25	582.4	540.2	42.2	561.3	0.127E 16	0.649E 23	4.60	1.53
26	590.2	548.9	41.3	569.5	0.125E 16	0.638E 23	4.32	1.44
27	597.7	557.4	40.3	577.6	0.123E 16	0.626E 23	4.04	1.35
28	604.9	565.7	39.2	585.3	0.120E 16	0.611E 23	3.74	1.25
29	611.8	573.8	38.1	592.8	0.117E 16	0.596E 23	3.46	1.15
30	618.4	581.6	36.8	600.0	0.114E 16	0.579E 23	3.17	1.06
31	624.5	589.0	35.5	606.7	0.110E 16	0.561E 23	2.89	0.96
32	630.5	596.2	34.3	613.4	0.107E 16	0.543E 23	2.64	0.88
33	636.4	603.3	33.2	619.9	0.103E 16	0.527E 23	2.41	0.80
34	642.4	610.2	32.2	626.3	0.101E 16	0.514E 23	2.22	0.74
35	648.7	617.2	31.6	632.9	0.993E 15	0.506E 23	2.08	0.69

T(IN) = TEMP OF INNER CLAD SURFACE.
DEL T = T(IN) - T(OUT)
PERC V = PERCENT CLAD VOLUME CHANGE.

TOUT = TEMP OF OUTER CLAD SURFACE.
T(M) = CLAD MEAN TEMP.
PERC D = PERCENT CLAD DIAMETER CHANGE.

PIN NO IS 7 TIME IN DAYS = 590. PEAK FLUX IS 1.80550E 15

POSI	T(IN) DEG C	T(OUT) DEG C	DEL T DEG C	T(M) DEG C	FLUX	FLUENCE	PERC V	PERC D
9	432.8	394.4	38.4	413.6	0.145E 16	0.737E 23	4.49	1.50
10	441.8	402.6	39.2	422.2	0.149E 16	0.758E 23	5.08	1.69
11	451.1	410.9	40.2	431.0	0.153E 16	0.781E 23	5.72	1.91
12	460.9	419.6	41.3	440.2	0.158E 16	0.807E 23	6.42	2.14
13	470.8	428.4	42.3	449.6	0.163E 16	0.832E 23	7.11	2.37
14	480.7	437.5	43.2	459.1	0.167E 16	0.853E 23	7.72	2.57
15	490.6	446.8	43.8	468.7	0.171E 16	0.872E 23	8.28	2.76
16	500.4	456.1	44.3	478.3	0.174E 16	0.888E 23	8.72	2.91
17	510.3	465.6	44.7	487.9	0.177E 16	0.901E 23	9.07	3.02
18	520.0	475.1	44.9	497.5	0.179E 16	0.910E 23	9.28	3.09
19	529.6	484.6	45.0	507.1	0.180E 16	0.916E 23	9.37	3.12
20	538.9	494.1	44.9	516.5	0.180E 16	0.920E 23	9.36	3.12
21	548.2	503.6	44.6	525.9	0.180E 16	0.920E 23	9.23	3.08
22	557.1	512.9	44.2	535.0	0.180E 16	0.915E 23	8.98	2.99
23	565.8	522.2	43.7	544.0	0.179E 16	0.910E 23	8.69	2.90
24	574.2	531.2	43.0	552.7	0.177E 16	0.900E 23	8.30	2.77
25	582.4	540.2	42.2	561.3	0.174E 16	0.869E 23	7.88	2.63
26	590.2	548.9	41.3	569.5	0.171E 16	0.873E 23	7.40	2.47
27	597.7	557.4	40.3	577.6	0.168E 16	0.856E 23	6.91	2.30
28	604.9	565.7	39.2	585.3	0.164E 16	0.837E 23	6.41	2.14
29	611.8	573.8	38.1	592.8	0.160E 16	0.816E 23	5.91	1.97
30	618.4	581.6	36.8	600.0	0.156E 16	0.793E 23	5.43	1.81
31	624.5	589.0	35.5	606.7	0.151E 16	0.768E 23	4.94	1.65
32	630.5	596.2	34.3	613.4	0.146E 16	0.744E 23	4.51	1.50
33	636.4	603.3	33.2	619.9	0.142E 16	0.722E 23	4.13	1.33
34	642.4	610.2	32.2	626.3	0.138E 16	0.704E 23	3.80	1.27
35	648.7	617.2	31.5	632.9	0.136E 16	0.693E 23	3.55	1.18

T(IN) = TEMP OF INNER CLAD SURFACE.
DEL T = T(IN) - T(OUT)
PERC V = PERCENT CLAD VOLUME CHANGE.

TOUT = TEMP OF OUTER CLAD SURFACE.
T(M) = CLAD MEAN TEMP.
PERC D = PERCENT CLAD DIAMETER CHANGE

PIN NO IS 8 TIME IN DAYS = 381. PEAK FLUX IS 1.77910E 15

PCSI	T(IN) DEG C	T(OUT) DEG C	DEL T DEG C	T(M) DEG C	FLUX	FLUENCE	PERC V	PERC D
9	432.1	394.2	37.8	413.1	0.142E 16	0.469E 23	2.06	0.69
10	440.9	402.2	38.7	421.5	0.147E 16	0.482E 23	2.33	0.78
11	450.1	410.4	39.7	430.2	0.151E 16	0.497E 23	2.63	0.88
12	459.7	418.9	40.7	439.3	0.156E 16	0.513E 23	2.95	0.98
13	469.4	427.7	41.7	448.6	0.161E 16	0.529E 23	3.27	1.09
14	479.2	436.6	42.6	457.9	0.165E 16	0.543E 23	3.55	1.18
15	489.1	445.8	43.3	467.4	0.169E 16	0.555E 23	3.81	1.27
16	498.8	455.0	43.8	476.9	0.172E 16	0.565E 23	4.02	1.34
17	508.4	464.3	44.1	486.4	0.174E 16	0.573E 23	4.18	1.39
18	518.1	473.7	44.4	495.9	0.176E 16	0.579E 23	4.28	1.43
19	527.4	483.1	44.4	505.2	0.177E 16	0.583E 23	4.33	1.44
20	536.7	492.4	44.3	514.6	0.178E 16	0.585E 23	4.33	1.44
21	545.8	501.7	44.1	523.7	0.178E 16	0.585E 23	4.27	1.42
22	554.6	510.9	43.6	532.7	0.177E 16	0.583E 23	4.17	1.39
23	563.2	520.1	43.2	541.6	0.176E 16	0.579E 23	4.04	1.35
24	571.5	529.1	42.4	550.3	0.174E 16	0.573E 23	3.86	1.29
25	579.6	537.9	41.7	558.7	0.172E 16	0.566E 23	3.67	1.22
26	587.2	546.5	40.7	566.9	0.169E 16	0.556E 23	3.45	1.15
27	594.7	554.9	39.8	574.8	0.166E 16	0.545E 23	3.23	1.08
28	601.8	563.1	38.7	582.4	0.162E 16	0.532E 23	3.00	1.00
29	608.6	571.0	37.6	589.8	0.158E 16	0.519E 23	2.77	0.92
30	615.0	578.7	36.3	596.8	0.153E 16	0.505E 23	2.55	0.85
31	621.1	586.0	35.1	603.6	0.148E 16	0.488E 23	2.32	0.77
32	627.0	593.2	33.8	610.1	0.144E 16	0.473E 23	2.12	0.71
33	632.8	600.1	32.7	616.5	0.140E 16	0.459E 23	1.94	0.65
34	638.7	606.9	31.8	622.8	0.136E 16	0.448E 23	1.79	0.60
35	645.0	613.8	31.2	629.4	0.134E 16	0.441E 23	1.68	0.56

T(IN) = TEMP OF INNER CLAD SURFACE.
DEL T = T(IN) - T(OUT)
PERC V = PERCENT CLAD VOLUME CHANGE.

TOUT = TEMP OF OUTER CLAD SURFACE.
T(M) = CLAD MEAN TEMP.
PERC D = PERCENT CLAD DIAMETER CHANGE.

PIN NO IS 9 TIME IN DAYS = 590. PEAK FLUX IS 1.75270E 15

POS I	T(IN) DEG C	T(OUT) DEG C	DEL T DEG C	T(M) DEG C	FLUX	FLUENCE	PERC V	PERC D
9	431.8	393.6	38.2	412.7	0.140E 16	0.715E 23	4.23	1.41
10	437.8	398.7	39.2	418.2	0.144E 16	0.736E 23	4.67	1.56
11	444.1	403.9	40.2	424.0	0.149E 16	0.758E 23	5.16	1.72
12	450.8	409.4	41.4	430.1	0.154E 16	0.783E 23	5.71	1.90
13	457.4	414.9	42.5	436.2	0.158E 16	0.807E 23	6.27	2.09
14	464.0	420.6	43.4	442.3	0.162E 16	0.828E 23	6.79	2.26
15	470.6	426.3	44.2	448.4	0.166E 16	0.846E 23	7.28	2.43
16	476.9	432.1	44.8	454.5	0.169E 16	0.862E 23	7.72	2.57
17	483.2	437.9	45.3	460.6	0.172E 16	0.874E 23	8.11	2.70
18	489.3	443.7	45.6	466.5	0.173E 16	0.883E 23	8.41	2.80
19	495.2	449.4	45.8	472.3	0.174E 16	0.889E 23	8.64	2.88
20	500.8	455.1	45.7	478.0	0.175E 16	0.893E 23	8.80	2.93
21	506.3	460.7	45.6	483.5	0.175E 16	0.893E 23	8.88	2.96
22	511.5	466.3	45.2	488.9	0.174E 16	0.889E 23	8.87	2.96
23	516.6	471.7	44.8	494.1	0.173E 16	0.883E 23	8.81	2.94
24	521.2	477.0	44.2	499.1	0.171E 16	0.874E 23	8.66	2.89
25	525.7	482.2	43.5	504.0	0.169E 16	0.863E 23	8.47	2.82
26	529.9	487.2	42.7	508.6	0.166E 16	0.848E 23	8.20	2.73
27	533.8	492.1	41.7	513.0	0.163E 16	0.831E 23	7.90	2.63
28	537.4	496.8	40.6	517.1	0.159E 16	0.812E 23	7.56	2.52
29	540.9	501.4	39.6	521.2	0.155E 16	0.792E 23	7.20	2.40
30	544.1	505.7	38.3	524.9	0.151E 16	0.770E 23	6.82	2.27
31	546.9	509.9	37.1	528.4	0.146E 16	0.745E 23	6.41	2.14
32	549.7	513.9	35.8	531.8	0.142E 16	0.722E 23	6.03	2.01
33	552.5	517.8	34.7	535.2	0.137E 16	0.701E 23	5.69	1.90
34	555.5	521.8	33.7	538.6	0.134E 16	0.683E 23	5.39	1.80
35	558.9	525.8	33.2	542.4	0.132E 16	0.673E 23	5.21	1.74

T(IN) = TEMP OF INNER CLAD SURFACE. TOUT = TEMP OF OUTER CLAD SURFACE.
DEL T = T(IN) - T(OUT) T(M) = CLAD MEAN TEMP.
PERC V = PERCENT CLAD VOLUME CHANGE. PERC D = PERCENT CLAD DIAMETER CHANGE

PIN NO IS 10 TIME IN DAYS = 254. PEAK FLUX IS 1.83190E 15

POSI	T(IN) DEG C	T(OUT) DEG C	DEL T DEG C	T(M) DEG C	FLUX	FLUENCE	PERC V	PERC D
9	430.8	393.3	37.6	412.1	0.147E 16	0.322E 23	1.07	0.36
10	436.7	398.2	38.5	417.5	0.151E 16	0.331E 23	1.18	0.39
11	442.9	403.4	39.5	423.1	0.155E 16	0.341E 23	1.31	0.44
12	449.4	408.7	40.7	429.1	0.161E 16	0.352E 23	1.45	0.48
13	456.0	414.2	41.8	435.1	0.166E 16	0.363E 23	1.59	0.53
14	462.4	419.8	42.7	441.1	0.170E 16	0.372E 23	1.72	0.57
15	468.9	425.4	43.5	447.1	0.174E 16	0.381E 23	1.85	0.62
16	475.1	431.1	44.1	453.1	0.177E 16	0.388E 23	1.96	0.65
17	481.3	436.7	44.6	459.0	0.179E 16	0.393E 23	2.06	0.69
18	487.3	440.7	46.5	464.0	0.181E 16	0.398E 23	2.13	0.71
19	493.1	448.1	45.0	470.6	0.182E 16	0.400E 23	2.20	0.73
20	498.7	453.7	45.0	476.2	0.183E 16	0.402E 23	2.24	0.75
21	504.0	459.2	44.8	481.6	0.183E 16	0.402E 23	2.26	0.75
22	509.1	464.6	44.5	486.9	0.182E 16	0.400E 23	2.26	0.75
23	514.1	469.9	44.1	492.0	0.181E 16	0.398E 23	2.25	0.75
24	518.7	475.2	43.5	496.9	0.179E 16	0.393E 23	2.21	0.74
25	523.1	480.3	42.8	501.7	0.177E 16	0.388E 23	2.16	0.72
26	527.2	485.2	41.9	506.2	0.174E 16	0.381E 23	2.10	0.70
27	531.1	490.0	41.1	510.5	0.170E 16	0.374E 23	2.02	0.67
28	534.6	494.6	40.0	514.6	0.167E 16	0.365E 23	1.93	0.64
29	538.0	499.1	38.9	518.6	0.162E 16	0.356E 23	1.85	0.62
30	541.1	503.4	37.7	522.2	0.158E 16	0.346E 23	1.75	0.58
31	543.9	507.4	36.4	525.7	0.153E 16	0.335E 23	1.64	0.55
32	546.6	511.4	35.2	529.0	0.148E 16	0.325E 23	1.55	0.52
33	549.4	515.3	34.1	532.3	0.144E 16	0.315E 23	1.46	0.49
34	552.3	519.1	33.2	535.7	0.140E 16	0.307E 23	1.39	0.46
35	555.7	523.1	32.6	539.4	0.138E 16	0.303E 23	1.34	0.45

T(IN) = TEMP OF INNER CLAD SURFACE. TOUT = TEMP OF OUTER CLAD SURFACS.
DEL T = T(IN) - T(OUT) T(M) = CLAD MEAN TEMP.
PERC V = PERCENT CLAD VOLUME CHANGE. PERC D = PERCENT CLAD DIAMETER CHANGE.

PIN NO IS 11 TIME IN DAYS = 590. PEAK FLUX IS 1.80550E 15

POSI	T(IN) DEG C	T(OUT) DEG C	DEL T DEG C	T(M) DEG C	FLUX	FLUENCE	PERC V	PERC D
9	432.8	394.4	38.4	413.6	0.145E 16	0.737E 23	4.49	1.50
10	441.8	402.6	39.2	422.2	0.149E 16	0.758E 23	5.08	1.69
11	451.1	410.9	40.2	431.0	0.153E 16	0.781E 23	5.72	1.91
12	460.3	419.6	41.3	440.2	0.158E 16	0.807E 23	6.42	2.14
13	470.8	428.4	42.3	449.6	0.163E 16	0.832E 23	7.11	2.37
14	480.7	437.5	43.2	459.1	0.167E 16	0.853E 23	7.72	2.57
15	490.6	446.8	43.8	468.7	0.171E 16	0.872E 23	8.28	2.76
16	500.4	456.1	44.3	478.3	0.174E 16	0.888E 23	8.72	2.91
17	510.3	465.6	44.7	487.9	0.177E 16	0.901E 23	9.07	3.02
18	520.0	475.1	44.9	497.5	0.179E 16	0.910E 23	9.28	3.09
19	529.6	484.6	45.0	507.1	0.180E 16	0.916E 23	9.37	3.12
20	538.9	494.1	44.9	516.5	0.180E 16	0.920E 23	9.36	3.12
21	548.2	503.6	44.6	525.9	0.180E 16	0.920E 23	9.23	3.08
22	557.1	512.9	44.2	535.0	0.180E 16	0.915E 23	8.98	2.99
23	565.8	522.2	43.7	544.0	0.179E 16	0.910E 23	8.69	2.90
24	574.2	531.2	43.0	552.7	0.177E 16	0.900E 23	8.30	2.77
25	582.4	540.2	42.2	561.3	0.174E 16	0.889E 23	7.88	2.63
26	590.2	548.9	41.3	569.5	0.171E 16	0.873E 23	7.40	2.47
27	597.7	557.4	40.3	577.6	0.168E 16	0.856E 23	6.91	2.30
28	604.9	565.7	39.2	585.3	0.164E 16	0.837E 23	6.41	2.14
29	611.8	573.8	38.1	592.8	0.160E 16	0.816E 23	5.91	1.97
30	618.4	581.6	36.8	600.0	0.156E 16	0.793E 23	5.43	1.81
31	624.5	589.0	35.5	606.7	0.151E 16	0.768E 23	4.94	1.65
32	630.5	596.2	34.3	613.4	0.146E 16	0.744E 23	4.51	1.50
33	636.4	603.3	33.2	619.9	0.142E 16	0.722E 23	4.13	1.38
34	642.4	610.2	32.2	626.3	0.138E 16	0.704E 23	3.80	1.27
35	648.7	617.2	31.6	632.9	0.136E 16	0.693E 23	3.55	1.18

T(IN) = TEMP OF INNER CLAD SURFACE
DEL T = T(IN) - T(OUT)
PERC V = PERCENT CLAD VOLUME CHANGE.

TOUT = TEMP OF OUTER CLAD SURFACE
T(M) = CLAD MEAN TEMP.
PERC D = PERCENT CLAD DIAMETER CHANGE.

PIN NC IS 12 TIME IN DAYS = 254. PEAK FLUX IS 1.77910E 15

POSI	T(IN) DEG C	T(OUT) DEG C	DEL T DEG C	T(M) DEG C	FLUX	FLUENCE	PERC V	PERC D
9	432.1	394.2	37.8	413.1	0.142E 16	0.313E 23	1.03	0.34
10	440.9	402.2	38.7	421.5	0.147E 16	0.322E 23	1.17	0.39
11	450.1	410.4	39.7	430.2	0.151E 16	0.331E 23	1.31	0.44
12	459.7	418.9	40.7	439.3	0.156E 16	0.342E 23	1.47	0.49
13	469.4	427.7	41.7	448.6	0.161E 16	0.353E 23	1.63	0.54
14	479.2	436.6	42.6	457.9	0.165E 16	0.362E 23	1.77	0.59
15	489.1	445.8	43.3	467.4	0.169E 16	0.370E 23	1.90	0.63
16	498.8	455.0	43.8	476.9	0.172E 16	0.376E 23	2.01	0.67
17	508.4	464.3	44.1	486.4	0.174E 16	0.382E 23	2.09	0.70
18	518.1	473.7	44.4	495.9	0.176E 16	0.386E 23	2.14	0.71
19	527.4	483.1	44.4	505.3	0.177E 16	0.389E 23	2.17	0.72
20	536.7	492.4	44.3	514.6	0.178E 16	0.390E 23	2.16	0.72
21	545.8	501.7	44.1	523.7	0.176E 16	0.390E 23	2.14	0.71
22	554.6	510.9	43.6	532.7	0.177E 16	0.388E 23	2.08	0.69
23	563.2	520.1	43.2	541.6	0.176E 16	0.386E 23	2.02	0.67
24	571.5	529.1	42.4	550.3	0.174E 16	0.382E 23	1.93	0.64
25	579.6	537.9	41.7	558.7	0.172E 16	0.377E 23	1.83	0.61
26	587.2	546.5	40.7	566.9	0.169E 16	0.370E 23	1.73	0.58
27	594.7	554.9	39.8	574.8	0.166E 16	0.363E 23	1.61	0.54
28	601.8	563.1	38.7	582.4	0.162E 16	0.355E 23	1.50	0.50
29	608.6	571.0	37.6	589.8	0.158E 16	0.346E 23	1.39	0.46
30	615.0	578.7	36.3	596.8	0.153E 16	0.336E 23	1.27	0.42
31	621.1	586.0	35.1	603.6	0.148E 16	0.326E 23	1.16	0.39
32	627.0	593.2	33.8	610.1	0.144E 16	0.315E 23	1.06	0.35
33	632.8	600.1	32.7	616.5	0.140E 16	0.306E 23	0.97	0.32
34	638.7	606.9	31.8	622.8	0.136E 16	0.298E 23	0.89	0.30
35	645.0	613.8	31.2	629.4	0.134E 16	0.294E 23	0.84	0.28

T(IN) = TEMP OF INNER CLAD SURFACE. TOUT = TEMP OF OUTER CLAD SURFACE
DEL T = T(IN) - T(OUT) T(M) = CLAD MEAN TEMP.
PERC V = PERCENT CLAD VOLUME CHANGE. PERC D = PERCENT CLAD DIAMETER CHANGE

PIN NO IS 13 TIME IN DAYS = 254. PEAK FLUX IS 1.75270E 15

POSI	T(IN) DEG C	T(OUT) DEG C	DEL T DEG C	T(M) DEG C	FLUX	FLUENCE	PERC V	PERC D
9	432.8	394.4	38.4	413.6	0.140E 16	0.308E 23	1.01	0.34
10	441.8	402.6	39.2	422.2	0.144E 16	0.317E 23	1.14	0.38
11	451.1	377.6	73.5	414.3	0.149E 16	0.326E 23	1.12	0.37
12	460.8	419.6	41.3	440.2	0.154E 16	0.337E 23	1.44	0.48
13	470.8	428.4	42.3	449.6	0.158E 16	0.348E 23	1.60	0.53
14	480.7	437.5	43.2	459.1	0.162E 16	0.356E 23	1.74	0.58
15	490.6	446.8	43.8	468.7	0.166E 16	0.364E 23	1.86	0.62
16	500.4	456.1	44.3	478.3	0.169E 16	0.371E 23	1.96	0.65
17	510.3	465.6	44.7	487.9	0.172E 16	0.376E 23	2.04	0.68
18	520.0	475.1	44.9	497.5	0.173E 16	0.380E 23	2.09	0.70
19	529.6	484.6	45.0	507.1	0.174E 16	0.383E 23	2.11	0.70
20	538.9	494.1	44.9	516.5	0.175E 16	0.384E 23	2.10	0.70
21	548.2	503.6	44.6	525.9	0.175E 16	0.384E 23	2.08	0.69
22	557.1	512.9	44.2	535.0	0.174E 16	0.383E 23	2.02	0.67
23	565.8	522.2	43.7	544.0	0.173E 16	0.380E 23	1.95	0.65
24	574.2	531.2	43.0	552.7	0.171E 16	0.376E 23	1.87	0.62
25	582.4	540.2	42.2	561.3	0.169E 16	0.371E 23	1.77	0.59
26	590.2	548.9	41.3	569.5	0.166E 16	0.365E 23	1.66	0.55
27	597.7	557.4	40.3	577.6	0.163E 16	0.358E 23	1.55	0.52
28	604.9	565.7	39.2	585.3	0.159E 16	0.350E 23	1.44	0.48
29	611.8	573.8	38.1	592.8	0.155E 16	0.341E 23	1.33	0.44
30	618.4	581.6	36.8	600.0	0.151E 16	0.331E 23	1.22	0.41
31	624.5	589.0	35.5	606.7	0.146E 16	0.321E 23	1.11	0.37
32	630.5	596.2	34.3	613.4	0.142E 16	0.311E 23	1.01	0.34
33	636.4	603.3	33.2	619.9	0.137E 16	0.302E 23	0.93	0.31
34	642.4	610.2	32.2	626.3	0.134E 16	0.294E 23	0.85	0.28
35	648.7	617.2	31.6	632.9	0.132E 16	0.290E 23	0.80	0.27

T(IN) = TEMP OF INNER CLAD SURFACE. TOUT = TEMP OF OUTER CLAD SURFACE.
DEL T = T(IN) - T(OUT) T(M) = CLAD MEAN TEMP.
PERC V = PERCENT CLAD VOLUME CHANGE. PERC D = PERCENT CLAD DIAMETER CHANGE

PIN NC IS 14 TIME IN DAYS = 381. PEAK FLUX IS 1.7263CE 15

POSI	T(IN) DEG C	T(OUT) DEG C	DEL T DEG C	T(M) DEG C	FLUX	FLUENCE	PERC V	PERC D
9	431.8	394.1	37.7	412.9	0.138E 16	0.455E 23	1.95	0.65
10	440.6	402.1	38.5	421.3	0.142E 16	0.468E 23	2.21	0.74
11	449.7	410.2	39.4	429.9	0.146E 16	0.482E 23	2.49	0.83
12	459.3	418.7	40.6	439.0	0.151E 16	0.498E 23	2.80	0.93
13	469.0	427.4	41.6	448.2	0.156E 16	0.513E 23	3.10	1.03
14	478.7	436.3	42.3	457.5	0.160E 16	0.526E 23	3.37	1.12
15	488.5	445.4	43.1	467.0	0.164E 16	0.538E 23	3.61	1.20
16	498.2	454.6	43.6	476.4	0.166E 16	0.548E 23	3.81	1.27
17	507.8	463.9	43.9	485.9	0.169E 16	0.556E 23	3.97	1.32
18	517.3	473.2	44.2	495.2	0.171E 16	0.562E 23	4.07	1.36
19	526.7	482.5	44.2	504.6	0.172E 16	0.566E 23	4.11	1.37
20	535.9	491.8	44.1	513.9	0.172E 16	0.568E 23	4.11	1.37
21	545.0	501.1	43.9	523.1	0.172E 16	0.568E 23	4.06	1.35
22	553.7	510.3	43.4	532.0	0.172E 16	0.565E 23	3.97	1.32
23	562.3	519.3	42.9	540.8	0.171E 16	0.562E 23	3.84	1.28
24	570.6	528.3	42.3	549.4	0.169E 16	0.556E 23	3.68	1.23
25	578.6	537.1	41.5	557.8	0.167E 16	0.549E 23	3.50	1.17
26	586.2	545.6	40.6	565.9	0.164E 16	0.539E 23	3.29	1.10
27	593.6	554.0	39.6	573.8	0.161E 16	0.529E 23	3.08	1.03
28	600.7	562.1	38.6	581.4	0.157E 16	0.517E 23	2.86	0.95
29	607.4	570.0	37.4	588.7	0.153E 16	0.504E 23	2.65	0.88
30	613.9	577.7	36.2	595.8	0.149E 16	0.490E 23	2.43	0.81
31	619.9	584.9	34.9	602.4	0.144E 16	0.474E 23	2.22	0.74
32	625.8	592.1	33.7	608.9	0.139E 16	0.459E 23	2.03	0.68
33	631.6	599.0	32.6	615.3	0.135E 16	0.446E 23	1.86	0.62
34	637.4	605.8	31.7	621.6	0.132E 16	0.434E 23	1.71	0.57
35	643.7	612.6	31.1	628.1	0.130E 16	0.428E 23	1.60	0.53

T(IN) = TEMP OF INNER CLAD SURFACE.
DEL T = T(IN) - T(OUT)
PERC V = PERCENT CLAD VOLUME CHANGE.

TCUT = TEMP OF OUTER CLAD SURFACS.
T(M) = CLAD MEAN TEMP.
PERC D = PERCENT CLAD DIAMETER CHANGE

PIN NO IS 15 TIME IN DAYS = 381. PEAK FLUX IS 1.69980E 15

POSI	T(IN) DEG C	T(OUT) DEG C	DEL T DEG C	T(M) DEG C	FLUX	FLUENCE	PERC V	PERC D
9	428.8	392.6	36.3	410.7	0.136E 16	0.448E 23	1.86	0.62
10	434.6	397.4	37.2	416.0	0.140E 16	0.461E 23	2.06	0.69
11	440.5	402.3	38.2	421.4	0.144E 16	0.475E 23	2.27	0.76
12	446.8	407.5	39.3	427.1	0.149E 16	0.491E 23	2.51	0.84
13	453.1	412.8	40.3	432.9	0.154E 16	0.506E 23	2.76	0.92
14	459.3	418.2	41.2	438.7	0.157E 16	0.518E 23	2.99	1.00
15	465.6	423.6	42.0	444.6	0.161E 16	0.530E 23	3.21	1.07
16	471.6	429.1	42.6	450.3	0.164E 16	0.540E 23	3.40	1.13
17	477.6	434.5	43.1	456.0	0.166E 16	0.548E 23	3.58	1.19
18	483.3	439.9	43.4	461.6	0.168E 16	0.553E 23	3.72	1.24
19	488.9	445.4	43.5	467.1	0.169E 16	0.557E 23	3.83	1.28
20	494.3	450.8	43.5	472.5	0.170E 16	0.559E 23	3.91	1.30
21	499.5	456.1	43.4	477.8	0.170E 16	0.559E 23	3.95	1.32
22	504.4	461.4	43.0	482.9	0.169E 16	0.557E 23	3.96	1.32
23	509.2	466.6	42.6	487.9	0.168E 16	0.553E 23	3.94	1.31
24	513.6	471.6	42.1	492.6	0.166E 16	0.547E 23	3.88	1.29
25	517.9	476.5	41.4	497.2	0.164E 16	0.540E 23	3.81	1.27
26	521.8	481.2	40.6	501.5	0.161E 16	0.531E 23	3.69	1.23
27	525.6	485.9	39.7	505.7	0.158E 16	0.521E 23	3.57	1.19
28	529.0	490.3	38.7	509.7	0.154E 16	0.509E 23	3.42	1.14
29	532.3	494.6	37.7	513.4	0.151E 16	0.496E 23	3.27	1.09
30	535.2	498.7	36.5	517.0	0.146E 16	0.482E 23	3.10	1.03
31	537.9	502.7	35.2	520.3	0.142E 16	0.467E 23	2.92	0.97
32	540.6	506.5	34.1	523.5	0.137E 16	0.452E 23	2.75	0.92
33	543.3	510.2	33.1	526.7	0.133E 16	0.439E 23	2.60	0.87
34	546.1	513.9	32.1	530.0	0.130E 16	0.428E 23	2.47	0.82
35	549.3	517.7	31.6	533.5	0.128E 16	0.421E 23	2.39	0.80

T(IN) = TEMP OF INNER CLAD SURFACE. TOUT = TEMP OF OUTER CLAD SURFACE
DEL T = T(IN) - T(OUT) T(M) = CLAD MEAN TEMP.
PERC V = PERCENT CLAD VOLUME CHANGE. PERC D = PERCENT CLAD DIAMETER CHANGE

PIN NO IS 16 TIME IN DAYS = 590. PEAK FLUX IS 1.80550E 15

POSI	T(IN) DEG C	T(OUT) DEG C	DEL T DEG C	T(M) DEG C	FLUX	FLUENCE	PERC V	PERC D
9	434.6	395.3	39.3	414.9	0.145E 16	0.737E 23	4.54	1.51
10	440.4	400.2	40.2	420.3	0.149E 16	0.758E 23	5.00	1.67
11	446.6	405.3	41.3	425.9	0.153E 16	0.781E 23	5.51	1.84
12	453.2	410.6	42.6	431.9	0.156E 16	0.807E 23	6.09	2.03
13	459.7	416.1	43.7	437.9	0.163E 16	0.832E 23	6.67	2.22
14	466.1	421.5	44.6	443.8	0.167E 16	0.853E 23	7.20	2.40
15	472.5	427.1	45.4	449.8	0.171E 16	0.872E 23	7.71	2.57
16	478.7	432.6	46.1	455.7	0.174E 16	0.888E 23	8.16	2.72
17	484.8	438.2	46.6	461.5	0.177E 16	0.901E 23	8.55	2.85
18	490.7	443.7	46.9	467.2	0.179E 16	0.910E 23	8.87	2.96
19	496.3	449.2	47.1	472.8	0.180E 16	0.916E 23	9.10	3.03
20	501.8	454.7	47.1	478.2	0.180E 16	0.920E 23	9.27	3.09
21	507.0	460.1	46.9	483.5	0.180E 16	0.920E 23	9.35	3.12
22	511.9	465.3	46.6	488.6	0.180E 16	0.915E 23	9.33	3.11
23	516.7	470.6	46.1	493.6	0.179E 16	0.910E 23	9.27	3.09
24	521.1	475.6	45.6	498.3	0.177E 16	0.900E 23	9.11	3.04
25	525.3	480.5	44.8	502.9	0.174E 16	0.889E 23	8.91	2.97
26	529.1	485.2	43.9	507.2	0.171E 16	0.873E 23	8.63	2.88
27	532.8	489.8	42.9	511.3	0.168E 16	0.856E 23	8.33	2.78
28	536.1	494.2	41.9	515.2	0.164E 16	0.837E 23	7.97	2.66
29	539.3	498.5	40.8	518.9	0.160E 16	0.816E 23	7.60	2.53
30	542.1	502.6	39.5	522.4	0.156E 16	0.793E 23	7.21	2.40
31	544.5	506.4	38.2	525.5	0.151E 16	0.768E 23	6.78	2.26
32	547.2	510.2	36.9	528.7	0.146E 16	0.744E 23	6.38	2.13
33	549.7	513.9	35.8	531.8	0.142E 16	0.722E 23	6.03	2.01
34	552.3	517.6	34.8	534.9	0.138E 16	0.704E 23	5.73	1.91
35	555.6	521.3	34.2	538.4	0.136E 16	0.693E 23	5.54	1.85

T(IN) = TEMP OF INNER CLAD SURFACE. TOUT = TEMP OF OUTER CLAD SURFACS.
DEL T = T(IN) - T(OUT) T(M) = CLAD MEAN TEMP.
PERC V = PERCENT CLAD VOLUME CHANGE. PERC D = PERCENT CLAD DIAMETER CHANGE.

PIN NO IS 17 TIME IN DAYS = 381. PEAK FLUX IS 1.77910E 15

POSI	T(IN) DEG C	T(OUT) DEG C	DEL T DEG C	T(M) DEG C	FLUX	FLUENCE	PERC V	PERC D
9	432.1	394.2	37.8	413.1	0.142E 16	0.469E 23	2.06	0.69
10	440.9	402.2	38.7	421.5	0.147E 16	0.482E 23	2.33	0.78
11	450.1	410.4	39.7	430.2	0.151E 16	0.497E 23	2.63	0.88
12	459.7	418.9	40.7	439.3	0.156E 16	0.513E 23	2.95	0.98
13	469.4	427.7	41.7	448.6	0.161E 16	0.529E 23	3.27	1.09
14	479.2	436.6	42.6	457.9	0.165E 16	0.543E 23	3.55	1.18
15	489.1	445.8	43.3	467.4	0.169E 16	0.555E 23	3.81	1.27
16	498.8	455.0	43.8	476.9	0.172E 16	0.565E 23	4.02	1.34
17	508.4	464.3	44.1	486.4	0.174E 16	0.573E 23	4.18	1.39
18	518.1	473.7	44.4	495.9	0.176E 16	0.579E 23	4.28	1.43
19	527.4	483.1	44.4	505.2	0.177E 16	0.583E 23	4.33	1.44
20	536.7	492.4	44.3	514.6	0.178E 16	0.585E 23	4.33	1.44
21	545.8	501.7	44.1	523.7	0.178E 16	0.585E 23	4.27	1.42
22	554.6	510.9	43.6	532.7	0.177E 16	0.583E 23	4.17	1.39
23	563.2	520.1	43.2	541.6	0.176E 16	0.579E 23	4.04	1.35
24	571.5	529.1	42.4	550.3	0.174E 16	0.573E 23	3.86	1.29
25	579.6	537.9	41.7	558.7	0.172E 16	0.566E 23	3.67	1.22
26	587.2	546.5	40.7	566.9	0.169E 16	0.556E 23	3.45	1.15
27	594.7	554.9	39.8	574.8	0.166E 16	0.545E 23	3.23	1.08
28	601.8	563.1	38.7	582.4	0.162E 16	0.532E 23	3.00	1.00
29	608.6	571.0	37.6	589.8	0.158E 16	0.519E 23	2.77	0.92
30	615.0	578.7	36.3	596.8	0.153E 16	0.505E 23	2.55	0.85
31	621.1	586.0	35.1	603.6	0.148E 16	0.488E 23	2.32	0.77
32	627.0	593.2	33.8	610.1	0.144E 16	0.473E 23	2.12	0.71
33	632.8	600.1	32.7	616.5	0.140E 16	0.459E 23	1.94	0.65
34	638.7	606.9	31.8	622.8	0.136E 16	0.448E 23	1.79	0.60
35	645.0	613.8	31.2	629.4	0.134E 16	0.441E 23	1.68	0.56

T(IN) = TEMP OF INNER CLAD SURFACE. TOUT = TEMP OF OUTER CLAD SURFACE.
DEL T = T(IN) - T(OUT) T(M) = CLAD MEAN TEMP.
PERC V = PERCENT CLAD VOLUME CHANGE. PERC D = PERCENT CLAD DIAMETER CHANGE.

PIN NO IS 18 TIME IN DAYS = 590. PEAK FLUX IS 1.75270E 15

POSI	T(IN) DEG C	T(OUT) DEG C	DEL T DEG C	T(M) DEG C	FLUX	FLUENCE	PERC V	PERC D
9	432.8	394.4	38.4	413.6	0.140E 16	0.715E 23	4.26	1.42
10	441.8	402.6	39.2	422.2	0.144E 16	0.736E 23	4.83	1.61
11	451.1	377.6	73.5	414.3	0.149E 16	0.758E 23	4.74	1.58
12	460.8	419.6	41.3	440.2	0.154E 16	0.783E 23	6.10	2.03
13	470.8	428.4	42.3	449.6	0.158E 16	0.807E 23	6.76	2.25
14	480.7	437.5	43.2	459.1	0.162E 16	0.828E 23	7.34	2.45
15	490.6	446.8	43.8	468.7	0.166E 16	0.846E 23	7.87	2.62
16	500.4	456.1	44.3	478.3	0.169E 16	0.862E 23	8.29	2.76
17	510.3	465.6	44.7	487.9	0.172E 16	0.874E 23	8.62	2.87
18	520.0	475.1	44.9	497.5	0.173E 16	0.883E 23	8.82	2.94
19	529.6	484.6	45.0	507.1	0.174E 16	0.889E 23	8.91	2.97
20	538.9	494.1	44.9	516.5	0.175E 16	0.893E 23	8.89	2.96
21	548.2	503.6	44.6	525.9	0.175E 16	0.892E 23	8.77	2.92
22	557.1	512.9	44.2	535.0	0.174E 16	0.889E 23	8.54	2.85
23	565.8	522.2	43.7	544.0	0.173E 16	0.883E 23	8.26	2.75
24	574.2	531.2	43.0	552.7	0.171E 16	0.874E 23	7.89	2.63
25	582.4	540.2	42.2	561.3	0.169E 16	0.863E 23	7.49	2.50
26	590.2	548.9	41.3	569.5	0.166E 16	0.848E 23	7.03	2.34
27	597.7	557.4	40.3	577.6	0.163E 16	0.831E 23	6.57	2.19
28	604.9	565.7	39.2	585.3	0.159E 16	0.812E 23	6.09	2.03
29	611.8	573.8	38.1	592.8	0.155E 16	0.792E 23	5.62	1.87
30	618.4	581.6	36.8	600.0	0.151E 16	0.770E 23	5.16	1.72
31	624.5	589.0	35.5	606.7	0.146E 16	0.745E 23	4.70	1.57
32	630.5	596.2	34.3	613.4	0.142E 16	0.722E 23	4.29	1.43
33	636.4	603.3	33.2	619.9	0.137E 16	0.701E 23	3.92	1.31
34	642.4	610.2	32.2	626.3	0.134E 16	0.683E 23	3.61	1.20
35	648.7	617.2	31.6	632.9	0.132E 16	0.673E 23	3.37	1.12

T(IN) = TEMP OF INNER CLAD SURFACE.
DEL T = T(IN) - T(OUT)
PERC V = PERCENT CLAD VOLUME CHANGE.

TOUT = TEMP OF OUTER CLAD SURFACE.
T(M) = CLAD MEAN TEMP.
PERC D = PERCENT CLAD DIAMETER CHANGE.

PIN NO IS 19 TIME IN DAYS = 381. PEAK FLUX IS 1.72630E 15

POS I	T(IN) DEG C	T(OUT) DEG C	DEL T DEG C	T(M) DEG C	FLUX	FLUENCE	PERC V	PERC D
9	431.8	394.1	37.7	412.9	0.138E 16	0.455E 23	1.95	0.65
10	440.6	402.1	38.5	421.3	0.142E 16	0.468E 23	2.21	0.74
11	449.7	410.2	39.4	429.9	0.146E 16	0.482E 23	2.49	0.83
12	459.3	418.7	40.6	439.0	0.151E 16	0.498E 23	2.80	0.93
13	469.0	427.4	41.6	448.2	0.156E 16	0.513E 23	3.10	1.03
14	478.7	436.3	42.3	457.5	0.160E 16	0.526E 23	3.37	1.12
15	488.5	445.4	43.1	467.0	0.164E 16	0.538E 23	3.61	1.20
16	498.2	454.6	43.6	476.4	0.166E 16	0.548E 23	3.81	1.27
17	507.8	463.9	43.9	485.9	0.169E 16	0.556E 23	3.97	1.32
18	517.3	473.2	44.2	495.2	0.171E 16	0.562E 23	4.07	1.36
19	526.7	482.5	44.2	504.6	0.172E 16	0.566E 23	4.11	1.37
20	535.9	491.8	44.1	513.9	0.172E 16	0.568E 23	4.11	1.37
21	545.0	501.1	43.9	523.1	0.172E 16	0.568E 23	4.06	1.35
22	553.7	510.3	43.4	532.0	0.172E 16	0.565E 23	3.97	1.32
23	562.3	519.3	42.9	540.8	0.171E 16	0.562E 23	3.84	1.28
24	570.6	528.3	42.3	549.4	0.169E 16	0.556E 23	3.68	1.23
25	578.6	537.1	41.5	557.8	0.167E 16	0.549E 23	3.50	1.17
26	586.2	545.6	40.5	565.9	0.164E 16	0.539E 23	3.29	1.10
27	593.6	554.0	39.6	573.8	0.161E 16	0.529E 23	3.08	1.03
28	600.7	562.1	38.6	581.4	0.157E 16	0.517E 23	2.86	0.95
29	607.4	570.0	37.4	588.7	0.153E 16	0.504E 23	2.65	0.88
30	613.9	577.7	36.2	595.8	0.149E 16	0.490E 23	2.43	0.81
31	619.9	584.9	34.9	602.4	0.144E 16	0.474E 23	2.22	0.74
32	625.8	592.1	33.7	608.9	0.139E 16	0.459E 23	2.03	0.68
33	631.6	599.0	32.6	615.3	0.135E 15	0.446E 23	1.86	0.62
34	637.4	605.8	31.7	621.6	0.132E 16	0.434E 23	1.71	0.57
35	643.7	612.6	31.1	628.1	0.130E 16	0.428E 23	1.60	0.53

T(IN) = TEMP OF INNER CLAD SURFACE. TOUT = TEMP OF OUTER CLAD SURFACE.
DEL T = T(IN) - T(OUT) T(M) = CLAD MEAN TEMP.
PERC V = PERCENT CLAD VOLUME CHANGE. PERC D = PERCENT CLAD DIAMETER CHANGE

PIN NO IS 20 TIME IN DAYS = 381. PEAK FLUX IS 1.69980E 15

POSI	T(IN) DEG C	T(OUT) DEG C	DEL T DEG C	T(M) DEG C	FLUX	FLUENCE	PERC V	PERC D
9	429.7	393.4	36.3	411.5	0.136E 16	0.448E 23	1.88	0.63
10	438.1	401.1	37.1	419.6	0.140E 16	0.461E 23	2.12	0.71
11	446.9	408.9	38.0	427.9	0.144E 16	0.475E 23	2.39	0.80
12	456.1	417.1	39.1	436.6	0.149E 16	0.491E 23	2.68	0.89
13	465.4	425.4	40.0	445.4	0.154E 16	0.506E 23	2.97	0.99
14	474.8	434.0	40.8	454.4	0.157E 16	0.518E 23	3.24	1.08
15	484.2	442.7	41.4	463.4	0.161E 16	0.530E 23	3.48	1.16
16	493.5	451.5	42.0	472.5	0.164E 16	0.540E 23	3.68	1.23
17	502.8	460.4	42.3	481.6	0.166E 16	0.548E 23	3.84	1.28
18	511.9	469.4	42.6	490.7	0.168E 16	0.553E 23	3.95	1.32
19	520.9	478.3	42.6	499.6	0.169E 16	0.557E 23	4.01	1.34
20	529.8	487.3	42.6	508.6	0.170E 16	0.559E 23	4.02	1.34
21	538.5	496.2	42.3	517.4	0.170E 16	0.559E 23	3.99	1.33
22	546.9	505.0	41.9	525.9	0.169E 16	0.557E 23	3.91	1.30
23	555.2	513.8	41.4	534.5	0.168E 16	0.553E 23	3.80	1.27
24	563.1	522.3	40.8	542.7	0.166E 16	0.547E 23	3.65	1.22
25	570.9	530.8	40.1	550.8	0.164E 16	0.540E 23	3.49	1.16
26	578.2	539.0	39.2	558.6	0.161E 16	0.531E 23	3.30	1.10
27	585.3	547.1	38.2	566.2	0.158E 16	0.521E 23	3.10	1.03
28	592.1	554.8	37.2	573.4	0.154E 16	0.509E 23	2.89	0.96
29	598.6	562.4	36.1	580.5	0.151E 16	0.496E 23	2.68	0.89
30	604.7	569.8	34.9	587.2	0.146E 16	0.482E 23	2.47	0.82
31	610.6	576.8	33.8	593.7	0.142E 16	0.467E 23	2.26	0.75
32	616.2	583.6	32.6	599.9	0.137E 16	0.452E 23	2.08	0.69
33	621.8	590.3	31.5	606.0	0.133E 16	0.439E 23	1.91	0.64
34	627.4	596.8	30.6	612.1	0.130E 16	0.428E 23	1.76	0.59
35	633.4	603.3	30.1	618.4	0.128E 16	0.421E 23	1.66	0.55

T(IN) = TEMP OF INNER CLAD SURFACE.
DEL T = T(IN) - T(OUT)
PERC V = PERCENT CLAD VOLUME CHANGE.

TOUT = TEMP OF OUTER CLAD SURFACS.
T(M) = CLAD MEAN TEMP.
PERC D = PERCENT CLAD DIAMETER CHANGE.

PIN NO IS 21 TIME IN DAYS = 254. PEAK FLUX IS 1.67340E 15

POSI	T(IN) DEG C	T(OUT) DEG C	DEL T DEG C	T(M) DEG C	FLUX	FLUENCE	PERC V	PERC D
9	428.8	393.2	35.7	411.0	0.134E 16	0.294E 23	0.91	0.30
10	437.2	400.7	36.5	418.9	0.138E 16	0.302E 23	1.03	0.34
11	445.8	408.4	37.4	427.1	0.142E 16	0.312E 23	1.15	0.38
12	454.9	416.4	38.4	435.7	0.147E 16	0.322E 23	1.30	0.43
13	464.1	424.7	39.4	444.4	0.151E 16	0.332E 23	1.44	0.48
14	473.3	433.1	40.2	453.2	0.155E 16	0.340E 23	1.57	0.52
15	482.5	441.7	40.8	462.1	0.159E 16	0.348E 23	1.69	0.56
16	491.7	450.3	41.4	471.0	0.161E 16	0.354E 23	1.78	0.59
17	500.8	459.1	41.7	480.0	0.164E 16	0.359E 23	1.86	0.62
18	509.8	467.9	41.9	488.9	0.165E 16	0.363E 23	1.92	0.64
19	518.7	476.7	42.0	497.7	0.167E 16	0.366E 23	1.95	0.65
20	527.5	485.6	41.9	506.5	0.167E 16	0.367E 23	1.96	0.65
21	536.0	494.3	41.7	515.2	0.167E 16	0.367E 23	1.95	0.65
22	544.3	503.0	41.3	523.6	0.166E 16	0.365E 23	1.91	0.64
23	552.4	511.6	40.8	532.0	0.165E 16	0.363E 23	1.86	0.62
24	560.3	520.1	40.2	540.2	0.164E 16	0.359E 23	1.79	0.60
25	567.9	528.3	39.6	548.1	0.162E 16	0.355E 23	1.71	0.57
26	575.1	536.4	38.7	555.8	0.159E 16	0.348E 23	1.62	0.54
27	582.1	544.4	37.7	563.2	0.156E 16	0.342E 23	1.52	0.51
28	588.7	552.1	36.7	570.4	0.152E 16	0.334E 23	1.42	0.47
29	595.2	559.6	35.6	577.4	0.148E 16	0.326E 23	1.32	0.44
30	601.2	566.7	34.5	584.0	0.144E 16	0.316E 23	1.22	0.41
31	606.9	573.7	33.3	590.3	0.140E 16	0.306E 23	1.12	0.37
32	612.5	580.4	32.1	596.4	0.135E 16	0.297E 23	1.03	0.34
33	618.0	586.9	31.1	602.5	0.131E 16	0.288E 23	0.95	0.32
34	623.6	593.3	30.2	608.4	0.128E 16	0.281E 23	0.88	0.29
35	629.4	599.8	29.7	614.6	0.126E 16	0.277E 23	0.83	0.28

T(IN) = TEMP OF INNER CLAD SURFACE.
DEL T = T(IN) - T(OUT)
PERC V = PERCENT CLAD VOLUME CHANGE.

TOUT = TEMP OF OUTER CLAD SURFACE.
T(M) = CLAD MEAN TEMP.
PERC D = PERCENT CLAD DIAMETER CHANGE.

PIN NO IS 22 TIME IN DAYS = 254. PEAK FLUX IS 1.64700E 15

POSI	T(IN) DEG C	T(OUT) DEG C	DEL T DEG C	T(M) DEG C	FLUX	FLUENCE	PERC V	PERC D
9	429.4	393.4	35.9	411.4	0.132E 16	0.289E 23	0.89	0.30
10	434.8	397.9	36.9	416.4	0.136E 16	0.298E 23	0.98	0.33
11	440.4	402.6	37.9	421.5	0.140E 16	0.307E 23	1.07	0.36
12	446.4	407.4	39.0	426.9	0.144E 16	0.317E 23	1.19	0.40
13	452.4	412.4	40.1	432.4	0.149E 16	0.327E 23	1.30	0.43
14	458.3	417.4	40.9	437.8	0.153E 16	0.335E 23	1.41	0.47
15	464.2	422.4	41.7	443.3	0.156E 16	0.342E 23	1.51	0.50
16	469.8	427.6	42.3	448.7	0.159E 16	0.349E 23	1.60	0.53
17	475.4	432.6	42.8	454.0	0.161E 16	0.354E 23	1.68	0.56
18	480.8	437.7	43.1	459.2	0.163E 16	0.357E 23	1.75	0.58
19	485.9	442.7	43.2	464.3	0.164E 16	0.360E 23	1.80	0.60
20	490.9	447.7	43.3	469.3	0.165E 16	0.361E 23	1.84	0.61
21	495.7	452.6	43.1	474.2	0.165E 16	0.361E 23	1.86	0.62
22	500.2	457.4	42.8	478.8	0.164E 16	0.360E 23	1.86	0.62
23	504.6	462.2	42.4	483.4	0.163E 16	0.357E 23	1.86	0.62
24	508.6	466.7	41.9	487.7	0.161E 16	0.354E 23	1.83	0.61
25	512.4	471.2	41.2	491.8	0.159E 16	0.349E 23	1.80	0.60
26	515.9	475.6	40.4	495.7	0.156E 16	0.343E 23	1.75	0.58
27	519.3	479.8	39.5	499.5	0.153E 16	0.336E 23	1.69	0.56
28	522.3	483.8	38.6	503.1	0.150E 16	0.329E 23	1.63	0.54
29	525.2	487.7	37.5	506.5	0.146E 16	0.320E 23	1.56	0.52
30	527.8	491.4	36.4	509.6	0.142E 16	0.311E 23	1.48	0.49
31	530.1	494.9	35.2	512.5	0.137E 16	0.301E 23	1.40	0.47
32	532.4	498.4	34.0	515.4	0.133E 16	0.292E 23	1.32	0.44
33	534.7	501.8	32.9	518.2	0.129E 16	0.284E 23	1.25	0.42
34	537.1	505.1	32.0	521.1	0.126E 16	0.276E 23	1.19	0.40
35	540.1	508.6	31.5	524.3	0.124E 16	0.272E 23	1.15	0.38

T(IN) = TEMP OF INNER CLAD SURFACE.
DEL T = T(IN) - T(OUT)
PERC V = PERCENT CLAD VOLUME CHANGE.

TOUT = TEMP OF OUTER CLAD SURFACE.
T(M) = CLAD MEAN TEMP.
PERC D = PERCENT CLAD DIAMETER CHANGE

PIN NO IS 23 TIME IN DAYS = 590. PEAK FLUX IS 1.75270E 15

POSI	T(IN) DEG C	T(OUT) DEG C	DEL T DEG C	T(M) DEG C	FLUX	FLUENCE	PERC V	PERC D
9	431.8	393.6	38.2	412.7	0.140E 16	0.715E 23	4.23	1.41
10	437.8	398.7	39.2	418.2	0.144E 16	0.736E 23	4.67	1.56
11	444.1	403.9	40.2	424.0	0.149E 16	0.758E 23	5.16	1.72
12	450.8	409.4	41.4	430.1	0.154E 16	0.783E 23	5.71	1.90
13	457.4	414.9	42.5	436.2	0.158E 16	0.807E 23	6.27	2.09
14	464.0	420.6	43.4	442.3	0.162E 16	0.828E 23	6.79	2.26
15	470.6	426.3	44.2	448.4	0.166E 16	0.846E 23	7.28	2.43
16	476.9	432.1	44.8	454.5	0.169E 16	0.862E 23	7.72	2.57
17	483.2	437.9	45.3	460.6	0.172E 16	0.874E 23	8.11	2.70
18	489.3	443.7	45.6	466.5	0.173E 16	0.883E 23	8.41	2.80
19	495.2	449.4	45.8	472.3	0.174E 16	0.889E 23	8.64	2.88
20	500.8	455.1	45.7	478.0	0.175E 16	0.893E 23	8.80	2.93
21	506.3	460.7	45.6	483.5	0.175E 16	0.893E 23	8.88	2.96
22	511.5	466.3	45.2	488.9	0.174E 16	0.889E 23	8.87	2.96
23	516.6	471.7	44.8	494.1	0.173E 16	0.883E 23	8.81	2.94
24	521.2	477.0	44.2	499.1	0.171E 16	0.874E 23	8.66	2.89
25	525.7	482.2	43.5	504.0	0.169E 16	0.863E 23	8.47	2.82
26	529.9	487.2	42.7	508.6	0.166E 16	0.848E 23	8.20	2.73
27	533.8	492.1	41.7	513.0	0.163E 16	0.831E 23	7.90	2.63
28	537.4	496.8	40.6	517.1	0.159E 16	0.812E 23	7.56	2.52
29	540.9	501.4	39.6	521.2	0.155E 16	0.792E 23	7.20	2.40
30	544.1	505.7	38.3	524.9	0.151E 16	0.770E 23	6.82	2.27
31	546.9	509.9	37.1	528.4	0.146E 16	0.745E 23	6.41	2.14
32	549.7	513.9	35.8	531.8	0.142E 16	0.722E 23	6.03	2.01
33	552.6	517.8	34.7	535.2	0.137E 16	0.701E 23	5.69	1.90
34	555.5	521.8	33.7	538.6	0.134E 16	0.683E 23	5.39	1.80
35	558.9	525.8	33.2	542.4	0.132E 16	0.673E 23	5.21	1.74

T(IN) = TEMP OF INNER CLAD SURFACE.
DEL T = T(IN) - T(OUT)
PERC V = PERCENT CLAD VOLUME CHANGE.

TOUT = TEMP OF OUTER CLAD SURFACE.
T(M) = CLAD MEAN TEMP.
PERC D = PERCENT CLAD DIAMETER CHANGE.

PIN NO IS 24 TIME IN DAYS = 590. PEAK FLUX IS 1.72630E 15

POS I	T(IN) DEG C	T(OUT) DEG C	DEL T DEG C	T(M) DEG C	FLUX	FLUENCE	PERC V	PERC D
9	431.8	394.1	37.7	412.9	0.138E 16	0.704E 23	4.13	1.38
10	440.6	402.1	38.5	421.3	0.142E 16	0.725E 23	4.67	1.56
11	449.7	410.2	39.4	429.9	0.146E 16	0.747E 23	5.26	1.75
12	459.3	418.7	40.6	439.0	0.151E 16	0.772E 23	5.91	1.97
13	469.0	427.4	41.6	448.2	0.156E 16	0.795E 23	6.54	2.18
14	478.7	436.3	42.3	457.5	0.160E 16	0.815E 23	7.11	2.37
15	488.5	445.4	43.1	467.0	0.164E 16	0.834E 23	7.63	2.54
16	498.2	454.6	43.6	476.4	0.166E 16	0.849E 23	8.05	2.68
17	507.8	463.9	43.9	485.9	0.169E 16	0.861E 23	8.38	2.79
18	517.3	473.2	44.2	495.2	0.171E 16	0.870E 23	8.59	2.86
19	526.7	482.5	44.2	504.6	0.172E 16	0.876E 23	8.69	2.90
20	535.9	491.8	44.1	513.9	0.172E 16	0.879E 23	8.69	2.90
21	545.0	501.1	43.9	523.1	0.172E 16	0.879E 23	8.59	2.86
22	553.7	510.3	43.4	532.0	0.172E 16	0.875E 23	8.38	2.79
23	562.3	519.3	42.9	540.8	0.171E 16	0.870E 23	8.12	2.71
24	570.6	528.3	42.3	549.4	0.169E 16	0.861E 23	7.77	2.59
25	578.6	537.1	41.5	557.8	0.167E 16	0.850E 23	7.39	2.46
26	586.2	545.6	40.6	565.9	0.164E 16	0.835E 23	6.95	2.32
27	593.6	554.0	39.6	573.8	0.161E 16	0.819E 23	6.51	2.17
28	600.7	562.1	38.6	581.4	0.157E 16	0.800E 23	6.04	2.01
29	607.4	570.0	37.4	588.7	0.153E 16	0.780E 23	5.59	1.86
30	613.9	577.7	36.2	595.8	0.149E 16	0.758E 23	5.14	1.71
31	619.9	584.9	34.9	602.4	0.144E 16	0.734E 23	4.69	1.56
32	625.8	592.1	33.7	608.9	0.139E 16	0.711E 23	4.29	1.43
33	631.6	599.0	32.6	615.3	0.135E 16	0.690E 23	3.93	1.31
34	637.4	605.8	31.7	621.6	0.132E 16	0.673E 23	3.62	1.21
35	643.7	612.6	31.1	628.1	0.130E 16	0.663E 23	3.39	1.13

T(IN) = TEMP OF INNER CLAD SURFACE.
DEL T = T(IN) - T(OUT)
PERC V = PERCENT CLAD VOLUME CHANGE.

TOUT = TEMP OF OUTER CLAD SURFACS.
T(M) = CLAD MEAN TEMP.
PERC D = PERCENT CLAD DIAMETER CHANGE.

PIN NO IS 25 TIME IN DAYS = 381. PEAK FLUX IS 1.69980E 15

POSI	T(IN) DEG C	T(OUT) DEG C	DEL T DEG C	T(M) DEG C	FLUX	FLUENCE	PERC V	PERC D
9	429.7	393.4	36.3	411.5	0.136E 16	0.448E 23	1.88	0.63
10	438.1	401.1	37.1	419.6	0.140E 16	0.461E 23	2.12	0.71
11	446.9	408.9	38.0	427.9	0.144E 16	0.475E 23	2.39	0.80
12	456.1	417.1	39.1	436.6	0.149E 16	0.491E 23	2.68	0.89
13	465.4	425.4	40.0	445.4	0.154E 16	0.506E 23	2.97	0.99
14	474.8	434.0	40.8	454.4	0.157E 16	0.518E 23	3.24	1.08
15	484.2	442.7	41.4	463.4	0.161E 16	0.530E 23	3.48	1.16
16	493.5	451.5	42.0	472.5	0.164E 16	0.540E 23	3.68	1.23
17	502.8	460.4	42.3	481.6	0.166E 16	0.548E 23	3.84	1.28
18	511.9	469.4	42.5	490.7	0.168E 16	0.553E 23	3.95	1.32
19	520.9	478.3	42.6	499.6	0.169E 16	0.557E 23	4.01	1.34
20	529.8	487.3	42.6	508.6	0.170E 16	0.559E 23	4.02	1.34
21	538.5	496.2	42.3	517.4	0.170E 16	0.559E 23	3.99	1.33
22	546.9	505.0	41.9	525.9	0.169E 16	0.557E 23	3.91	1.30
23	555.2	513.8	41.4	534.5	0.168E 16	0.553E 23	3.80	1.27
24	563.1	522.3	40.8	542.7	0.166E 16	0.547E 23	3.65	1.22
25	570.8	530.8	40.1	550.8	0.164E 16	0.540E 23	3.49	1.16
26	578.2	539.0	39.2	558.6	0.161E 16	0.531E 23	3.30	1.10
27	585.3	547.1	38.2	566.2	0.158E 16	0.521E 23	3.10	1.03
28	592.1	554.8	37.2	573.4	0.154E 16	0.509E 23	2.89	0.96
29	598.6	562.4	36.1	580.5	0.151E 16	0.496E 23	2.69	0.89
30	604.7	569.8	34.9	587.2	0.146E 16	0.482E 23	2.47	0.82
31	610.6	576.8	33.8	593.7	0.142E 16	0.467E 23	2.26	0.75
32	616.2	583.6	32.6	599.9	0.137E 16	0.452E 23	2.08	0.69
33	621.8	590.3	31.5	606.0	0.133E 16	0.439E 23	1.91	0.64
34	627.4	596.8	30.6	612.1	0.130E 16	0.428E 23	1.76	0.59
35	633.4	603.3	30.1	618.4	0.128E 16	0.421E 23	1.66	0.55

T(IN) = TEMP OF INNER CLAD SURFACE.
DEL T = T(IN) - T(OUT)
PERC V = PERCENT CLAD VOLUME CHANGE.

TOUT = TEMP OF OUTER CLAD SURFACS.
T(M) = CLAD MEAN TEMP.
PERC D = PERCENT CLAD DIAMETER CHANGE

PIN NO IS 26 TIME IN DAYS = 254. PEAK FLUX IS 1.67340E 15

POSI	T(IN) DEG C	T(OUT) DEG C	DEL T DEG C	T(M) DEG C	FLUX	FLUENCE	PERC V	PERC D
9	428.8	393.2	35.7	411.0	0.134E 16	0.294E 23	0.91	0.30
10	437.2	400.7	36.5	418.9	0.138E 16	0.302E 23	1.03	0.34
11	445.8	408.4	37.4	427.1	0.142E 16	0.312E 23	1.15	0.38
12	454.9	416.4	38.4	435.7	0.147E 16	0.322E 23	1.30	0.43
13	464.1	424.7	39.4	444.4	0.151E 16	0.332E 23	1.44	0.48
14	473.3	433.1	40.2	453.2	0.155E 16	0.340E 23	1.57	0.52
15	482.5	441.7	40.8	462.1	0.159E 16	0.348E 23	1.69	0.56
16	491.7	450.3	41.4	471.0	0.161E 16	0.354E 23	1.78	0.59
17	500.8	459.1	41.7	480.0	0.164E 16	0.359E 23	1.86	0.62
18	509.8	467.9	41.9	488.9	0.165E 16	0.363E 23	1.92	0.64
19	518.7	476.7	42.0	497.7	0.167E 16	0.366E 23	1.95	0.65
20	527.5	485.6	41.9	506.5	0.167E 16	0.367E 23	1.96	0.65
21	536.0	494.3	41.7	515.2	0.167E 16	0.367E 23	1.95	0.65
22	544.3	503.0	41.3	523.6	0.166E 16	0.365E 23	1.91	0.64
23	552.4	511.6	40.8	532.0	0.165E 16	0.363E 23	1.86	0.62
24	560.3	520.1	40.2	540.2	0.164E 16	0.359E 23	1.79	0.60
25	567.9	528.3	39.6	548.1	0.162E 16	0.355E 23	1.71	0.57
26	575.1	536.4	38.7	555.8	0.159E 16	0.348E 23	1.62	0.54
27	582.1	544.4	37.7	563.2	0.156E 16	0.342E 23	1.52	0.51
28	588.7	552.1	36.7	570.4	0.152E 16	0.334E 23	1.42	0.47
29	595.2	559.6	35.6	577.4	0.148E 16	0.326E 23	1.32	0.44
30	601.2	566.7	34.5	584.0	0.144E 16	0.316E 23	1.22	0.41
31	606.9	573.7	33.3	590.3	0.140E 16	0.306E 23	1.12	0.37
32	612.5	580.4	32.1	596.4	0.135E 16	0.297E 23	1.03	0.34
33	618.0	586.9	31.1	602.5	0.131E 16	0.288E 23	0.95	0.32
34	623.6	593.3	30.2	608.4	0.128E 16	0.281E 23	0.88	0.29
35	629.4	599.8	29.7	614.6	0.126E 16	0.277E 23	0.83	0.28

T(IN) = TEMP OF INNER CLAD SURFACE.
DEL T = T(IN) - T(OUT)
PERC V = PERCENT CLAD VOLUME CHANGE.

TOUT = TEMP OF OUTER CLAD SURFACS.
T(M) = CLAD MEAN TEMP.
PERC D = PERCENT CLAD DIAMETER CHANGE

PIN NO IS 27 TIME IN DAYS = 254. PEAK FLUX IS 1.64700E 15

POSI	T(IN) DEG C	T(OUT) DEG C	DEL T DEG C	T(M) DEG C	FLUX	FLUENCE	PERC V	PERC D
9	429.2	393.3	35.9	411.2	0.132E 16	0.289E 23	0.89	0.30
10	437.7	400.8	36.8	419.2	0.136E 16	0.298E 23	1.00	0.33
11	446.3	408.7	37.7	427.5	0.140E 16	0.307E 23	1.13	0.38
12	455.5	416.8	38.7	436.1	0.144E 16	0.317E 23	1.27	0.42
13	464.8	425.1	39.7	444.9	0.149E 16	0.327E 23	1.40	0.47
14	474.1	433.6	40.5	453.8	0.153E 16	0.335E 23	1.53	0.51
15	483.4	442.2	41.2	462.8	0.156E 16	0.342E 23	1.64	0.55
16	492.6	450.9	41.7	471.8	0.159E 16	0.349E 23	1.74	0.58
17	501.8	459.8	42.1	480.8	0.161E 16	0.354E 23	1.82	0.61
18	510.9	468.7	42.3	489.8	0.163E 16	0.357E 23	1.87	0.62
19	519.9	477.6	42.3	498.7	0.164E 16	0.360E 23	1.90	0.63
20	528.7	486.4	42.2	507.6	0.165E 16	0.361E 23	1.91	0.64
21	537.3	495.3	42.0	516.3	0.165E 16	0.361E 23	1.89	0.63
22	545.7	504.1	41.6	524.9	0.164E 16	0.360E 23	1.85	0.62
23	553.8	512.7	41.1	533.3	0.163E 16	0.357E 23	1.81	0.60
24	561.7	521.2	40.5	541.5	0.161E 16	0.354E 23	1.74	0.58
25	569.4	529.6	39.8	549.5	0.159E 16	0.349E 23	1.66	0.55
26	576.7	537.8	38.9	557.2	0.156E 16	0.343E 23	1.57	0.52
27	583.7	545.7	38.0	564.7	0.153E 16	0.336E 23	1.48	0.49
28	590.4	553.5	36.9	572.0	0.150E 16	0.329E 23	1.38	0.46
29	596.9	561.1	35.9	579.0	0.146E 16	0.320E 23	1.28	0.43
30	603.1	568.3	34.8	585.7	0.142E 16	0.311E 23	1.18	0.39
31	608.8	575.3	33.5	592.0	0.137E 16	0.301E 23	1.08	0.36
32	614.4	582.1	32.4	598.2	0.133E 16	0.292E 23	0.99	0.33
33	619.9	588.7	31.3	604.3	0.129E 16	0.284E 23	0.91	0.30
34	625.5	595.1	30.4	610.3	0.126E 16	0.276E 23	0.84	0.28
35	631.4	601.6	29.8	616.5	0.124E 16	0.272E 23	0.79	0.26

T(IN) = TEMP OF INNER CLAD SURFACE.
DEL T = T(IN) - T(OUT)
PERC V = PERCENT CLAD VOLUME CHANGE.

TOUT = TEMP OF OUTER CLAD SURFACS.
T(M) = CLAD MEAN TEMP.
PERC D = PERCENT CLAD DIAMETER CHANGE

PIN NO IS 28 TIME IN DAYS = 590. PEAK FLUX IS 1.61870E 15

POS I	T(IN) DEG C	T(OUT) DEG C	DEL T DEG C	T(M) DEG C	FLUX	FLUENCE	PERC V	PERC D
9	426.2	391.7	34.6	408.9	0.130E 16	0.660E 23	3.55	1.18
10	431.7	396.3	35.4	414.0	0.133E 16	0.680E 23	3.92	1.31
11	437.4	401.0	36.4	419.2	0.137E 16	0.700E 23	4.32	1.44
12	443.4	405.9	37.4	424.7	0.142E 16	0.723E 23	4.79	1.60
13	449.4	410.9	38.5	430.2	0.146E 16	0.746E 23	5.25	1.75
14	455.4	416.1	39.3	435.7	0.150E 16	0.764E 23	5.69	1.90
15	461.3	421.2	40.1	441.2	0.153E 16	0.782E 23	6.12	2.04
16	467.1	426.4	40.7	446.7	0.156E 16	0.796E 23	6.50	2.17
17	472.7	431.6	41.1	452.2	0.158E 16	0.807E 23	6.84	2.28
18	478.2	436.8	41.4	457.5	0.160E 16	0.816E 23	7.12	2.37
19	483.6	442.0	41.6	462.8	0.161E 16	0.821E 23	7.34	2.45
20	488.7	447.2	41.5	467.9	0.162E 16	0.824E 23	7.51	2.50
21	493.6	452.2	41.4	472.9	0.162E 16	0.824E 23	7.60	2.53
22	498.3	457.2	41.1	477.7	0.161E 16	0.821E 23	7.62	2.54
23	502.9	462.1	40.8	482.5	0.160E 16	0.816E 23	7.61	2.54
24	507.1	466.9	40.2	487.0	0.158E 16	0.807E 23	7.51	2.50
25	511.2	471.6	39.6	491.4	0.156E 16	0.797E 23	7.37	2.46
26	514.9	476.1	38.8	495.5	0.154E 16	0.783E 23	7.17	2.39
27	518.4	480.6	37.9	499.5	0.151E 16	0.768E 23	6.94	2.31
28	521.7	484.8	36.9	503.2	0.147E 16	0.750E 23	6.67	2.22
29	524.8	488.8	36.0	506.8	0.144E 16	0.732E 23	6.38	2.13
30	527.7	492.8	34.9	510.2	0.139E 16	0.711E 23	6.06	2.02
31	530.2	496.6	33.7	513.4	0.135E 16	0.688E 23	5.72	1.91
32	532.8	500.2	32.6	516.5	0.131E 16	0.667E 23	5.40	1.80
33	535.3	503.7	31.6	519.5	0.127E 16	0.647E 23	5.11	1.70
34	538.0	507.3	30.7	522.6	0.124E 16	0.631E 23	4.87	1.62
35	541.1	510.9	30.2	526.0	0.122E 16	0.621E 23	4.72	1.57

T(IN) = TEMP OF INNER CLAD SURFACE.
DEL T = T(IN) - T(OUT)
PERC V = PERCENT CLAD VOLUME CHANGE.

TOUT = TEMP OF OUTER CLAD SURFACS.
T(M) = CLAD MEAN TEMP.
PERC D = PERCENT CLAD DIAMETER CHANGE.

PIN NO IS 29 TIME IN DAYS = 381. PEAK FLUX IS 1.69980E 15

POS I	T(IN) DEG C	T(OUT) DEG C	DEL T DEG C	T(M) DEG C	FLUX	FLUENCE	PERC V	PERC D
9	428.8	392.6	36.3	410.7	0.136E 16	0.448E 23	1.86	0.62
10	434.6	397.4	37.2	416.0	0.140E 16	0.461E 23	2.06	0.69
11	440.5	402.3	38.2	421.4	0.144E 16	0.475E 23	2.27	0.76
12	446.8	407.5	39.3	427.1	0.149E 16	0.491E 23	2.51	0.84
13	453.1	412.8	40.3	432.9	0.154E 16	0.506E 23	2.76	0.92
14	459.3	418.2	41.2	438.7	0.157E 16	0.518E 23	2.99	1.00
15	465.6	423.6	42.0	444.6	0.161E 16	0.530E 23	3.21	1.07
16	471.6	429.1	42.6	450.3	0.164E 16	0.540E 23	3.40	1.13
17	477.6	434.5	43.1	456.0	0.166E 16	0.548E 23	3.58	1.19
18	483.3	439.9	43.4	461.6	0.168E 16	0.553E 23	3.72	1.24
19	488.9	445.4	43.5	467.1	0.169E 16	0.557E 23	3.83	1.28
20	494.3	450.8	43.5	472.5	0.170E 16	0.559E 23	3.91	1.30
21	499.5	456.1	43.4	477.8	0.170E 16	0.559E 23	3.95	1.32
22	504.4	461.4	43.0	482.9	0.169E 16	0.557E 23	3.96	1.32
23	509.2	466.6	42.6	487.9	0.168E 16	0.553E 23	3.94	1.31
24	513.6	471.6	42.1	492.6	0.166E 16	0.547E 23	3.88	1.29
25	517.9	476.5	41.4	497.2	0.164E 16	0.540E 23	3.81	1.27
26	521.8	481.2	40.6	501.5	0.161E 16	0.531E 23	3.69	1.23
27	525.6	485.9	39.7	505.7	0.158E 16	0.521E 23	3.57	1.19
28	529.0	490.3	38.7	509.7	0.154E 16	0.509E 23	3.42	1.14
29	532.3	494.6	37.7	513.4	0.151E 16	0.496E 23	3.27	1.09
30	535.2	498.7	36.5	517.0	0.146E 16	0.482E 23	3.10	1.03
31	537.9	502.7	35.2	520.3	0.142E 16	0.467E 23	2.92	0.97
32	540.6	506.5	34.1	523.5	0.137E 16	0.452E 23	2.75	0.92
33	543.3	510.2	33.1	526.7	0.133E 16	0.439E 23	2.60	0.87
34	546.1	513.9	32.1	530.0	0.130E 16	0.428E 23	2.47	0.82
35	549.3	517.7	31.6	533.5	0.128E 16	0.421E 23	2.39	0.80

T(IN) = TEMP OF INNER CLAD SURFACE. TOUT = TEMP OF OUTER CLAD SURFACS
DEL T = T(IN) - T(OUT) T(M) = CLAD MEAN TEMP.
PERC V = PERCENT CLAD VOLUME CHANGE. PERC D = PERCENT CLAD DIAMETER CHANGE

PIN NO IS 30 TIME IN DAYS = 254. PEAK FLUX IS 1.67340E 15

POSI	T(IN) DEG C	T(OUT) DEG C	DEL T DEG C	T(M) DEG C	FLUX	FLUENCE	PERC V	PERC D
9	428.8	393.2	35.7	411.0	0.134E 16	0.294E 23	0.91	0.30
10	437.2	400.7	36.5	418.9	0.138E 16	0.302E 23	1.03	0.34
11	445.8	408.4	37.4	427.1	0.142E 16	0.312E 23	1.15	0.38
12	454.9	416.4	38.4	435.7	0.147E 16	0.322E 23	1.30	0.43
13	464.1	424.7	39.4	444.4	0.151E 16	0.332E 23	1.44	0.48
14	473.3	433.1	40.2	453.2	0.155E 16	0.340E 23	1.57	0.52
15	482.5	441.7	40.8	462.1	0.159E 16	0.348E 23	1.69	0.56
16	491.7	450.3	41.4	471.0	0.161E 16	0.354E 23	1.78	0.59
17	500.8	459.1	41.7	480.0	0.164E 16	0.359E 23	1.86	0.62
18	509.8	467.9	41.9	488.9	0.165E 16	0.363E 23	1.92	0.64
19	518.7	476.7	42.0	497.7	0.167E 16	0.366E 23	1.95	0.65
20	527.5	485.6	41.9	506.5	0.167E 16	0.367E 23	1.96	0.65
21	536.0	494.3	41.7	515.2	0.167E 16	0.367E 23	1.95	0.65
22	544.3	503.0	41.3	523.6	0.166E 16	0.365E 23	1.91	0.64
23	552.4	511.6	40.8	532.0	0.165E 16	0.363E 23	1.86	0.62
24	560.3	520.1	40.2	540.2	0.164E 16	0.359E 23	1.79	0.60
25	567.9	528.3	39.6	548.1	0.162E 16	0.355E 23	1.71	0.57
26	575.1	536.4	38.7	555.8	0.159E 16	0.348E 23	1.62	0.54
27	582.1	544.4	37.7	563.2	0.156E 16	0.342E 23	1.52	0.51
28	588.7	552.1	36.7	570.4	0.152E 16	0.334E 23	1.42	0.47
29	595.2	559.6	35.6	577.4	0.148E 16	0.326E 23	1.32	0.44
30	601.2	566.7	34.5	584.0	0.144E 16	0.316E 23	1.22	0.41
31	606.9	573.7	33.3	590.3	0.140E 16	0.306E 23	1.12	0.37
32	612.5	580.4	32.1	596.4	0.135E 16	0.297E 23	1.03	0.34
33	618.0	586.9	31.1	602.5	0.131E 16	0.288E 23	0.95	0.32
34	623.6	593.3	30.2	608.4	0.128E 16	0.281E 23	0.88	0.29
35	629.4	599.8	29.7	614.6	0.126E 16	0.277E 23	0.83	0.28

T(IN) = TEMP OF INNER CLAD SURFACE.
DEL T = T(IN) - T(OUT)
PERC V = PERCENT CLAD VOLUME CHANGE.

TOUT = TEMP OF OUTER CLAD SURFACS.
T(M) = CLAD MEAN TEMP.
PERC D = PERCENT CLAD DIAMETER CHANGE.

PIN NO IS 31 TIME IN DAYS = 254. PEAK FLUX IS 1.64700E 15

POSI	T(IN) DEG C	T(OUT) DEG C	DEL T DEG C	T(M) DEG C	FLUX	FLUENCE	PERC V	PERC D
9	429.2	393.3	35.9	411.2	0.132E 16	0.289E 23	0.89	0.30
10	437.7	400.8	36.8	419.2	0.136E 16	0.298E 23	1.00	0.33
11	446.3	408.7	37.7	427.5	0.140E 16	0.307E 23	1.13	0.38
12	455.5	416.8	38.7	436.1	0.144E 16	0.317E 23	1.27	0.42
13	464.8	425.1	39.7	444.9	0.149E 16	0.327E 23	1.40	0.47
14	474.1	433.6	40.5	453.8	0.153E 16	0.335E 23	1.53	0.51
15	483.4	442.2	41.2	462.8	0.156E 16	0.342E 23	1.64	0.55
16	492.6	450.9	41.7	471.8	0.159E 16	0.349E 23	1.74	0.58
17	501.8	459.8	42.1	480.8	0.161E 16	0.354E 23	1.82	0.61
18	510.9	468.7	42.3	489.8	0.163E 16	0.357E 23	1.87	0.62
19	519.9	477.6	42.3	498.7	0.164E 16	0.360E 23	1.90	0.63
20	528.7	486.4	42.2	507.6	0.165E 16	0.361E 23	1.91	0.64
21	537.3	495.3	42.0	516.3	0.165E 16	0.361E 23	1.89	0.63
22	545.7	504.1	41.6	524.9	0.164E 16	0.360E 23	1.85	0.62
23	553.8	512.7	41.1	533.3	0.163E 16	0.357E 23	1.81	0.60
24	561.7	521.2	40.5	541.5	0.161E 16	0.354E 23	1.74	0.58
25	569.4	529.6	39.9	549.5	0.159E 16	0.349E 23	1.66	0.55
26	576.7	537.8	38.9	557.2	0.156E 16	0.343E 23	1.57	0.52
27	583.7	545.7	38.0	564.7	0.153E 16	0.336E 23	1.48	0.49
28	590.4	553.5	36.9	572.0	0.150E 16	0.329E 23	1.38	0.46
29	596.9	561.1	35.9	579.0	0.146E 16	0.320E 23	1.28	0.43
30	603.1	568.3	34.8	585.7	0.142E 16	0.311E 23	1.18	0.39
31	608.8	575.3	33.5	592.0	0.137E 16	0.301E 23	1.08	0.36
32	614.4	582.1	32.4	598.2	0.133E 16	0.292E 23	0.99	0.33
33	619.9	588.7	31.3	604.3	0.129E 16	0.284E 23	0.91	0.30
34	625.5	595.1	30.4	610.3	0.126E 16	0.276E 23	0.84	0.28
35	631.4	601.6	29.8	616.5	0.124E 16	0.272E 23	0.79	0.26

T(IN) = TEMP OF INNER CLAD SURFACE.
DEL T = T(IN) - T(OUT)
PERC V = PERCENT CLAD VOLUME CHANGE.

TOUT = TEMP OF OUTER CLAD SURFACS.
T(M) = CLAD MEAN TEMP.
PERC D = PERCENT CLAD DIAMETER CHANGE.

PIN NO IS 32 TIME IN DAYS = 590. PEAK FLUX IS 1.61870E 15

POSI	T(IN) DEG C	T(OUT) DEG C	DEL T DEG C	T(M) DEG C	FLUX	FLUENCE	PERC V	PERC D
9	427.2	392.6	34.6	409.9	0.130E 16	0.660E 23	3.59	1.20
10	435.2	399.8	35.4	417.5	0.133E 16	0.680E 23	4.05	1.35
11	443.6	407.3	36.2	425.4	0.137E 16	0.700E 23	4.55	1.52
12	452.4	415.1	37.3	433.7	0.142E 16	0.723E 23	5.12	1.71
13	461.3	423.1	38.2	442.2	0.146E 16	0.746E 23	5.67	1.89
14	470.2	431.2	38.9	450.7	0.150E 16	0.764E 23	6.19	2.06
15	479.1	439.6	39.6	459.3	0.153E 16	0.782E 23	6.66	2.22
16	488.0	447.9	40.1	468.0	0.156E 16	0.796E 23	7.06	2.35
17	496.9	456.4	40.5	476.6	0.158E 16	0.807E 23	7.40	2.47
18	505.6	464.9	40.7	485.3	0.160E 16	0.816E 23	7.63	2.54
19	514.2	473.4	40.7	493.8	0.161E 16	0.821E 23	7.78	2.59
20	522.7	482.0	40.7	502.3	0.162E 16	0.824E 23	7.84	2.61
21	530.9	434.9	96.1	482.9	0.162E 16	0.824E 23	7.75	2.58
22	538.9	498.8	40.1	518.9	0.161E 16	0.821E 23	7.68	2.56
23	546.8	507.2	39.7	527.0	0.160E 16	0.816E 23	7.50	2.50
24	554.4	515.3	39.1	534.9	0.158E 16	0.807E 23	7.25	2.42
25	561.7	523.4	38.3	542.6	0.156E 16	0.797E 23	6.95	2.32
26	568.7	531.2	37.5	550.0	0.154E 16	0.783E 23	6.59	2.20
27	575.5	538.9	36.6	557.2	0.151E 16	0.768E 23	6.22	2.07
28	581.9	546.3	35.6	564.1	0.147E 16	0.750E 23	5.83	1.94
29	588.2	553.6	34.6	570.9	0.144E 16	0.732E 23	5.44	1.81
30	594.1	560.5	33.6	577.3	0.139E 16	0.711E 23	5.03	1.68
31	599.6	567.2	32.3	583.4	0.135E 16	0.688E 23	4.63	1.54
32	604.9	573.7	31.2	589.3	0.131E 16	0.667E 23	4.26	1.42
33	610.3	580.1	30.2	595.2	0.127E 16	0.647E 23	3.93	1.31
34	615.6	586.3	29.3	600.9	0.124E 16	0.631E 23	3.65	1.22
35	621.3	592.5	28.8	606.9	0.122E 16	0.621E 23	3.44	1.15

T(IN) = TEMP OF INNER CLAD SURFACE. TOUT = TEMP OF OUTER CLAD SURFACS.
DEL T = T(IN) - T(OUT) T(M) = CLAD MEAN TEMP.
PERC V = PERCENT CLAD VOLUME CHANGE. PERC D = PERCENT CLAD DIAMETER CHANGE.

PIN NO IS 33 TIME IN DAYS = 254. PEAK FLUX IS 1.59230E 15

POSI	T(IN) DEG C	T(OUT) DEG C	DEL T DEG C	T(M) DEG C	FLUX	FLUENCE	PERC V	PERC D
9	429.7	392.9	36.8	411.3	0.127E 16	0.280E 23	0.84	0.28
10	435.5	397.7	37.8	416.6	0.131E 16	0.288E 23	0.92	0.31
11	441.5	402.8	38.7	422.1	0.135E 16	0.296E 23	1.02	0.34
12	447.9	408.1	39.9	428.0	0.140E 16	0.306E 23	1.13	0.38
13	454.4	413.4	40.9	433.9	0.144E 16	0.316E 23	1.24	0.41
14	460.7	418.8	41.8	439.7	0.148E 16	0.324E 23	1.34	0.45
15	467.0	424.4	42.6	445.7	0.151E 16	0.331E 23	1.44	0.48
16	473.1	429.9	43.2	451.5	0.154E 16	0.337E 23	1.53	0.51
17	479.2	435.5	43.7	457.3	0.156E 16	0.342E 23	1.61	0.54
18	485.0	441.1	43.9	463.0	0.157E 16	0.346E 23	1.67	0.56
19	490.7	446.6	44.1	468.6	0.159E 16	0.348E 23	1.72	0.57
20	496.2	452.1	44.1	474.1	0.159E 16	0.349E 23	1.75	0.58
21	501.4	457.4	44.0	479.4	0.159E 16	0.349E 23	1.77	0.59
22	506.4	462.8	43.7	484.6	0.158E 16	0.348E 23	1.77	0.59
23	511.3	468.0	43.3	489.6	0.157E 16	0.346E 23	1.76	0.59
24	515.8	473.1	42.7	494.4	0.156E 16	0.342E 23	1.74	0.58
25	520.1	478.1	42.0	499.1	0.154E 16	0.337E 23	1.70	0.57
26	524.1	483.9	41.2	503.5	0.151E 16	0.331E 23	1.65	0.55
27	527.9	487.7	40.2	507.8	0.148E 16	0.325E 23	1.59	0.53
28	531.4	492.2	39.2	511.8	0.145E 16	0.318E 23	1.53	0.51
29	534.7	496.6	38.2	515.6	0.141E 16	0.310E 23	1.46	0.49
30	537.8	500.8	37.0	519.3	0.137E 16	0.301E 23	1.38	0.46
31	540.5	504.7	35.8	522.6	0.133E 16	0.291E 23	1.30	0.43
32	543.2	508.6	34.6	525.9	0.129E 16	0.282E 23	1.23	0.41
33	545.9	512.4	33.5	529.2	0.125E 16	0.274E 23	1.16	0.39
34	548.8	516.2	32.6	532.5	0.122E 16	0.267E 23	1.10	0.37
35	552.1	520.1	32.0	536.1	0.120E 16	0.263E 23	1.06	0.35

T(IN) = TEMP OF INNER CLAD SURFACE.
DEL T = T(IN) - T(OUT)
PERC V = PERCENT CLAD VOLUME CHANGE.

TOUT = TEMP OF OUTER CLAD SURFACE.
T(M) = CLAD MEAN TEMP.
PERC D = PERCENT CLAD DIAMETER CHANGE.

PIN NO IS 34 TIME IN DAYS = 254. PEAK FLUX IS 1.64760E 15

POS I	T(IN) DEG C	T(OUT) DEG C	DEL T DEG C	T(M) DEG C	FLUX	FLUENCE	PERC V	PERC D
9	429.4	393.4	35.9	411.4	0.132E 16	0.289E 23	0.89	0.30
10	434.8	397.9	36.9	416.4	0.136E 16	0.298E 23	0.98	0.33
11	440.4	402.6	37.9	421.5	0.140E 16	0.307E 23	1.07	0.36
12	446.4	407.4	39.0	426.9	0.144E 16	0.317E 23	1.19	0.40
13	452.4	412.4	40.1	432.4	0.149E 16	0.327E 23	1.30	0.43
14	458.3	417.4	40.9	437.8	0.153E 16	0.335E 23	1.41	0.47
15	464.2	422.4	41.7	443.3	0.156E 16	0.342E 23	1.51	0.50
16	469.8	427.6	42.3	448.7	0.159E 16	0.349E 23	1.60	0.53
17	475.4	432.6	42.8	454.0	0.161E 16	0.354E 23	1.68	0.56
18	480.8	437.7	43.1	459.2	0.163E 16	0.357E 23	1.75	0.58
19	485.9	442.7	43.2	464.3	0.164E 16	0.360E 23	1.80	0.60
20	490.9	447.7	43.3	469.3	0.165E 16	0.361E 23	1.84	0.61
21	495.7	452.6	43.1	474.2	0.165E 16	0.361E 23	1.86	0.62
22	500.2	457.4	42.8	478.8	0.164E 16	0.360E 23	1.86	0.62
23	504.6	462.2	42.4	483.4	0.163E 16	0.357E 23	1.86	0.62
24	508.6	466.7	41.9	487.7	0.161E 16	0.354E 23	1.83	0.61
25	512.4	471.2	41.2	491.8	0.159E 16	0.349E 23	1.80	0.60
26	515.9	475.6	40.4	495.7	0.156E 16	0.343E 23	1.75	0.58
27	519.3	479.8	39.5	499.5	0.153E 16	0.336E 23	1.69	0.56
28	522.3	483.8	38.6	503.1	0.150E 16	0.329E 23	1.63	0.54
29	525.2	487.7	37.5	506.5	0.146E 16	0.320E 23	1.56	0.52
30	527.8	491.4	36.4	509.6	0.142E 16	0.311E 23	1.48	0.49
31	530.1	494.9	35.2	512.5	0.137E 16	0.301E 23	1.40	0.47
32	532.4	498.4	34.0	515.4	0.133E 16	0.292E 23	1.32	0.44
33	534.7	501.8	32.9	518.2	0.129E 16	0.284E 23	1.25	0.42
34	537.1	505.1	32.0	521.1	0.126E 16	0.276E 23	1.19	0.40
35	540.1	508.6	31.5	524.3	0.124E 16	0.272E 23	1.15	0.38

T(IN) = TEMP OF INNER CLAD SURFACE.
DEL T = T(IN) - T(OUT)
PERC V = PERCENT CLAD VOLUME CHANGE.

TOUT = TEMP OF OUTER CLAD SURFACS.
T(M) = CLAD MEAN TEMP.
PERC D = PERCENT CLAD DIAMETER CHANGE.

PIN NO IS 35 TIME IN DAYS = 590. PEAK FLUX IS 1.61870E 15

POS I	T(IN) DEG C	T(OUT) DEG C	DEL T DEG C	T(M) DEG C	FLUX	FLUENCE	PERC V	PERC D
9	426.2	391.7	34.6	408.9	0.130E 16	0.660E 23	3.55	1.18
10	431.7	396.3	35.4	414.0	0.133E 16	0.680E 23	3.92	1.31
11	437.4	401.0	36.4	419.2	0.137E 16	0.700E 23	4.32	1.44
12	443.4	405.9	37.4	424.7	0.142E 16	0.723E 23	4.79	1.60
13	449.4	410.9	38.5	430.2	0.146E 16	0.746E 23	5.25	1.75
14	455.4	416.1	39.3	435.7	0.150E 16	0.764E 23	5.69	1.90
15	461.3	421.2	40.1	441.2	0.153E 16	0.782E 23	6.12	2.04
16	467.1	426.4	40.7	446.7	0.156E 16	0.796E 23	6.50	2.17
17	472.7	431.6	41.1	452.2	0.158E 16	0.807E 23	6.84	2.28
18	478.2	436.8	41.4	457.5	0.160E 16	0.816E 23	7.12	2.37
19	483.6	442.0	41.6	462.8	0.161E 16	0.821E 23	7.34	2.45
20	488.7	447.2	41.5	467.9	0.162E 16	0.824E 23	7.51	2.50
21	493.6	452.2	41.4	472.9	0.162E 16	0.824E 23	7.60	2.53
22	498.3	457.2	41.1	477.7	0.161E 16	0.821E 23	7.62	2.54
23	502.9	462.1	40.8	482.5	0.160E 16	0.816E 23	7.61	2.54
24	507.1	466.9	40.2	487.0	0.158E 16	0.807E 23	7.51	2.50
25	511.2	471.6	39.6	491.4	0.156E 16	0.797E 23	7.37	2.46
26	514.9	476.1	38.8	495.5	0.154E 16	0.783E 23	7.17	2.39
27	518.4	480.6	37.9	499.5	0.151E 16	0.768E 23	6.94	2.31
28	521.7	484.8	36.9	503.2	0.147E 16	0.750E 23	6.67	2.22
29	524.8	488.8	36.0	506.8	0.144E 16	0.732E 23	6.38	2.13
30	527.7	492.8	34.9	510.2	0.139E 16	0.711E 23	6.06	2.02
31	530.2	496.6	33.7	513.4	0.135E 16	0.688E 23	5.72	1.91
32	532.8	500.2	32.6	516.5	0.131E 16	0.667E 23	5.40	1.80
33	535.3	503.7	31.6	519.5	0.127E 16	0.647E 23	5.11	1.70
34	538.0	507.3	30.7	522.6	0.124E 16	0.631E 23	4.87	1.62
35	541.1	510.9	30.2	526.0	0.122E 16	0.621E 23	4.72	1.57

T(IN) = TEMP OF INNER CLAD SURFACE.
DEL T = T(IN) - T(OUT)
PERC V = PERCENT CLAD VOLUME CHANGE.

TOUT = TEMP OF OUTER CLAD SURFACE
T(M) = CLAD MEAN TEMP.
PERC D = PERCENT CLAD DIAMETER CHANGE.

PIN NO IS 36 TIME IN DAYS = 590. PEAK FLUX IS 1.59230E 15

POSI	T(IN) DEG C	T(OUT) DEG C	DEL T DEG C	T(M) DEG C	FLUX	FLUENCE	PERC V	PERC D
9	429.7	392.9	36.8	411.3	0.127E 16	0.650E 23	3.54	1.18
10	435.5	397.7	37.8	416.6	0.131E 16	0.669E 23	3.91	1.30
11	441.5	402.8	38.7	422.1	0.135E 16	0.689E 23	4.31	1.44
12	447.9	408.1	39.9	428.0	0.140E 16	0.712E 23	4.78	1.59
13	454.4	413.4	40.9	433.9	0.144E 16	0.733E 23	5.24	1.75
14	460.7	418.8	41.8	439.7	0.148E 16	0.752E 23	5.68	1.89
15	467.0	424.4	42.6	445.7	0.151E 16	0.769E 23	6.10	2.03
16	473.1	429.9	43.2	451.5	0.154E 16	0.783E 23	6.47	2.16
17	479.2	435.5	43.7	457.3	0.156E 16	0.794E 23	6.80	2.27
18	485.0	441.1	43.9	463.0	0.157E 16	0.803E 23	7.06	2.35
19	490.7	446.6	44.1	468.6	0.159E 16	0.808E 23	7.27	2.42
20	496.2	452.1	44.1	474.1	0.159E 16	0.811E 23	7.41	2.47
21	501.4	457.4	44.0	479.4	0.159E 16	0.811E 23	7.49	2.50
22	506.4	462.8	43.7	484.6	0.158E 16	0.807E 23	7.49	2.50
23	511.3	468.0	43.3	489.6	0.157E 16	0.803E 23	7.46	2.49
24	515.8	473.1	42.7	494.4	0.156E 16	0.794E 23	7.34	2.45
25	520.1	478.1	42.0	499.1	0.154E 16	0.784E 23	7.19	2.40
26	524.1	482.9	41.2	503.5	0.151E 16	0.770E 23	6.97	2.32
27	527.9	487.7	40.2	507.8	0.148E 16	0.755E 23	6.73	2.24
28	531.4	492.2	39.2	511.8	0.145E 16	0.738E 23	6.45	2.15
29	534.7	496.6	38.2	515.6	0.141E 16	0.720E 23	6.16	2.05
30	537.8	500.8	37.0	519.3	0.137E 16	0.699E 23	5.84	1.95
31	540.5	504.7	35.8	522.6	0.133E 16	0.677E 23	5.49	1.83
32	543.2	508.6	34.6	525.9	0.129E 16	0.656E 23	5.18	1.73
33	545.9	512.4	33.5	529.2	0.125E 16	0.637E 23	4.89	1.63
34	548.8	516.2	32.6	532.5	0.122E 16	0.620E 23	4.65	1.55
35	552.1	520.1	32.0	536.1	0.120E 16	0.611E 23	4.49	1.50

T(IN) = TEMP OF INNER CLAD SURFACE.
DEL T = T(IN) - T(OUT)
PERC V = PERCENT CLAD VOLUME CHANGE.

TOUT = TEMP OF OUTER CLAD SURFACS.
T(M) = CLAD MEAN TEMP.
PERC D = PERCENT CLAD DIAMETER CHANGE.

PIN NO IS 37 TIME IN DAYS = 590. PEAK FLUX IS 1.56590E 15

POSI	T(IN) DEG C	T(OUT) DEG C	DEL T DEG C	T(M) DEG C	FLUX	FLUENCE	PERC V	PERC D
9	425.4	392.1	33.4	408.7	0.125E 16	0.639E 23	3.35	1.12
10	430.5	396.2	34.3	413.4	0.129E 16	0.657E 23	3.68	1.23
11	435.7	400.5	35.2	418.1	0.133E 16	0.677E 23	4.05	1.35
12	441.3	405.0	36.3	423.1	0.137E 16	0.700E 23	4.47	1.49
13	446.9	409.6	37.3	428.2	0.141E 16	0.721E 23	4.89	1.63
14	452.3	414.3	38.1	433.3	0.145E 16	0.739E 23	5.29	1.76
15	457.8	418.9	38.8	438.4	0.148E 16	0.756E 23	5.68	1.89
16	463.1	423.7	39.4	443.4	0.151E 16	0.770E 23	6.03	2.01
17	468.2	428.4	39.8	448.3	0.153E 16	0.781E 23	6.35	2.12
18	473.2	433.1	40.1	453.2	0.155E 16	0.789E 23	6.61	2.20
19	478.1	437.8	40.3	457.9	0.156E 16	0.795E 23	6.82	2.27
20	482.7	442.4	40.3	462.5	0.156E 16	0.798E 23	6.97	2.32
21	487.1	446.9	40.2	467.0	0.156E 16	0.798E 23	7.07	2.36
22	491.3	451.4	39.9	471.3	0.156E 16	0.794E 23	7.10	2.37
23	495.4	455.8	39.6	475.6	0.155E 16	0.789E 23	7.10	2.37
24	499.1	460.1	39.1	479.6	0.153E 16	0.781E 23	7.02	2.34
25	502.7	464.2	38.4	483.4	0.151E 16	0.771E 23	6.91	2.30
26	505.9	468.2	37.7	487.1	0.149E 16	0.757E 23	6.73	2.24
27	509.0	472.2	36.8	490.6	0.146E 16	0.743E 23	6.53	2.18
28	511.8	475.9	35.9	493.9	0.142E 16	0.726E 23	6.29	2.10
29	514.5	479.5	35.0	497.0	0.139E 16	0.708E 23	6.04	2.01
30	516.9	482.9	34.0	499.9	0.135E 16	0.688E 23	5.75	1.92
31	519.1	486.2	32.8	502.6	0.131E 16	0.666E 23	5.44	1.81
32	521.2	489.4	31.7	505.3	0.127E 16	0.645E 23	5.15	1.72
33	523.3	492.6	30.8	507.9	0.123E 16	0.626E 23	4.89	1.63
34	525.6	495.7	29.9	510.6	0.120E 16	0.610E 23	4.67	1.56
35	528.3	498.9	29.4	513.6	0.118E 16	0.601E 23	4.54	1.51

T(IN) = TEMP OF INNER CLAD SURFACE.
DEL T = T(IN) - T(OUT)
PERC V = PERCENT CLAD VOLUME CHANGE.

TOUT = TEMP OF OUTER CLAD SURFACS.
T(M) = CLAD MEAN TEMP.
PERC D = PERCENT CLAD DIAMETER CHANGE.

APPENDIX B

ORNL Quality Assurance Specifications and Procedures

MET-FCT-FQ-1 Fabrication and Quality Assurance Plan, Series II Pins (EBR-II)

1. Tubing for Cladding

2. End Fittings

a. Procurement Specifications

MET-NDT-4 Tentative Methods for Liquid-Penetrant Inspection

MET-FR-4 Tentative Specification for the Ultrasonic Inspection of Metal Tubing

MET-FR-3 Specification for Inconel X Springs for $(U,Pu)O_2$ Fuel Rod Extensometers, Purchase Requisition N-1455

b. Inspection and Testing Procedures

MET-FCT-TS-5 Procedure for Visual Inspection of Incoming Metallic Materials

MET-FCT-TS-9 Use of Dermitron with Chart Recorder

MET-FCT-TS-10 Procedure for Ultrasonic Wall Thickness Measurement of Stainless Steel Tubing

MET-NDT-13 Inside Diameter Measurements of Tubing by Eddy Currents

ORNL Inspection Engineering Standards, Section 5 – Ultrasonic Testing

c. Reports

MAT-19- Certification of Tests – The Carpenter Steel Company (dated 12/12/68 and 2/27/69)

MAT-19- Material Report CH-19-1 – Summary of ORNL Analyses

MAT-20- Test Report – Crucible Steel Company of America (dated 2/24/69)

MAT-20- Material Report CH-20-1 – Summary of ORNL Analyses

Photomicrographs of Tubing and End Fittings (Fig. B.1)

3. Welds of End Fittings to Cladding Tube

a. Welding Procedure

MET-FCT-PP-7 General Welding Procedure for EBR-II, Series II

MET-FCT-PP-7-1 Bottom End Plug Weld

MET-FCT-PP-7-2 Capillary to Top Plug Weld

MET-FCT-PP-7-3 Top End Plug to Clad Welding

Fig. B.1. Photomicrographs of Tubing and End Fittings. (a) Base metal cladding tube; (b) base metal end plug.

3(a) Continued

MET-FCT-PP-7-4	Capillary Edge Weld
MET-FCT-PP-7-5	Top End Cap to Top End Plug Weld
MET-FCT-OP-9	Fuel Pin Welding

c. Photomicrographs of Qualification Welds on W-1, W-2, W-3, W-4, and W-5 (Fig. B.2)

e. Summary of Weld Repairs

4. Helium Leak Testing

b. Procedure. ORNL Inspection Engineering Standards, Section 7.

5. Xenon Tag Insertion

MET-FCT-OP-10	Procedure for Initial Loading of Xenon and Helium into Fuel Rods
MET-FCT-OP-10-1	Procedure for Subsequent Loading of Xenon and Helium into Fuel Rods
MET-FCT-D-137	Data Sheet for Measuring Fuel Pin Free Volume (XE-1)
MET-FCT-D-138	Xenon Tagging Calculation Work Sheet No. 1
MET-FCT-D-139	Xenon Tagging Calculation Work Sheet No. 2
MET-FCT-D-140	Data Sheet for Loading Xenon and Helium into Fuel Pins (XE-1)

8. Dimensional Inspections

a. Procedures

MET-FCT-TS-6	Length Measurement of Finished Fuel Pins
MET-FCT-TS-7	Outside Diameter Measurement of Finished Fuel Pins
MET-FCT-TS-8	Method for Measuring Total Indicated Runout of Finished Fuel Pins
MET-FCT-TS-1	Micrometer Standardization

9. Fuel Element Weights

a. Procedures

MET-FCT-TS-2	Procedure for Balance Standardization

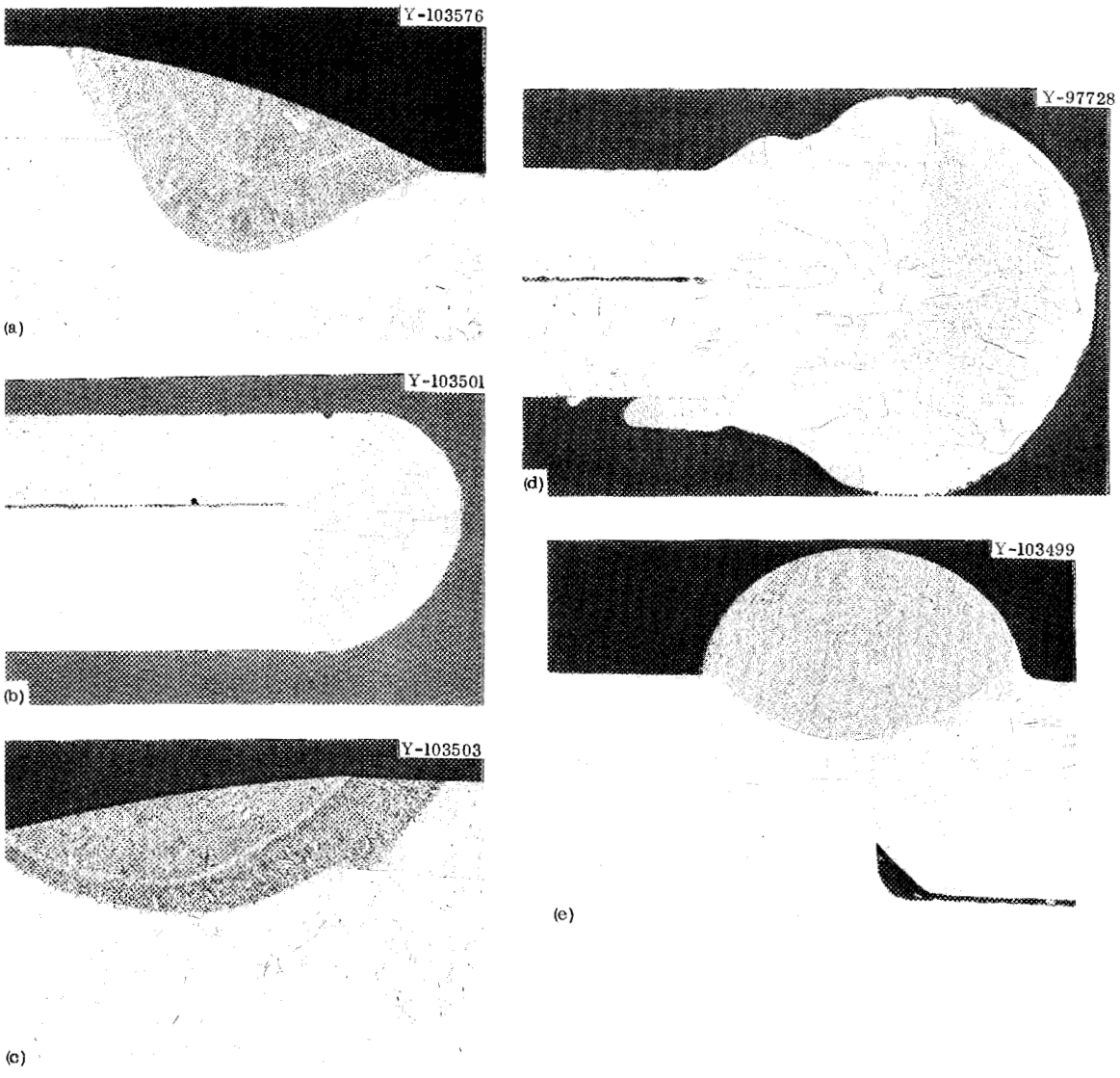

Fig. B-2. Photomicrographs of Qualification Welds. (a) Weld W-1, 75×. (b) Weld W-2, 75×. (c) Weld W-3, 75×. (d) Weld W-4, 100×. (e) Weld W-5, 75×. Reduced 34%.

WELD REPAIRS

Bottom End Plug to Clad Tube Weld W-1

Fuel Rod OS-2, OP-3, OP-5 – minimum weld thickness < 1 T, rewelded by procedure MET-FCT-PP-7-1; visual, radiographic, dye-penetrant, and helium leak check inspection. Weld met all requirements of specification.

Top End Plug to Clad Tube W-3

Fuel Rod OS-8, OP-2, OP-4 – excessive weld buildup on diameter by visual inspection; rewelded by procedure MET-FCT-PP-7-3; visual, radiographic, dye-penetrant, and helium leak check inspection. Weld met all requirements of specification.

Fuel Rod OS-11, OP-6 – minimum weld thickness < 1 T, rewelded by procedure MET-FCT-PP-7-3; visual, radiographic, dye-penetrant, and helium leak check inspection. Weld met all requirements of specification.

Top End Cap Top End Plug Weld W-5

Fuel Rod OP-1, OS-7, OP-4, OS-12 – depth of penetration < 1 T, rewelded using procedure MET-FCT-PP-7-5; visual, radiographic, dye-penetrant, and helium leak check inspection. Weld met requirements of specification.

Fuel Rod OP-3 – weld ammeter showed only 4–5 amperes; cold weld; weld repassed using procedure MET-FCT-7-5 at proper current; visual, radiographic, dye-penetrant, and helium leak check inspection. Weld met requirements of specification.

Summary of Welds Repaired on EBR-II Fuel Rod

Fuel Rod	Weld
OS-2	W-1
OP-3	W-1, W-5
OP-5	W-1
OP-4	W-3, W-5
OP-2	W-3
OS-8	W-3
OP-1	W-5
OS-7	W-5
OS-12	W-5
OS-11	W-3
OP-6	W-3

INTERNAL DISTRIBUTION

1–3. Central Research Library
4. ORNL – Y-12 Technical Library
Document Reference Section
5–24. Laboratory Records
25. Laboratory Records, ORNL-RC
26. ORNL Patent Office
27. E. E. Bloom
28. W. D. Bond
29. R. A. Bradley
30. R. E. Brooksbank
31. K. B. Brown
32. J. M. Chandler
33. S. D. Clinton
34. J. H. Coobs
35. F. L. Culler
36. D. R. Cuneo
37. J. E. Cunningham
38. H. G. Duggan
39. D. A. Dyslin
40. D. E. Ferguson
41. R. B. Fitts
42. J. H Frye, Jr.
43–44. W. O. Harms
45–47. M. R. Hill
48. F. J. Homan
49. A. R. Irvine
50. F. J. Kitts
51. W. J. Lackey
52. J. M. Leitnaker
53. R. E. Leuze
54. E. L. Long, Jr.
55. A. L. Lotts
56. E. J. Manthos
57. J. P. McBride
58. R. W. McClung
59. W. T. McDuffie
60. D. L. McElroy
61–65. A. R. Olsen
66. P. Patriarca
67. W. H. Pechin
68. M. K. Preston
69. C. F. Sanders
70. J. L. Scott
71. J. D. Sease
72. D. B. Trauger
73. W. D. Turner
74. W. E. Unger
75. T. N. Washburn
76. J. R. Weir, Jr.
77. R. G. Wymer
78. A. F. Zulliger

EXTERNAL DISTRIBUTION

AEC ADVISORY COMMITTEE ON REACTOR SAFEGUARDS, Washington, DC 20545

79. Executive Secretary

AEC DIVISION OF REACTOR DEVELOPMENT AND TECHNOLOGY, Washington, DC 20545

80. Director
81. Assistant Director, Project Management
82. Assistant Director, Reactor Technology
83. Assistant Director, Plant Engineering
84. Assistant Director, Reactor Engineering
85. Assistant Director, Nuclear Safety
86. Assistant Director, Program Analysis
87. Assistant Director, Engineering Standards
88–90. Chief, Fuels and Materials Branch
91. Chief, Fuels Engineering Branch
92. Chief, Gas Cooled Projects Branch

AEC DIVISION OF REACTOR DEVELOPMENT AND TECHNOLOGY, Washington, DC 20545 (continued)

93. Chief, Liquid Metal Projects Branch
94. EBR-II Program Manager
95. LMFBR Program Manager

AEC DIVISION OF REACTOR LICENSING, Washington, DC 20545

96–98. Director

AEC DIVISION OF REACTOR STANDARDS, Washington, DC 20545

99–100. Director

AEC DIVISION OF TECHNICAL INFORMATION EXTENSION, P.O. Box 62, Oak Ridge, TN 37830

101–102. Director

AEC NEW YORK OPERATIONS OFFICE, 376 Hudson Street, New York, NY 10014

103–104. Development Contracts Division

AEC OAK RIDGE OPERATIONS OFFICE, P.O. Box E, Oak Ridge, TN 37830

105. Laboratory and University Division

AEC SAN FRANCISCO OPERATIONS OFFICE, 2111 Bancroft Way, Berkeley, CA 94704

106. E. C. Shute

AEC SENIOR SITE REPRESENTATIVES

107. Argonne National Laboratory, 9700 S. Cass Avenue, Argonne, IL 60439
108. Argonne National Laboratory, P.O. Box 2108, Idaho Falls, ID 83401
109. Oak Ridge National Laboratory, P.O. Box X, Oak Ridge, TN 37830

ARGONNE NATIONAL LABORATORY, 9700 S. Cass Avenue, Argonne, IL 60439

110–111. Director, EBR-II Project
112. Director, LMFBR Program Office
113–127. Experimental Manager, EBR-II Project
128–129. B.R.T. Frost
130–131. Irradiation Coordinator, EBR-II Project
132–138. R. C. Vogel

ATOMICS INTERNATIONAL, P.O. Box 309, Canoga Park, CA 91304

139. H. Pearlman
140. S. Siegel

ATOMIC POWER DEVELOPMENT ASSOCIATES, INC., 1911 First Street, Detroit, MI 48226

141. A. A. Shoudy

BABCOCK & WILCOX, Research and Development Division, Alliance, OH 44601

142. H. H. Poor

BABCOCK & WILCOX, Power Generation Division, Lynchburg, VA 24505

143. H. S. Barringer
144. M. W. Croft
145. S. H. Esleeck
146. C. R. Johnson
147. R. S. Kingsley
148. E. C. Moncrief
149. R. A. Webb
150. B. W. Whitaker

BABCOCK & WILCOX, Research and Development Division, Lynchburg, VA 24505

151. C. J. Baroch
152. W. N. Bishop
153. A. H. Bremser
154. R. V. Carlson
155. E. H. Dewell
156. T. C. Engelder
157. L. J. Ferrell
158. L. B. Gross
159. E. N. Harbinson
160. J. M. Kerr
161. E. J. Kosiancic
162. E. D. Lynch

COMBUSTION ENGINEERING, INC., Prospect Hill Road, Windsor, CT 06095

163. W. P. Chernock

GENERAL ELECTRIC COMPANY, Breeder Reactor Development Department, 310 DeGuigne Drive, Sunnyvale, CA 94086

164–165. E. L. Zebroski

GULF GENERAL ATOMIC, INC., P.O. Box 111, San Diego, CA 92112

166. J. Lindgren
167. R. F. Turner

HANFORD ENGINEERING DEVELOPMENT LABORATORY, P.O. Box 1970, Richland, WA 99352

168–169. W. E. Roake

LOS ALAMOS SCIENTIFIC LABORATORY, P.O. Box 1663, Los Alamos, NM 87544

170. R. D. Baker

NUCLEAR FUEL SERVICES, INC., Erwin, TN 37650

171. Erik Pedersen

UNITED NUCLEAR CORPORATION, 5 New Street, White Plains, NY 10601

172. A. Strasser

WESTINGHOUSE ADVANCED REACTOR DIVISION, Waltz Mill Site, P.O. Box 158, Madison, PA 15663

173. P. Murray